Swimming Pools as Heat Sinks and Sources for Heat Pumps

By

CURTIS HARRINGTON
THESIS

Submitted in partial satisfaction of the requirements for the degree of

MASTER OF SCIENCE

in

Mechanical and Aerospace Engineering

in the

OFFICE OF GRADUATE STUDIES

of the

UNIVERSITY OF CALIFORNIA

DAVIS

Approved:

Vinod Narayanan, Chair

Mark Modera

Paul Erickson

Committee in Charge

2024

Acknowledgments

I dedicate this work to my family, whose unwavering support has been my anchor throughout this journey. To my grandparents, Kay and Harvey, for always reminding me of my potential and the value of lifelong learning. To my parents, Beth and Craig, for their steadfast encouragement as I navigated my winding path through college and into my career. And finally, to my wife, Angie, whose constant motivation and patience have inspired me daily, all while gracefully balancing the joys and challenges of raising our two wonderful children, Avery and Carter.

Abstract

This thesis describes the results from field demonstrations and model simulations of a retrofit technology that facilitates the rejection of air conditioner waste heat to a swimming pool. There are two primary advantages when rejecting waste heat to a swimming pool instead of ambient air: 1) swimming pool temperatures are typically colder than ambient air during peak cooling periods, and 2) water is a superior heat transfer medium than air resulting in better heat exchanger effectiveness allowing for more compact heat exchanger design. These both allow for lower compressor head pressures and associated energy use. This process also has the added benefit of providing "free" pool heating which would increase the benefits to consumers and spur market adoption. The technology demonstrated allows a maximum pool temperature to be set by the user, and switches between the existing air-source condenser and the water-source condenser depending on the heating needs of the pool. The performance of the existing air-source condensers was monitored for a period of three months. Subsequently, the air conditioners were retrofitted with the pool-source condenser and monitoring continued for another nine weeks. The results showed that the air conditioning energy use was reduced by 13% over the nine-week period, with 31% reduction when ambient conditions were above 90°F. Furthermore, a pool thermal model was developed and validated against field data to simulate the performance of the retrofit technology in different California climate zones. Simulations showed reductions in annual air conditioning energy use of more than 500 kWh in some climates. Savings were highly dependent on climate zone, with colder climates showing little or even negative cooling energy savings. The model is intended to be used as a tool for determining the potential energy savings for this technology in different scenarios given limited input data. The simulation tool was also used to evaluate the use of the pool as a heat source for a heat pump in the winter. Using the pool as a heat source in the winter showed energy savings potential with savings for many climate zones between 50-100 kWh, but this savings was significantly lower compared to the application as a heat sink in the summer.

Table of Contents

List of Figures

List of Tables

Nomenclature

A_{cond}	Surface Area of Conduction to Ground (m^2)
A_s	Surface Area used for shape factor calculations (m^2)
A	Surface Area of pool at air-water interface (m^2)
B	Bowen ratio $(-)$
C_B	Bowen Coefficient = 61.3 $(Pa/°C)$
COP	Coefficient of Performance $(-)$
$c_{p_{pool}}$	Pool Water Specific Heat $\left(\frac{kJ}{kg\ K}\right)$
CZ	Climate Zone
DB	Dry-bulb
$d_{poolavg}$	Average Pool Depth (m)
e_a	Vapor Pressure in ambient air (Pa)
e_s	Saturation Vapor Pressure of Air at the Pool Temperature (Pa)
E_{sky}	Emissivity of Sky $(-)$
E_w	Emissivity of water $(-)$
$G_{diffuse}$	Diffuse Component of Global Horizontal Radiation
G_{direct}	Direct Component of Global Horizontal Radiation
h	Specific Enthalpy $\left(\frac{kJ}{kg}\right)$
h_{evap}	Heat Transfer Coefficient for Evaporation $\left(\frac{W}{m^2 Pa}\right)$
HSPF	Heating Seasonal Performance Factor
k_{soil}	Thermal Conductivity of Soil $\left(\frac{W}{m\ K}\right)$
kW	Kilowatt
kWh	Kilowatt-hour
L_c	Characteristic Length used for shape factor calculations (m)
$\dot{m}_{air}$	Air Conditioner Mass Air Flow Rate $\left(\frac{kg}{s}\right)$
O_{sky}	Opaque Sky Cover $(in\ tenths)$
p_a	Ambient Pressure (Pa)

P_{AC}	Air Conditioner Power (kW)
P_{HP}	Heat Pump Power (kW)
p_o	Reference Pressure (Pa)
q_{ss}^*	Dimensionless Conduction Heat Rate $(-)$
Q_C	Heat absorbed from cold reservoir
q_{cond}	Conduction Heat Flux $\left(\frac{W}{m^2}\right)$
q_{conv}	Convection Heat Flux $\left(\frac{W}{m^2}\right)$
q_{evap}	Evaporation Heat Flux $\left(\frac{W}{m^2}\right)$
$Q_{EvapCoil}$	Air Conditioner Cooling Capacity (kW)
Q_H	Heat rejected to hot reservoir
q_{rad}	Radiation Heat Flux $\left(\frac{W}{m^2}\right)$
q_{solar}	Solar Heat Flux $\left(\frac{W}{m^2}\right)$
RMS	Root-mean Square
SEER	Seasonal Energy Efficiency Rating
SF	Shading Factor (–)
SHGC	Solar Heat Gain Coefficient (–)
T_a	Ambient Air Temperature (℃)
T_C	Cold Reservoir Temperature (℃)
T_{dew}	Dew Point Temperature (℃)
T_H	Hot Reservoir Temperature (℃)
$T_{HX,in}$	Pool Heat Exchanger Inlet Temperature (℃)
$T_{HX,out}$	Pool Heat Exchanger Outlet Temperature (℃)
T_{sky}	Effective Sky Temperature (℃)
T_{soil}	Soil Temperature (℃)
T_w	Swimming Pool Water Temperature (℃)
V	Wind Speed $\left(\frac{m}{s}\right)$

$\dot{V}_{air}$	Air Conditioner Volume Air Flow Rate $\left(\frac{m^3}{s}\right)$
$\dot{\mathrm{V}}_{\mathrm{pool}}$	Pool Heat Exchanger Volume Flow Rate $\left(\frac{m^3}{s}\right)$
W	Work Performed by Heat Pump System (kW)
WB	Wet-Bulb
α_{direct}	Absorptivity of Water under direct beam radiation $(-)$
$\alpha_{diffuse}$	Absorptivity of Water under diffuse radiation $(-)$
ρ_{pool}	Pool Water Density $\left(\frac{kg}{m^3}\right)$
ρ_{air}	Density of Air $\left(\frac{kg}{m^3}\right)$
σ	Stefan-Boltzmann Constant = 5.67×10^{-8} $\left(\frac{W}{m^2K^4}\right)$

Chapter 1. Introduction and Background

Introduction

Energy efficiency is a key component to reducing greenhouse gas emissions related to human activity and combating climate change. Many countries have adopted goals to decarbonize their energy portfolios by electrifying end-uses and developing renewable energy resources. The International Energy Agency, which has 31 member countries and more associated countries, has a goal to double the rate of improvement in energy efficiency by 2030 from its current rate of around 2% per year to over 4% (IEA, 2023). The California Energy Efficiency Strategic Plan, adopted in 2008, provides a roadmap for achieving aggressive goals related to buildings including a goal for net-zero energy in new residential and commercial buildings by 2020 and 2030, respectively (CPUC, 2011). These are just some of the examples of energy efficiency roadmaps that governments are using to address climate change.

Decarbonizing energy resources is another critical pathway toward reducing global warming impacts and is primarily aimed at reducing fossil-fuel use. Electrification is only one step in the process of decarbonization as it reduces on-site fuel use but must be paired with an effort to reduce fossil-fuels used for electricity production. According to the U.S. Energy Information Association, fossil fuel accounted for 80% of global energy consumption in 2022 with 60% of electricity generation coming from fossil fuel sources (EIA, 2023). Transitioning to renewable energy sources will encounter several challenges related to transmission, storage, and capital investment, but is necessary to achieving the aggressive goals to reduce global emissions.

One strategy for decarbonization that does not have broader implications for existing infrastructure and supply lines is energy efficiency, which is the process of reducing the energy required to achieve the same result. Some examples of these efforts include insulating buildings and reducing air infiltration to reduce heat gain or loss, improving the fuel efficiency of vehicles, and improving the efficiency of heat pumps used for conditioning buildings. Each of these examples demonstrate an effort that results in

lower energy consumption at the end-use without sacrificing comfort or performance. In some cases, systems can be retrofitted to improve performance without the need to replace the entire system. This thesis describes the results of a study evaluating the efficiency improvement of an air conditioning system retrofit that allows air conditioner waste heat to be rejected to a swimming pool rather than ambient air. Heat rejected from air conditioners is generally directed to outdoor air, which is hottest when air conditioning is most required. By rejecting air conditioner heat to a swimming pool, the efficiency of the air conditioner improves for the following reasons: 1) swimming pools are cooler than outdoor air during the hottest part of the day, and 2) rejecting heat to water is more effective than rejecting heat to air due to the higher density and heat capacity. These result in lower temperature lift (i.e. differential) required by the compressor. Previous research has indicated that rejecting heat to a swimming pool can save 25-30% on annual air conditioning electricity consumption in California (Harrington and Modera, 2013). A secondary benefit of this approach is that the heat rejected from the air conditioner provides pool heating that improves comfort. Running a 10.5 kW (3-ton) air conditioner for 2 hours would provide pool heating roughly equivalent to 29 kWh (1 therm) of natural gas used in a 90% efficient gas pool heater. The technology utilized is designed to be installed in combination with standard air conditioning equipment with controls to avoid overheating the swimming pool. The efficiency improvement of the air conditioner when rejecting heat to the pool was evaluated to determine the energy savings of the technology. Furthermore, this project provided further validation of a pool thermal model developed in (Woolley et al., 2011) that can be used to predict performance of the system in different applications.

Literature Review

Buildings require heating and cooling to maintain a safe and comfortable environment for their occupants. Heating of buildings has largely been accomplished through burning of fuels, including wood, oil, and natural gas. While building heating systems are still dominated by fossil fuel sources, heating

systems have advanced to become more efficient and allow for improved indoor air quality. Before the advent of current air conditioning systems, cooling was often accomplished through passive strategies that relied on the thermal mass of the building, insulation, and thoughtful design strategies (Samuel et al. 2012). For example, the design of a building can allow for natural ventilation to cool the space by taking advantage of wind or stack effects on a building. With the prevalence of mechanical heating and cooling systems, the construction of modern buildings does not generally implement advanced passive design strategies for maintaining comfortable indoor environments but instead relies on active space conditioning.

Recent efforts to reduce greenhouse gas emissions associated with building heating systems have led to higher rates of adoption of vapor-compression heat pump systems that use a refrigeration cycle to move heat between the conditioned zone (i.e. a home or business) and a heat source/sink. Most of these systems use outside air as the heat source/sink (air-source) but there have been a wide range of examples of using alternative heat exchange strategies for vapor-compression heat pump systems. Often these alternative methods arise from the desire to improve the efficiency of the heat pump system by changing the temperature of the heat source/sink. Carnot efficiency describes the maximum theoretical efficiency that can be achieved by a heat pump which is illustrated in Figure 1 using the conservation of energy and second law principles.

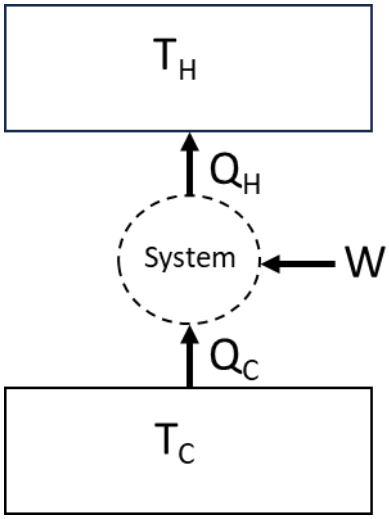

Figure 1. Schematic of energy flows in Carnot heat pump cycle

The Carnot efficiency for the heat pump in Figure 1 can be expressed through a simple relationship of the system heat flows as follows:

$$COP = \frac{Q_C}{W} \qquad \textit{Equation 1}$$

$$COP = \frac{Q_C}{Q_H - Q_C} \qquad \textit{Equation 2}$$

$$COP = \frac{1}{\frac{Q_H}{Q_C} - 1} \qquad \textit{Equation 3}$$

The maximum (Carnot) efficiency can be expressed in terms of the sink and source temperatures as follows:

$$COP_{cool} = \frac{1}{\frac{T_H}{T_C} - 1} \qquad \textit{Equation 4}$$

Equation 4 states that the maximum efficiency for an air conditioner is a function of the temperature of the building being cooled and the temperature of the heat sink to which the air conditioner is rejecting

heat. This is often referred to as the temperature lift of an air conditioner. A similar analysis can be performed for heating with a heat pump which ultimately gives the relationship shown in Equation 5.

$$COP_{heat} = \frac{1}{1 - \frac{T_C}{T_H}} \qquad \textit{Equation 5}$$

Equation 4 and Equation 5 demonstrate the theoretical maximum efficiency for a heat pump system is related to the indoor and outdoor temperatures. One strategy for reducing energy use from a heat pump system is to raise the air conditioner temperature setpoint in the home or reduce the heat pump temperature setpoint when in heating mode. This reduces the temperature lift of the system and results in higher efficiency. Unfortunately, there is limited opportunity to modify indoor temperatures without causing the occupants to become uncomfortable. There have been significant efforts, however, to identify different sources (or sinks) for exchanging heat with the outdoor environment.

Ground-Source Heat Pumps

Ground-source heat pumps are a category of systems that exchange heat with the ground. Ground temperatures are much more stable than outdoor air temperatures due to the large thermal mass of the ground, which reduces the temperature extremes experienced by refrigeration systems. Shallow ground temperatures are approximately constant below about four meters and are roughly 10-16°C (50-60°F) degrees which is very close to comfortable indoor room temperatures (Singh and Sharma, 2017; NREL, 2024). This led to the design of heat exchangers that can exchange heat with the ground to reduce the temperature lift associated with heat pump heating and cooling. The simplest design is the u-tube is comprised of a tube going down 30-120 meters (100-400 feet) below the surface where it turns around and returns to the surface. The tube carries the heat transfer fluid (often water and glycol) which is either absorbing heat from the ground for heat pump heating or rejecting heat to the ground for air-conditioning. This allows heat exchange with a medium that is generally warmer in the winter when heating is required and cooler in the summer when cooling is required leading to efficiency gains relative

to air-source systems. These deep bore systems are costly to install due to the specialized equipment needed to drill down in the earth and there are also regulations that require the borehole to be grouted to avoid ground water contamination from the heat transfer fluid.

Other shallow-bore ground-source systems have been developed to lower installation cost by reducing the depth of the system in the ground. Figure 2 shows a few shallow ground heat exchanger designs that can be installed with more readily available equipment. These systems generally require more land area which may not be an option for some installations. The exception to this is the vertical helix heat exchanger design which trades off depth with a wider bore. These bores can have diameters of roughly 0.5 meters, but the helical design allows similar heat transfer area to a deep bore design. Previous research for the shallow-bore helical heat exchanger design has developed modeling tools and performance estimates for this ground-source heat pump design that shows lower energy use than air-source systems in multiple climate zones (Najib et al., 2020).

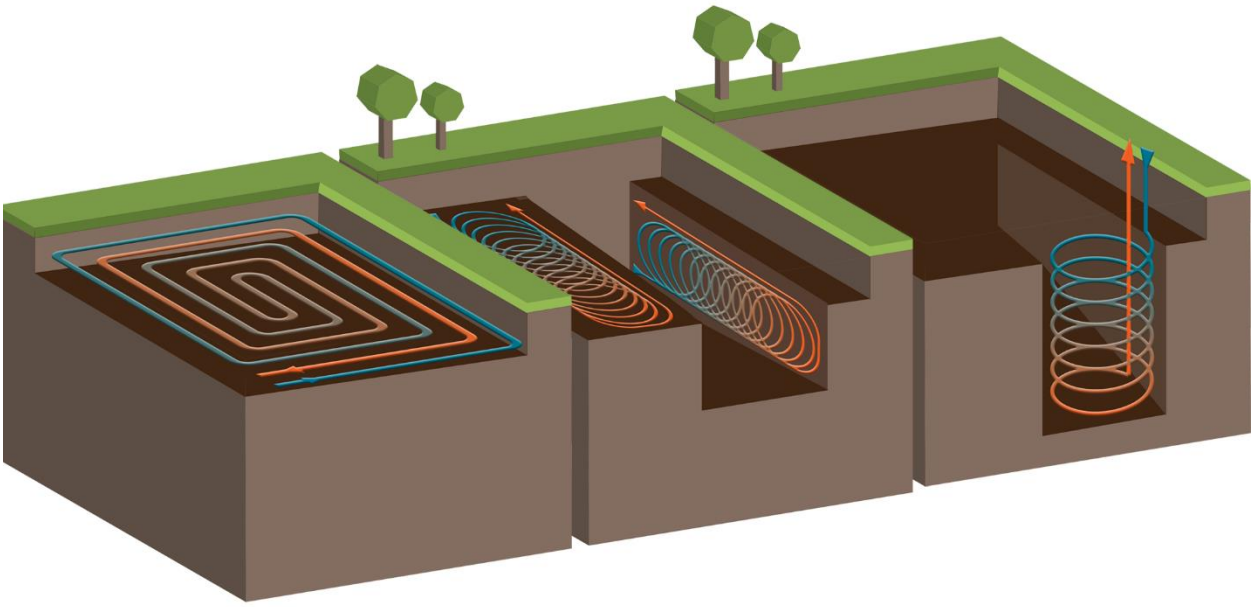

Figure 2. Diagram of several shallow ground heat exchanger designs including snail type, horizontal slinky type, vertical slinky type, and the vertical helix type.

There are also examples of using ponds or rivers as heat sources or sinks for heat pumps. These can be designed as either open loop systems where the water is pumped directly to the heat pump or closed

loop systems where a secondary heat transfer fluid is pumped through a heat exchanger submerged in the water. The water temperature would depend on the source of water or depth of the pond (Spitler and Mitchel, 2016). Surface water heat pumps are largely driven by convenience where the body of water is in proximity of the building, but these strategies can encounter regulatory barriers due to the ecological impact on the water body.

Background

Pool Thermal Model

This thesis focuses on the use of a swimming pool as the heat source and sink for heat pumps. Past research has developed and validated a thermal model of a pool that allows pool temperature to be calculated based on pool characteristics and local weather conditions (Woolley et al., 2011). This model was then used to evaluate the energy savings potential for a pool-coupled air conditioner in multiple California climate zones (Harrington and Modera, 2013) showing a potential for 25-30% reduction in air conditioner energy use. That paper also developed resources for helping determine appropriate pool size for different climate zones and building loads to avoid overheating of the pool. The following section outlines the basic principles of the model, but more detail can be found in the reference papers.

The pool thermal model was based on (Woolley et al., 2011) and simulates several heat transfer mechanisms including solar insolation, evaporation, convection, conduction, and longwave radiation. These heat transfer mechanisms are driven primarily by weather conditions and pool temperature. Other heat flows accounted for but not described below are the impacts of makeup water to replace water lost through evaporation, rain, and heat exchange with the heat pump which is described in more detail in the Heat Pump Performance Modeling section in Chapter 2. The heat transfer into and out of the pool is calculated for each mechanism on an hourly basis to determine the net heating or cooling effect on the pool. Previous testing has shown that it is appropriate to treat the pool as well-mixed with a single effective pool temperature, especially since pool filtering occurs daily (Woolley et al., 2011).

Figure 3 shows a schematic of the pool showing the heat flows included in the model. The boundary condition for the model is the pool water boundary.

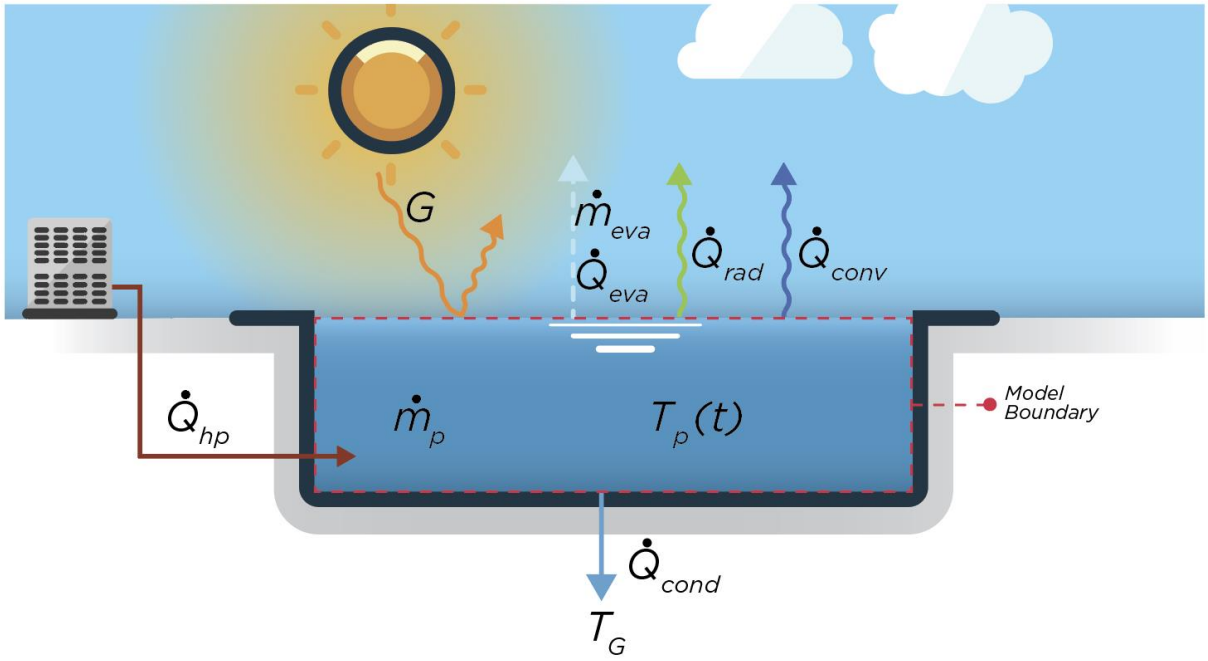

Figure 3. Schematic of pool thermal model showing control volume and heat transfer mechanisms

Solar Insolation

Heat gain from solar radiation is calculated using the global horizontal radiation, absorptivity of the pool water, and a shading factor (Equation 6). The direct and diffuse components of global horizontal radiation are treated differently in the model with the direct portion impacted by shading conditions of the pool. The shading factor is a value between 0-1 (0 used for the condition where there is no shading on the surface and 1 means the entire surface is shaded) and is used to correct the amount of direct solar radiation that is incident on the pool surface.

One adjustment made to the (Woolley et al., 2011) model is the fraction of diffuse radiation that is absorbed by the pool. Hahne and Kubler (Hahne and Kubler, 1994) describe the relationship between solar incident angle on the pool and its impact on absorptance of the pool water. Hahne and Kubler make the assumption that diffuse radiation has an isotropic distribution resulting in an effective incident

angle of 71° and a calculated absorptance of 0.836. A similar analysis for the pool absorptance under direct solar radiation was performed by (Woolley et al., 2011) which accounted for incident angle and resulted in an average absorptance of 0.91.

$$q_{solar} = (G_{direct} \cdot SF \cdot \alpha_{direct}) + (G_{diffuse} \cdot \alpha_{diffuse}) \quad \textit{Equation 6}$$

Where q_{solar} is the heat flux to the pool, G_{direct} is the direct component of global horizontal radiation, $G_{diffuse}$ is the diffuse component of global horizontal radiation, SF is the shading factor, and α is the absorptivity of the pool water.

Longwave Radiation

Longwave radiation was calculated based on radiation between two objects. The pool radiates to an effective sky temperature with an emissivity that was calculated based on ambient temperature, dewpoint, and cloud cover (Equation 7 through Equation 9). On cloudy days the effective sky temperature is much warmer reducing longwave radiation to the sky. In hot dry climates, like California, longwave radiation with the sky is the largest single mechanism for cooling the pool during the summer followed closely be evaporation. The pool was assumed to have an emissivity of 0.96 for this calculation.

$$q_{rad} = \sigma E_w \left[(T_{sky} + 273)^4 - (T_w + 273)^4\right] \quad \textit{Equation 7}$$

$$T_{sky} = (T_a + 273) \cdot \left({E_{sky}}^{0.25}\right) - 273 \quad \textit{Equation 8}$$

$$E_{sky} = \left[0.787 + 0.764 \cdot LOG\left(\frac{T_{dew} + 273}{273}\right)\right]\left[1 + 0.0224 \cdot O_{sky} - 0.0035 \cdot \left({O_{sky}}^2\right) + 0.00028 \cdot \left({O_{sky}}^3\right)\right] \quad \textit{Equation 9}$$

Where q_{rad} is the radiation heat flux emitted from the pool, σ is the Stefan-Boltzmann constant, E_w is the emissivity of the pool water, T_{sky} is the effective sky temperature, T_w is the temperature of the pool water, T_a is the temperature of the ambient air, E_{sky} is the emissivity of the sky, T_{dew} is the dewpoint temperature of the ambient air, and O_{sky} is the cloud cover in tenths. The

calculation does not distinguish between clouds at different altitudes which would have an impact on the effective sky temperature.

Evaporation

Evaporation is driven by differences in partial pressure of water in ambient air and the partial pressure of water in air saturated at the pool temperature. This driving force is multiplied by a mass transfer coefficient that determines the amount of water evaporated in each hour (Equation 10 and Equation 11). While there is no commonly accepted theoretical approach for evaluating the mass transfer coefficient, there is considerable research evaluating mass transfer coefficients for different applications. The coefficient used in the model is based on empirical equations based on evaporation from a free water surface and varies in a similar way that convection heat transfer coefficients vary with surrounding air velocity. This value combined with the heat of vaporization of water gives the thermal energy required to evaporate the water from the pool. Evaporation is one of the primary cooling mechanisms for the pool accounting for nearly half of heat loss during the summer.

$$q_{evap} = -h_{evap} \cdot (e_s - e_a) \qquad \textit{Equation 10}$$

$$h_{evap} = 0.0360 + 0.0250V \qquad \textit{Equation 11}$$

Where q_{evap} is the evaporation heat flux, h_{evap} is the evaporation heat transfer coefficient, e_s is the saturated vapor pressure at the pool temperature, e_a is the ambient air vapor pressure, and V is the wind velocity corrected to a height of three meters.

Convection

Convection was calculated based on the Bowen relationship that associates the convection energy from a pool surface with the evaporation from that surface (Equation 12 and Equation 13). Bowen (Bowen, 1926) considered the diffusion of both heat and mass into a differentially small element of air above the water surface subject to molecular and thermal diffusivity and forced air movement. When no wind speed is present, convection was calculated based on free convection from a surface.

Convection has a relatively small effect on the overall heat balance of the pool accounting for only 2% of the pool cooling during the summer. Convection plays more of a role in the winter when pool conditions are cold relative to air conditions and can even result in condensation causing a heat gain in the pool.

$$B = \frac{q_{conv}}{q_{evap}} = C_B \cdot \frac{p_a}{p_o} \cdot \frac{(T_w - T_a)}{(e_s - e_a)} \qquad \textit{Equation 12}$$

$$q_{conv} = B \cdot q_{evap} \qquad \textit{Equation 13}$$

Where B is the Bowen ratio, C_B is the Bowen coefficient, p_a is the ambient pressure, and p_o is the reference pressure of 1 atmosphere.

Conduction

Conduction was calculated based on a shape factor analysis for a body in an infinite medium outlined in (Incropera, 2007) using Equation 14 through Equation 18. The pool surface is assumed adiabatic for this analysis since the conduction heat flow was calculated only for the interaction between the pool and the ground. Conduction to the ground had the lowest heat transfer impact of all modes accounting for only 1% of the average heat flows.

$$q_{cond} = \frac{1}{2L_c} q_{ss}^* k_{soil} \frac{A_s}{A} (T_{soil} - T_w) \qquad \textit{Equation 14}$$

Where q_{ss}^* using

Table 1. Conduction shape factors based on aspect ratio of pool volume

d/D	q_{ss}^*
0.1	0.943
1.0	0.956
2.0	0.961

$$A_s = 2D^2 + 4Dd \qquad \textit{Equation 15}$$

$$d = 2d_{poolavg}$$ *Equation 16*

$$L_c = (A_s/4\pi)^{0.5}$$ *Equation 17*

$$D = (A_{cond} + d^2)^{0.5} - d$$ *Equation 18*

Where q_{cond} is the conduction heat flux from the pool to the ground, L_c is the characteristic length, q^*_{ss} is the shape factor, k_{soil} is the soil conductivity, A_s is the surface are used for shape factor calculations, A is the pool water surface area, T_{soil} is the soil temperature, d is double the average pool depth, and L_c is the characteristic length.

Previous Field Studies

An earlier study performed a field demonstration of this approach on a hotel swimming pool in San Diego, CA, showing a 29% reduction in natural gas used to heat the pool and 5% air conditioning energy savings (Harrington et al., 2015). There was no prior research identified that evaluated heat pump heating using a swimming pool as a heat source in the winter.

The prior research related to using a swimming pool as a heat sink for air conditioning highlighted the potential for energy savings in different applications including for offsetting pool heating energy use and improving air conditioner efficiency. Prior field studies of the technology relied on custom-designed systems to facilitate the process. A commercial product (FPH) that allows an existing air conditioner or heat pump to be modified for rejecting waste heat to a swimming pool was identified, and field studies of the technology were funded by the California Statewide Emerging Technologies research program. The CalNEXT project is evaluating the energy savings potential of the retrofit system as well as developing an analysis tool that allows utility program managers to estimate savings in different applications.

Thesis Overview

The objectives of this thesis are to:

- Measure performance of an air conditioner employing heat rejection to a pool with the FPH technology relative to the existing baseline air conditioning equipment
- Validate the pool thermal model used for predicting the performance of the technology
- Develop a tool for estimating energy savings that can be used in utility programs
- Assess the potential of the technology when used as a heat source for a heat pump

Chapter 2 provides the details of the experimental methods for the field test of the pool-coupled air conditioning technology, and the modeling effort to evaluate the impact of the technology in different applications in California. Chapter 3 presents the results of both the field test and parametric modeling for the technology as it is currently applied, as well as investigation of its potential use as a heat source for heat pump systems. Finally, Chapter 4 provides conclusions and recommendations for the technology for applications in California.

Chapter 2. Experimental and Modeling Methods

Experimental Methods

The FPH technology was installed on two residential swimming pools in California. The field tests measured the air conditioner performance when rejecting heat to the swimming pool compared to the performance of the existing baseline air conditioning equipment. The installation process was documented to evaluate the cost and complexity of the retrofit. A pool thermal model was validated based on the results of the field test, and ultimately used to predict performance of other potential installations. This provides energy efficiency program administrators with a tool for determining deemed energy savings based on information provided about the potential site.

Technology Description

The FPH technology demonstrated in the project is a secondary condenser that is installed beside the existing condenser unit (Figure 4). A controller can direct refrigerant to the existing air-source condenser or FPH condenser using a three-way refrigerant valve depending on the pool temperature conditions. The controls allow for management of pool temperature by switching to the existing air-source condenser when pool temperatures meet or exceed the setpoint temperature. The resident can adjust this temperature to their desired comfort. The controls allow the use of the existing air conditioning condenser when pool temperatures exceed the setpoint avoiding the issue of overheating the pool. When a call for cooling occurs, the air conditioner starts in its traditional mode and a signal is sent to the pool pump to direct water to the FPH. After a preset delay to allow fresh pool water into the plumbing, the pool water temperature is measured, and it is determined whether the pool is below the setpoint temperature. If the pool temperature is below the setpoint, the system switches the refrigerant valve to the pool-source condenser and shuts down the condenser fan. The controller continues to monitor pool temperature and may switch back to the air-source condenser if the setpoint is met.

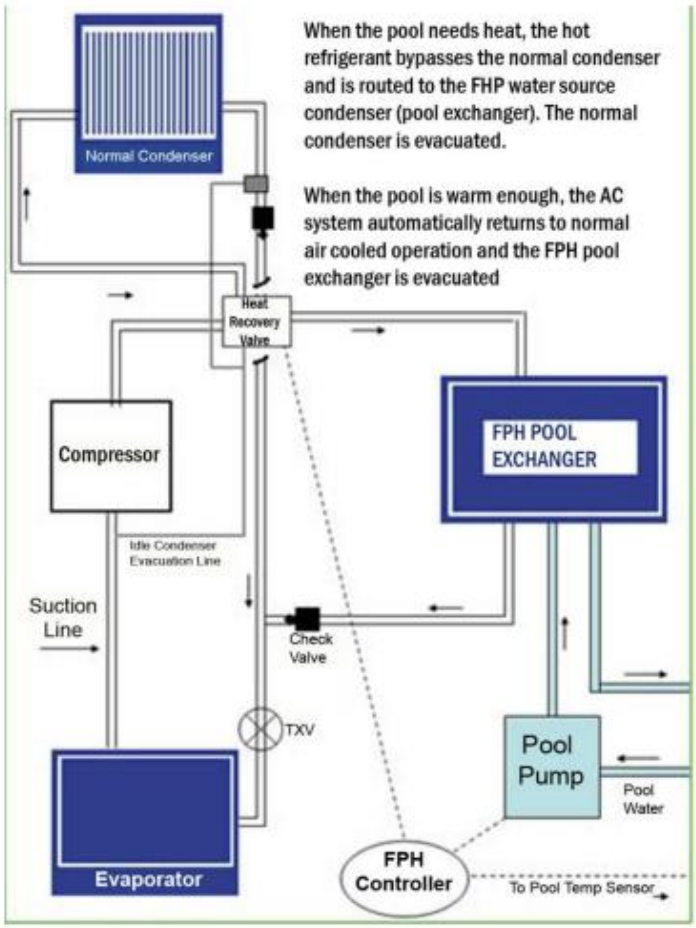

Figure 4: Schematic of FPH integration with existing air conditioning unit (source: HotSpot Energy)

Installation of FPH

The installation of the technology was challenging due to the number of field-installed components and lack of prior experience by the contractor installing this technology. The components included: a three-way valve, two check valves, a solenoid valve, a restrictor, and refrigerant receiver. Figure 5 provides a diagram of where the components are placed in the refrigerant circuit, and Figure 6 shows photos of the installed components.

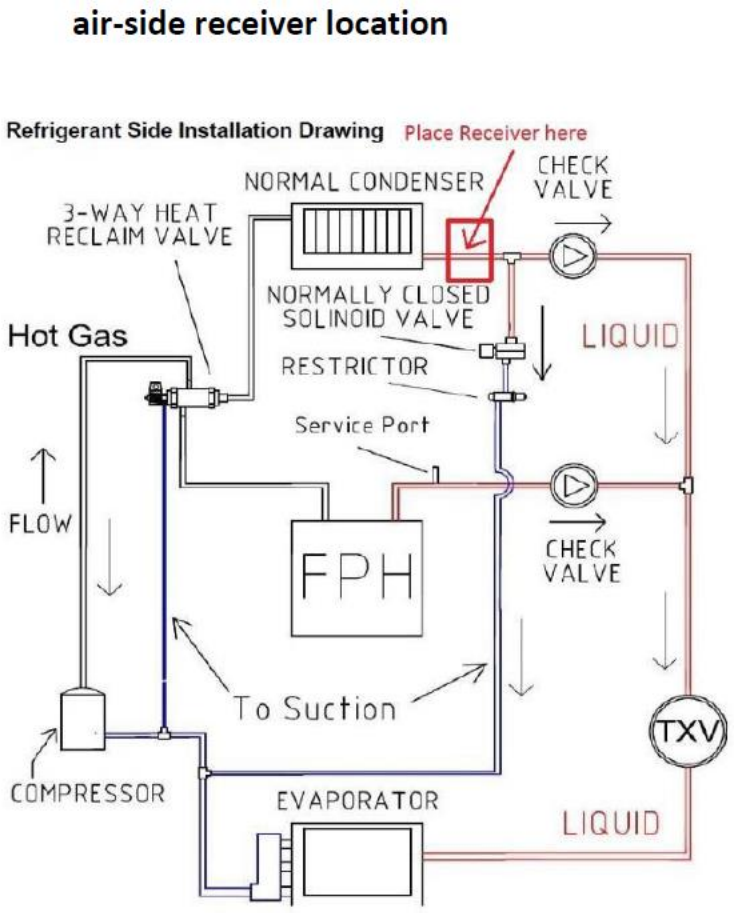

Figure 5. Diagram of refrigerant component placement (source: HotSpot Energy)

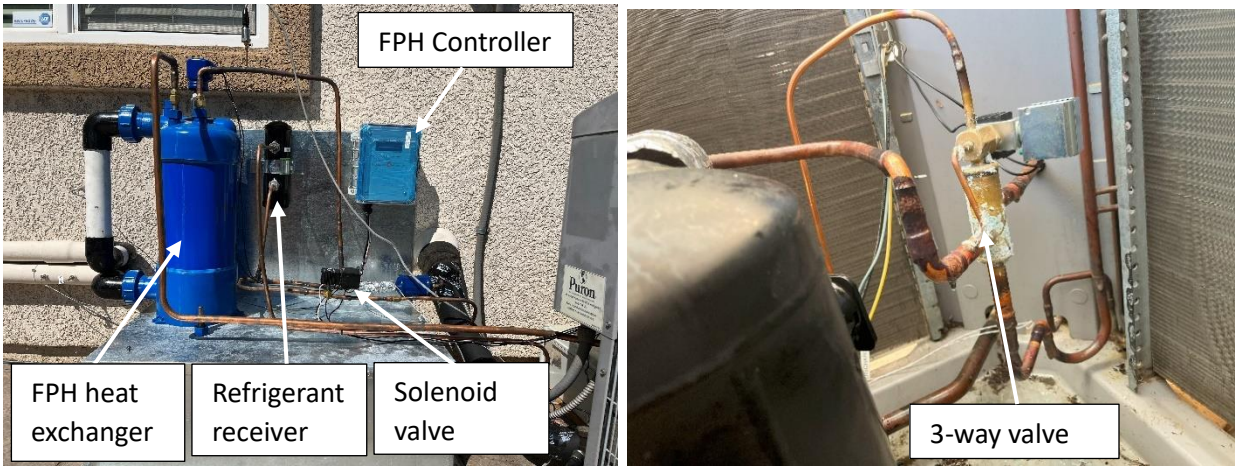

Figure 6. Photos of refrigerant components installed for FPH system

After installing the refrigerant components, the controller was installed. The controller is powered by a 24 VAC power transformer mounted inside the electrical cabinet of the air conditioner and pulling

power from the 240 VAC power supply to the unit. The thermistor is installed on the water line entering the water-to-refrigerant heat exchanger to sense pool temperature during operation. The controller has 24 VAC output signals to the refrigerant solenoid valve, the relay to cut power to the condenser fan motor, and the three-way refrigerant valve to change the mode of the system from air-source to pool-source.

The integration with the pool pumping system depends on the pool pump controls. For the field demonstrations performed for this project, the control scheme required simulating a solar thermal heating operation by connecting a fixed resistor signal to the thermistor input for the solar thermal system on the pool controller. The pool controller interprets the resistance value as a temperature in a solar thermal system, and if the temperature exceeds the pool temperature by a set amount it will trigger the pool pump to send water to the FPH refrigerant-to-water heat exchanger. A relay was installed to switch between two resistor values depending on the status of the air conditioner. When there is no air conditioning operation, a 15k Ohm resistor is used to simulate the solar thermistor measuring a colder water temperature of 15.6°C (60°F), and when the air conditioning starts a 5k Ohm resistor is used to simulate a warmer water temperature of 40.6°C (105°F).

Methodology & Approach

Instrumentation was installed to measure the performance parameters of the air conditioning systems, weather conditions, the heat delivered to the pool, and the power draw of the pool pump. The ratio of capacity to power draw of the air conditioner is defined as the coefficient of performance (COP) and describes the efficiency of the system. There are several parameters that impact the COP of an air conditioner including the outdoor air or pool water temperature, as well as the indoor air conditions. Data were collected to characterize the efficiency of the air conditioning system when rejecting heat to pool water and to outdoor air. A comparison was made between the efficiency of the cooling operation when rejecting heat to the pool versus the cooling operation when rejecting to outdoor air. This allowed

for the determination of the performance improvement of the technology.

The measurement period occurred over two cooling seasons. Baseline data was collected on the air conditioning system before the retrofit which provided the basis for energy savings calculations. After collecting data on the existing air conditioner performance across a range of outdoor air conditions, the FPH technology was installed, and post-retrofit performance data collection began.

Test Sites

The sites for the project were single-family residences in West Sacramento, CA (Figure 7). One pool was heavily shaded located in a north-facing yard while the other had minimal shading in a south-facing yard. The baseline systems were monitored for a period of about three months before the retrofit occurred. This allowed measurement of the baseline performance across a range of outdoor air temperatures. The FPH system retrofit occurred on August 16th, 2024, at which point the post-retrofit monitoring period began and continued for about nine weeks before air conditioner use was limited by cooler weather conditions. The installation required the following steps: 1) remove the refrigerant from the air conditioner, 2) add refrigerant components including a three-way valve, refrigerant solenoid valves, check valves, liquid line receiver, and water-to-refrigerant heat exchanger, install condenser fan relay, 3) recharging the unit, and 4) install the controller. No additional refrigerant was required when installing the FPH technology, however a low charge was discovered at one of the sites when performing the retrofit that required additional refrigerant charge to be added. The retrofit does not require additional refrigerant volume due to the refrigerant circuit design. The solenoid and restrictor installed allows refrigerant trapped in the air-source condenser when switching to pool-source mode to migrate back to the suction side of the compressor. Furthermore, the pool-source condenser is sized to match the approximate volume of the air-source condenser to avoid a mismatch in the required refrigerant charge.

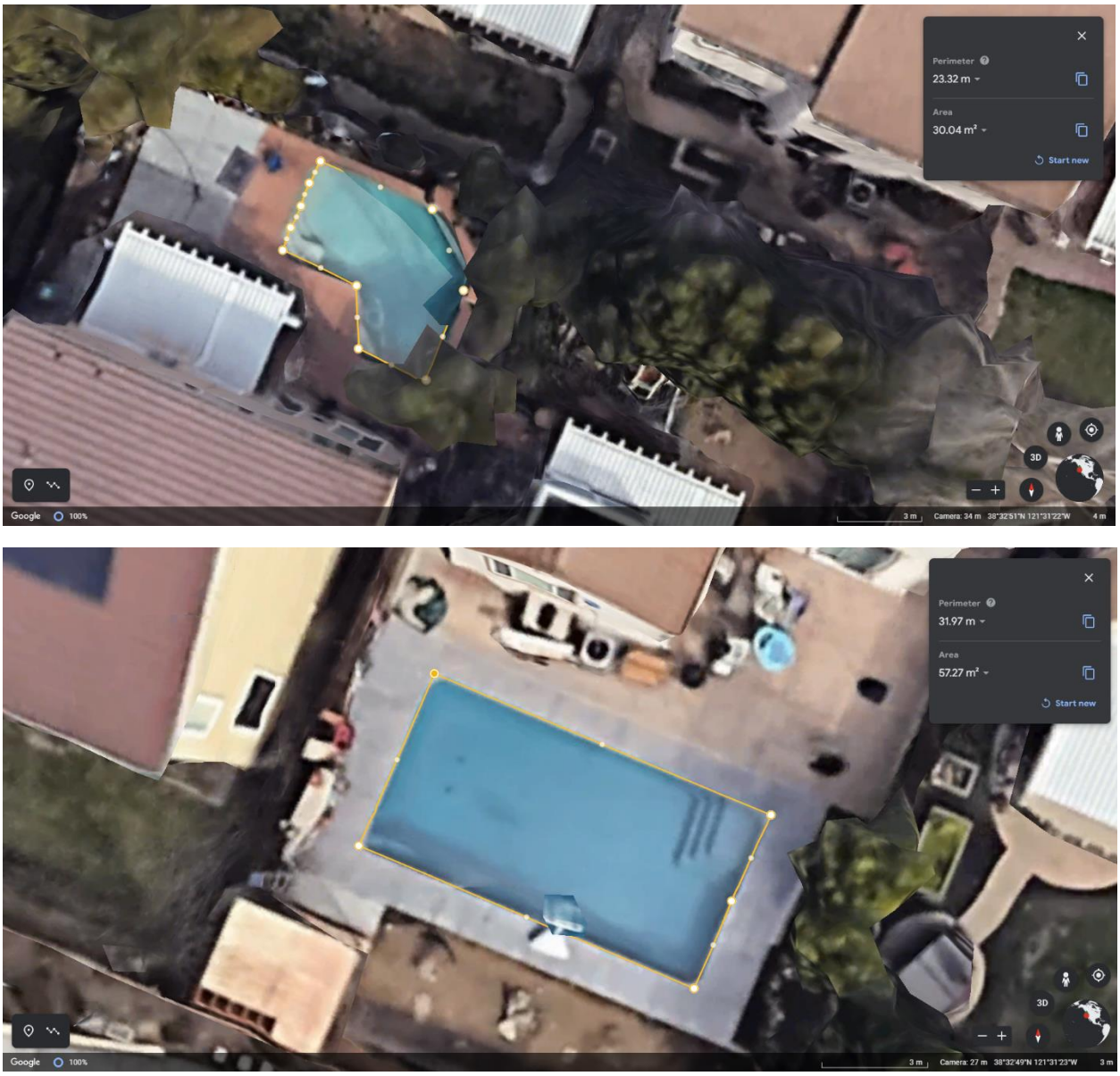

Figure 7: Residences used for testing FPH product. The pool in the top image is heavily shaded in a north-facing yard, and the pool in the bottom of image is minimally shaded in a south-facing yard.

Instrumentation Plan

A general schematic of the system components and measurement points is shown in Figure 8. This outlines the plumbing connections that connect the FPH water-to-refrigerant heat exchanger to the pool system as well as the relative location of various sensors. Note that some of the instruments are only required for the retrofit period (i.e. water flow and temperatures at the pool-source condenser) and will be added during the technology installation. These include the pool water flow, and temperatures

entering and exiting the water-to-refrigerant heat exchanger. The specific sensors installed our outlined in Table 2 below.

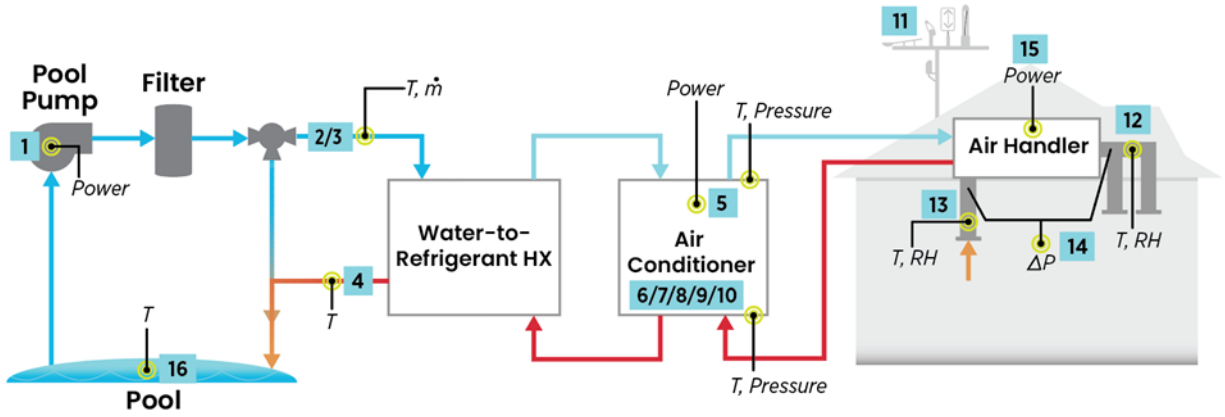

Figure 8: Instrumentation schematic showing points of measurement (T – temperature, $\dot{m}$ – flowrate, RH- relative humidity, ΔP – differential pressure)

Pool Heating

The heat absorbed by the pool from the air conditioner was measured by collecting data on the temperature entering and exiting the water-to-refrigerant heat exchanger of the FPH combined with the water flow rate. This should agree with the air conditioner (AC) performance data collected (pool heating = AC cooling capacity + AC electrical power – thermal losses).

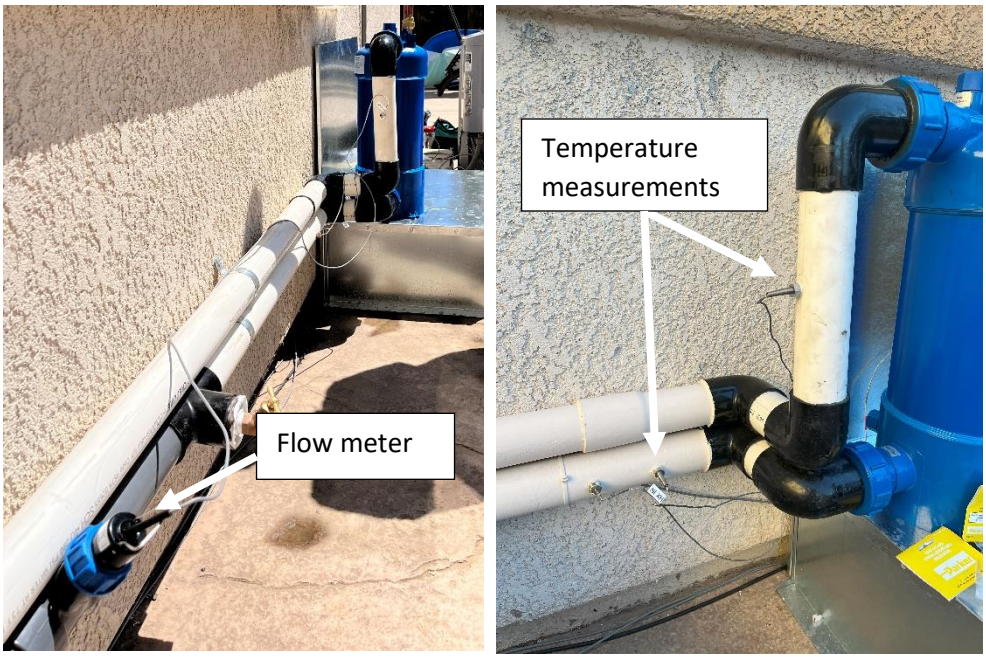

Figure 9. Instrumentation installed to measure heat transferred to pool from air conditioner

Air Conditioner Performance

Cooling capacity was determined by monitoring the temperature and humidity of air at the supply and return of the air handler. The airflow of the air conditioner was mapped to a differential pressure across the air handler fan and calibrated with a tracer gas airflow measurement device. The tracer gas system injects a known mass of CO_2 in the air stream and measures the change in CO_2 concentration between upstream and downstream from the injection allowing the volume flow of air to be determined. The power consumed by both the outdoor and indoor units was monitored and used along with the cooling capacity to determine the overall system performance. Pool pumping power was also considered when evaluating air conditioner performance.

Pool Pumping

Pool pump power was monitored to determine what impact the new system had on overall pumping power use. The heat exchanger in the FPH does cause additional pressure drop to the existing filtering loop but this effect had to be modeled due to the limitations of the field data collected. It could be argued that pool pumping power could be attributed to the standard pool filtering process, but due to

the control method employed by the retrofit system, the pumping schedule needed to be adjusted to maximize the time the system rejected heat to the pool which included running the pump during peak electricity hours. This is discussed in more detail in the results.

Weather Data

Weather data was collected near the installations to monitor ambient weather conditions including air temperature and humidity, wind speed and direction, barometric pressure, and precipitation. Outdoor temperature data was used to map the performance of the air conditioner while the other parameters were used to validate the pool thermal model used for simulating performance.

Data Collection and Remote Monitoring

A central data acquisition system was used to record the measurements (Figure 10). All data was remotely transferred to a UC Davis FTP server once each day to monitor the system.

Figure 10. Data acquisition enclosure in attic of Site 2

This allowed data to be evaluated for quality to assure everything was working appropriately. Table 2 shows the instrumentation used for each measurement outlined in Figure 8.

Table 2: Table of Instruments

Measurement #	Measurement Type	Manufacturer and Model #	Accuracy	Signal Type
1	Pool Pump Power	Dent Powerscout 3	±1%	RS-485
2	Pool Water Flowrate	Omega FP5600	±1% of reading	Pulse
3	Water Temperature Entering FPH	Omega TH-44006	±0.2°C	Ohms
4	Water Temperature Exiting FPH	Omega TH-44006	±0.2°C	Ohms
5	Condenser Power	Dent Powerscout 3	±1%	RS-485
6	Compressor Discharge Pressure	Climacheck S22	±1%	1-5 VDC
7	Compressor Discharge Temperature	Omega TH-44006	±0.2°C	Ohms
8	Compressor Suction Pressure	Climacheck S22	±1%	1-5 VDC
9	Compressor Suction Temperature	Omega TH-44006	±0.2°C	Ohms
10	Condenser Outlet Temperature	Omega TH-44006	±0.2°C	Ohms
11	Outdoor Air Temperature	Vaisala WXT520	±0.3°C	RS-485
11	Outdoor Air Humidity	Vaisala WXT520	±3%	RS-485
11	Wind Speed	Vaisala WXT520	±3% at 10 m/s	RS-485
11	Wind Direction	Vaisala WXT520	±3°	RS-485
11	Precipitation	Vaisala WXT520	<5%	RS-485
11	Barometric Pressure	Vaisala WXT520	±50 Pa	RS-485
12	Supply Air Temperature	Vaisala HUMICAP HMP110	±0.2°C	0-10 VDC
12	Supply Air Humidity	Vaisala HUMICAP HMP110	±1.7%	0-10 VDC
13	Return Air Temperature	Vaisala HUMICAP HMP110	±0.2°C	0-10 VDC
13	Return Air Humidity	Vaisala HUMICAP HMP110	±1.7%	0-10 VDC

14	Air Handler External Static Pressure	Dwyer 668	±2.5 Pa	4-20mA
15	Air Handler Power	Dent Powerscout 3	±1%	RS-485
16	Pool Temperature	HOBO TidbiT mX	±0.2°C	Internal Logging

Data Analysis

The data collected served two primary purposes. One was to evaluate the energy performance of the retrofit system compared to the baseline equipment, and the other was to validate the pool thermal model used to predict performance of the technology in other applications. For the energy savings analysis, the key parameters are air conditioning capacity and power use. For the pool thermal model, the key parameters are physical characteristics of the pool, weather conditions, and heat added to the pool through the heat exchange with the air conditioning equipment.

Air Conditioner Capacity

Air conditioner capacity is a measurement of the cooling provided to the home. Both homes in the study had a two-zone, ducted air conditioning system serving upstairs and downstairs zones that could operate in three different modes. A one-time measurement of air volume flow was conducted at each test site with a tracer-gas airflow measurement tool in each of the different operating modes for the system (i.e. upstairs only, downstairs only, and both upstairs and downstairs modes). Pressure sensors were installed at different locations in the duct system to identify which mode was active and allowing the appropriate airflow to be selected. The mass flow rate was determined from the volumetric flow rate and air density according to Equation 19, and the measured volumetric flows are presented inTable 3. Volumetric flow rates measured at both test sites in each mode of operation Table 3.

$$\dot{m} = \rho_{air} * \dot{V}_{air} \qquad \textit{Equation 19}$$

Table 3. Volumetric flow rates measured at both test sites in each mode of operation

	Upstairs	Downstairs	Both
Site 1	0.9005 m^3/s (1,908 CFM)	0.8245 (1,747)	0.9576 (2,029)
Site 2	0.8151 m^3/s (1,727 CFM)	0.8448 m^3/s (1,790 CFM)	0.9080 m^3/s (1,924 CFM)

Temperature and humidity measurements were collected in the return and supply duct to and combined with Equation 19 to evaluate the capacity delivered. The capacity was calculated according to Equation 20, where the enthalpy, h, was determined from psychrometric functions using measured temperature and relative humidity.

$$Q_{EvapCoil} = \dot{m}_{air} * \left[h(T, RH)_{return} - h(T, RH)_{supply} \right] \quad \textit{Equation 20}$$

Coefficient of Performance

The COP was calculated as:

$$COP = Q_{EvapCoil}/P_{AC} \quad \textit{Equation 21}$$

Where air conditioning equipment power, P_{AC}, included both the indoor air handler and outdoor condenser unit.

Heat Delivered to Pool

To calculate the heating provided to the pool by the air conditioner, the water temperature entering and exiting the water-to-refrigerant heat exchanger was used along with the water flow rate. A primary assumption in Equation 22 is that there is negligible heat loss or gain in the pipes between the water-source-condenser and the pool.

$$q_{CondCoil/Pool} = \rho_{pool} * \dot{V}_{\text{pool}} * c_{p_{pool}} * (T_{HX,out} - T_{HX,in}) \quad \textit{Equation 22}$$

Uncertainty Analysis

The uncertainty of the calculated results shown above are provided in Table 4. Uncertainties were calculated by propagating the errors of each individual measured value using the accuracy of each measurement outlined in Table 2. The error propagation method used is based on a root-sum-squared

method accounting for each elemental error in the calculation. Uncertainties in dependent parameters were estimated using the propagation of errors method (Figliola and Beasley, 2006) and performed in Engineering Equation Solver (F-Chart Inc.) A representative sample of data was used for the analysis to evaluate the uncertainty while the air conditioner was operating. The results show that the measurement uncertainty of air conditioner capacity, COP, and heating delivered to the pool are accurate to within 10%, 10%, and 20%, respectively. The uncertainty in heating delivered to the pool is largest due to the relatively small temperature change across the FPH heat exchanger.

Table 4. Uncertainty in calculated results

Calculated Value	Uncertainty in Calculated Value
$\dot{m}$	1.078 ±0.0323 [kg/s]
$q_{EvapCoil}$	12.62 ±1.246 [kW]
COP	3.713 ±0.3675
$q_{CondCoil/Pool}$	14.72 ±2.978 [kW]

Modeling Methods

This project is largely focused on developing and validating a simulation tool that can allow accurate estimates of the energy savings that can be expected from the pool-coupled air conditioning or heat pump system. The pool thermal model is a key component for making accurate energy savings estimates. As noted previously, the temperature of the heat sink/source for the heat pump system has significant influence on the performance of the system including both cooling or heating capacity delivered and power draw. For air-source systems, this requires knowledge of the ambient temperature and humidity conditions for the climate of interest which is widely available and frequently updated. For the pool-source system, this requires simulating accurate pool temperatures for the simulation period. Pool temperatures are influenced by local climate, physical characteristics including surface area and volume, shading of the pool and wind obstruction from nearby objects, and heat exchange with the heat pump.

Pool Thermal Model Inputs

An overview of the pool model details was provided in Chapter 1 including the various heat flows between the pool and its surroundings. This section describes the input data used for the model including how global horizontal solar insolation from weather data was broken into direct and diffuse components. For field validation of the thermal model, solar radiation data was collected from a weather station proximate to the field test site (CIMIS, 2024) and the direct and diffuse components were estimated using the DISC model developed by the National Renewable Energy Laboratory (NREL) that uses the specific longitude and latitude of the location (Maxwell, 1987). For the model simulations, the direct and diffuse components of radiation are included in the Typical Meteorological Year weather (TMY) data (Vignola et al., 2013). The direct component was adjusted based on shading parameters of the site while the diffuse component was not. Multiple shading parameters are considered from highly shaded to low shade which provides an hourly fractional shading of the pool. These shading factors were developed based on observations of residential pools in previous studies and are only approximations to evaluate the sensitivity of this parameter on performance results. Table 5 shows the shading factors that were used for the simulations which considered three shading levels for the pools. The fraction of the pool surface that is shaded reduces the direct radiation incident on the pool proportionally.

Table 5. Hourly shading factors considered for simulations

Hour	Low Shading	Some Shading	High Shading
0	0	0	0
1	0	0	0
2	0	0	0
3	0	0	0
4	0	0	0
5	0	0	0
6	0	0	0
7	0.25	0.25	0.25
8	0.5	0.5	0.25
9	0.75	0.5	0.5

10	1	0.75	0.5
11	1	1	0.75
12	1	1	1
13	1	1	1
14	1	0.75	0.75
15	1	0.75	0.5
16	0.75	0.5	0.5
17	0.5	0.5	0.25
18	0.25	0.25	0.25
19	0	0	0
20	0	0	0
21	0	0	0
22	0	0	0
23	0	0	0

Another component of the model is the building cooling and heating loads that were used to calculate the energy use of the conditioning equipment as well as have influence on the pool temperature condition. Building loads are highly variable which makes accurate predictions challenging. The model presented here considers multiple prototypical building types to simulate the expected load in a particular instance but could be expanded to other building types in the future.

Lastly, the heat pump model must also account for differences in performance between one heat pump and another. Heat pump performance has improved as technology changes and due to efficiency mandates from regulatory agencies including the U.S. Department of Energy. Again, obtaining detailed performance data for each potential installation is not feasible so the model presented here considers multiple heat pump performance parameters depending on the standardized efficiency rating of the equipment utilized.

Building Load Simulation

EnergyPlus (DOE, 2024) modeling software was used to generate building heating and cooling loads for use as inputs to the pool thermal model. EnergyPlus is an established whole building energy modeling software developed and maintained by NREL and funded by the DOE. Two residential building types

were considered for estimating the performance of the pool-coupled heat pump system. One was an older one-story home based on information from the Mayfair Central Valley Research Home (Proctor Engineering, 2013) which is a single-family home built in 1953. The second model was a two-story, single-family home meeting the 2006 International Energy Conservation Code (ICC, 2006) recommendations for Climate Zone 3. These models were chosen to provide two reasonable load profiles for single-family homes in California. The model allows more representative load profiles to be used for specific applications. For each model, cooling and heating loads are generated for simulating with the pool heat pump system in each of the 16 California Climate zones. Descriptions of each model are included in the sections below.

One-Story Model

A model representing a smaller single-family home (872 ft^2) with building envelope properties representing an older vintage home was created in EnergyPlus 23.2. The construction of the building shell was modeled to represent the as-built construction of the Mayfair house (Figure 11). This house is meant to be representative of an older vintage home on a raised foundation with moderate levels of insulation in the wall and attic.

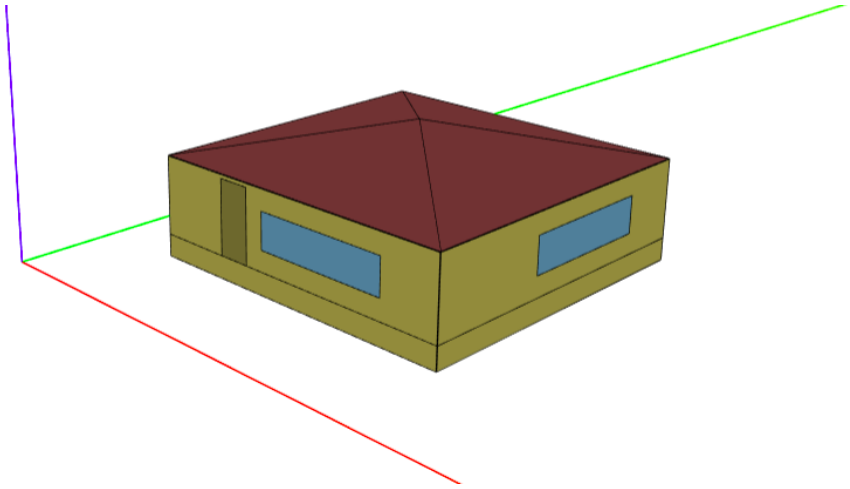

Figure 11. Three-dimensional rendering of the Mayfair model

The key thermal properties of the opaque surfaces of the building envelope were based on a survey conducted on insulation levels in existing homes by the California Energy Commission (Miller and Griffin,

1986). It is common for older single-pane windows to get replaced as part of the general maintenance of a home, so it was assumed that the windows meet the 2006 IECC requirements. Table 6 summarizes these key model input variables including the thermal properties of the windows including Solar Heat Gain Coefficient (SHGC) which provides the fraction of solar radiation that is transmitted, and U-Factor which is a measurement of the conductivity of the window unit including the frame, and wall and ceiling insulation levels. EnergyPlus uses a 1-dimensional heat transfer model to approximate heat flows through the building envelope so the actual input values for the opaque surfaces differ slightly from the values reported in Table 6 to account for thermal bridging of the studs in a wall assembly.

Table 6. Mayfair model building envelope thermal properties

Fenestration U-Factor	Glazed Fenestration SHGC	Ceiling U-Factor	Wall U-Factor
W/m-K (h-ft^2-F/Btu)		W/m-K (h-ft^2-F/Btu)	W/m-K (h-ft^2-F/Btu)
3.69 (0.650)	0.40	0.351 (0.062)	0.644 (0.113)

Two-Story Model

A model representing two-story single-family home meeting the 2006 IECC was also simulated. This model was based on a DOE prototype single-family residential home with a conditioned floor area of 2,400 ft^2. The home is representative of a newer vintage home with higher levels of insulation relative to the one-story model. Table 7 provides a summary of some of the key performance characteristics of the home.

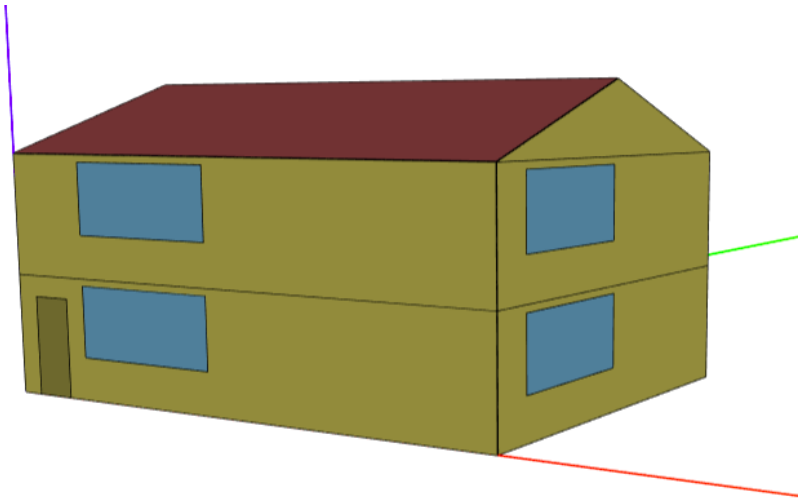

Figure 12. Three-dimensional rendering of Title 24 new construction model

Table 7. Two-story model building envelope thermal properties

Fenestration U-Factor	Glazed Fenestration SHGC	Ceiling U-Factor	Wall U-Factor
W/m-K (h-ft^2-F/Btu)		W/m-K (h-ft^2-F/Btu)	W/m-K (h-ft^2-F/Btu)
3.69 (0.650)	0.33	0.213 (0.038)	0.532 (0.094)

Meteorological Conditions

The CEC has divided California into 16 distinct climate regions for the purposes of developing appropriate building codes based on a particular climate (Figure 13). The simulation tool allows the pool-source heat pump to be simulated in any of the 16 California climate zones (CACZ) depending on the location of the installation using TMY data. The weather conditions for a particular simulation are used for both the pool thermal model and the building load model.

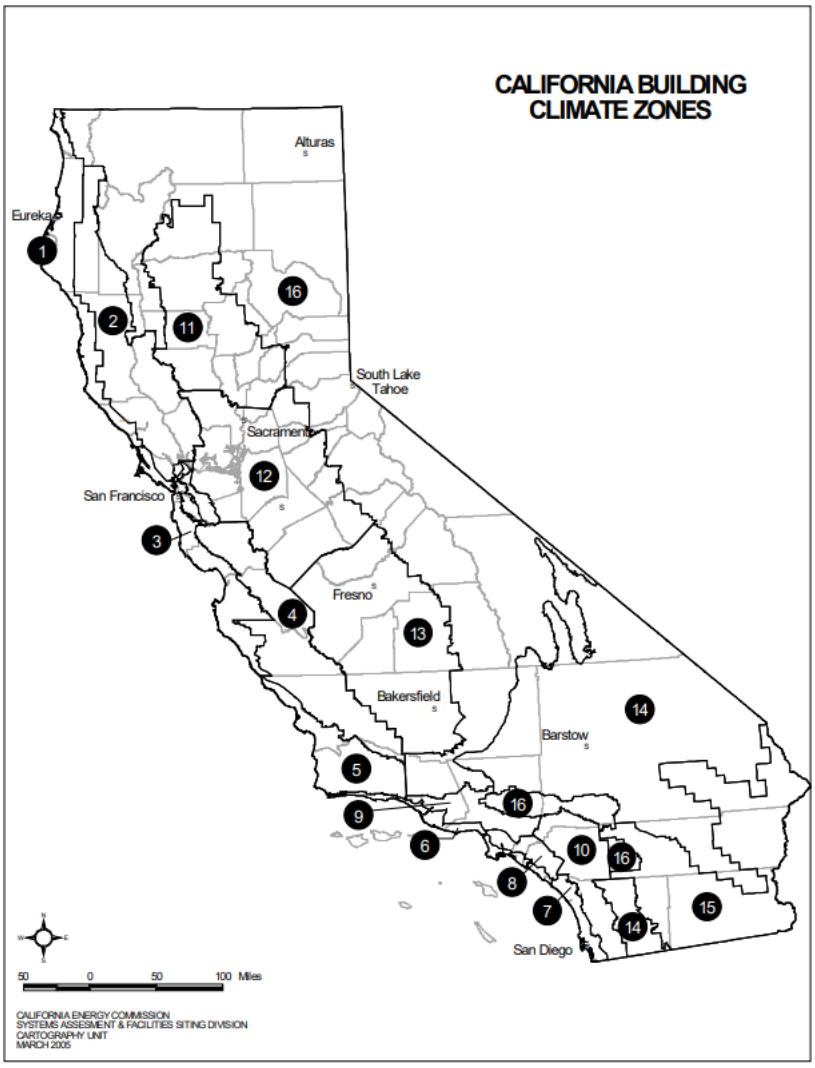

Figure 13. California Climate Zone map (source: CEC Title 24 Residential Compliance Manual)

Heat Pump Performance Modeling

The pool-source heat pump system impacts the refrigeration cycle performance in two key ways relative to the air-source operation. One is that the temperature conditions of the pool can be very different from the temperature conditions of ambient air, and the other is that the heat exchanger fluid is changing from air to water. A typical condenser design strategy is to target a particular temperature difference between the fluid exiting the heat exchanger and the refrigerant condensing temperature, which for air-source condensers is typically 11°C (20°F) and water-cooled condensers is 6°C (10°F) (Smith and Parmenter (2016). This approach suggests that using water as the heat transfer fluid for a condenser can result in lower condensing temperatures reducing the energy required from the compressor. Data

collected on one of the air conditioners in this project showed a 1.5% reduction in COP for every one-degree Fahrenheit increase in outdoor air conditions.

The field data collected in this project did show that the pool-source mode operated at similar COPs as the air-source at slightly elevated temperatures. The impact was lower than the general rule suggested by Smith and Parmenter (2016). Figure 14 shows a plot of the performance difference between pool-source and air-source modes compared to the temperature difference between the pool and air. This trend shows the COPs in the two modes being the same when pool temperatures are about 1.8°C warmer than the air temperature. This demonstrates the improved heat transfer performance of the pool-refrigerant condenser versus the air-refrigerant condenser.

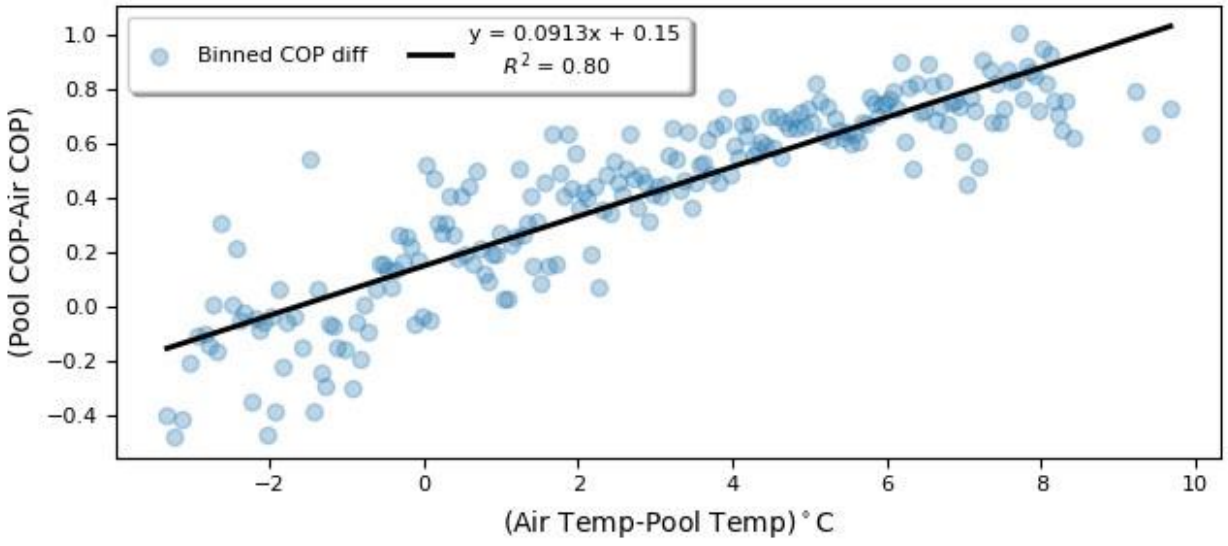

Figure 14. Performance comparison between pool-source and air-source modes relative to the temperature difference between the pool and the air.

For the model tool, a heat pump curve describing the efficiency (COP) of the system relative to the heat sink/source temperature was used to predict energy use to meet a modeled building load using Equation 21.

$$P_{HP} = \frac{Q_{load}}{COP(T)} \qquad \textit{Equation 23}$$

Where P_{AC} (W) is the heat pump electricity power draw, Q_{load} (W) is the building thermal load, and

COP(T) is the COP as a function of sink/source temperature. The efficiency curves will change depending on many factors including the specific equipment, installation, and maintenance of a heat pump. The current model allows a selection of different heat pump curves based on their rated performance. The rated performance is based on required testing outlined by Air-Conditioning, Heating, and Refrigeration Institute (AHRI, 2023) standard 210/240. Generic curves are included for heat pumps with the rated performance outlined in Table 8. These performance selections were based on minimum efficiency requirements over the past 15 years (EIA 2019) to cover a range of system types installed. Each equipment type in Table 8 gives the year in which that minimum efficiency was mandated by DOE in parenthesis. The performance data does not exactly match the minimum requirement but is intended to be representative of equipment installed during those periods. The efficiency ratings are provided in seasonal energy efficiency ratio (SEER) and heating seasonal performance factor (HSPF) for heat pumps. SEER and HSPF are performance metrics that use the rated performance at different conditions to estimate the average efficiency of a heat pump in cooling and heating modes, respectively. The performance of the heat pump at the different conditions are weighted to account for the number of hours a system is expected to run at moderate outdoor conditions and more extreme conditions. This process is standardized across heat pump manufacturers by AHRI.

Table 8. Performance ratings used for heat pump selection in model

Equipment	SEER	HSPF
Low Efficiency (2006)	10	7.0
Medium Efficiency (2015)	13	7.7
High Efficiency (2023)	15	8.5

Performance curves were generated using data provided by the manufacturers for heat pumps and air conditioners meeting the performance ratings outlined in Table 8. The performance curves provide the

COP(T) function used in Equation 23 to evaluate the energy use of the heat pump. An assumed indoor condition of 23.9°C (75°F) dry-bulb (DB) and a 17.2°C (63°F) wet-bulb (WB) temperature for cooling was used for generating the curves which matched the setpoints used in the building energy models. In addition, the cooling performance was based on an airflow rate of 0.189 m^3/s (400 cfm) per 3.52 kW (12,000 Btu/hr) of capacity. The performance curves used for the modeling are provided in Figure 15. The performance data for heat pump cooling was taken from a Carrier 38TKB series air conditioner for the 10 SEER and a Goodman GSX series air conditioner for the 13 SEER and 15 SEER.

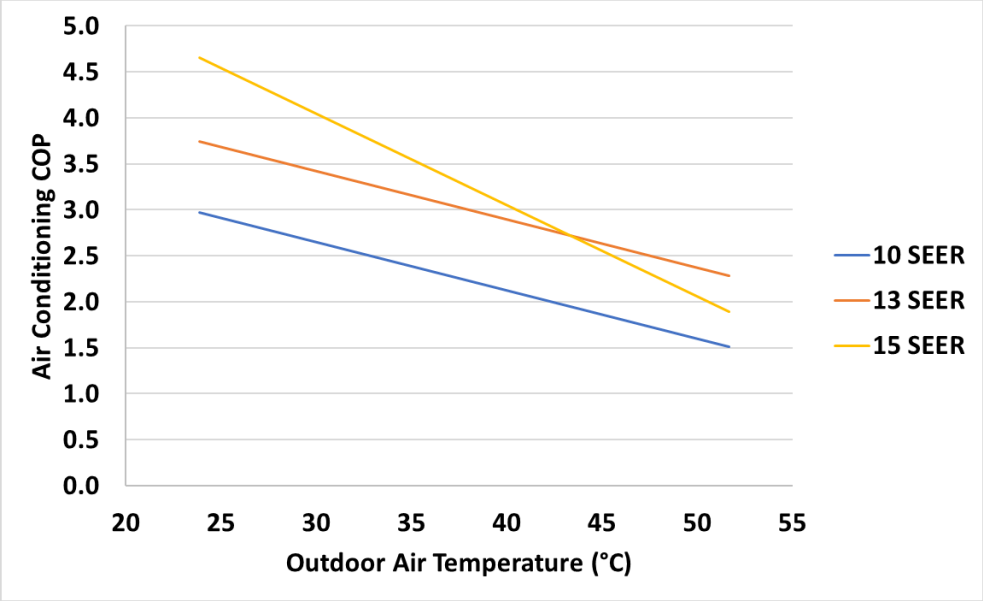

Figure 15. Performance curves used to calculate air conditioner energy use of heat pump simulations

A similar process was used for generating COP(T) curves for heat pump heating. For heating, the indoor condition was 21.1°C (70°F) DB. The outdoor coil WB temperatures were not published other than for the AHRI standard conditions of 8.3°C /6.1°C (47°F/43°F) (DB/WB) and -8.3°C /-9.4°C (17°F/15°F) (DB/WB). In addition, the effect of supplemental electric heat is not included in the curves. Supplemental heaters are used during defrost cycles and during peak conditions where the heat pump cannot meet the house load. The use of supplemental heat in an actual install would result in lower heat loads being extracted from the pool. Since the load served by the supplemental heater represents a

small fraction of the overall load, this impact was neglected for the purposes of this analysis. The performance data for the curves presented in Figure 16 are taken from three different Carrier heat pump units (38YCC-8PD for the 7.0 HSPF, 38YRA for the 7.7 HSPF, and 25HCA4 for the 8.5 HSPF).

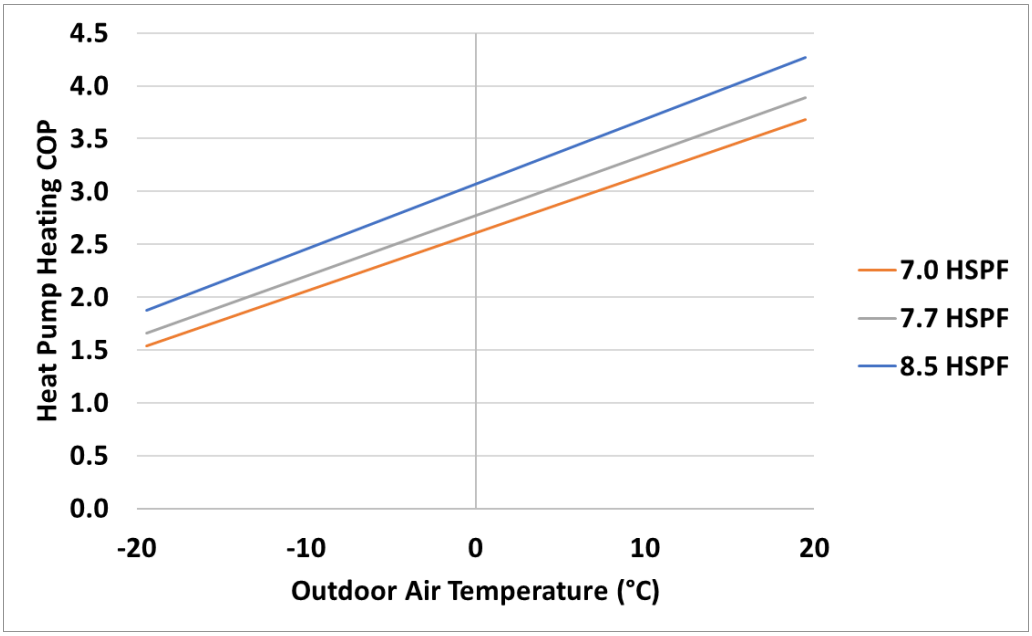

Figure 16. Performance curves used to calculate heating energy use of heat pump simulations

The temperature, T, used for determining the operating COP of the heat pump at any timestep depends on the mode in which the system is operating. In air-source mode, T is the ambient temperature condition during that timestep. For pool-source mode, the pool temperature is used in place of the air temperature. An offset for the appropriate temperature to use was considered based on the data provided in Figure 14 to account for the improved performance of the water-to-refrigerant coil. The data in Figure 14 suggested an offset of about 3°F between the water temperature and the effective air temperature (air temperature at which the performance is similar between air-source and pool-source operation) when operating in pool-source mode. It was decided to use a 0°F offset to provide conservative estimates of performance and account for the fact that the data provided in Figure 14 was only for a single field test unit.

The heat load added or removed from the pool is based on the outdoor coil load of the heat pump.

Rearranging Equation 2 from Chapter 1, which describes the basic energy flow of a heat pump system, the heat exchange with the pool was determined and outlined in Equation 24 and Equation 25. Equation 24 describes how the heat added to the pool was calculated during cooling operations while Equation 25 describes how the heat removed was calculated during heating operations.

$$Q_P = Q_H = W + Q_C = Q_C(1 + \frac{1}{COP}) \qquad \textit{Equation 24}$$

$$Q_P = -Q_C = -(Q_H - W) = -Q_H(1 - \frac{1}{COP}) \qquad \textit{Equation 25}$$

In Equation 24 and Equation 25, Q_P represents the heat exchange between the heat pump and the pool, Q_H is the heat pump condenser heat load during cooling operations, and Q_C is the heat pump evaporator load during heating operations.

Chapter 3. Field Evaluation and Modeling Results

Results and Discussion

The results for this thesis are divided into three main sections: 1) the first section provides results from the field testing of the technology, 2) the second provides the results from the model validation based on field test results, and 3) the third section provides results from simulations of the pool-coupled heat pump using the validated model.

Field Test Results

Baseline Equipment Performance

Baseline data was collected to establish the existing air conditioners' performance before the retrofit. The baseline systems both had dual-zone setups with damper control for upstairs and downstairs zones. Air conditioning equipment performance is primarily dependent on outdoor air temperature since indoor conditions are relatively constant. Performance data was evaluated at different outdoor air dry-bulb conditions for each site to develop a baseline performance map. The performance was evaluated as close to steady-state as reasonable by only considering data after the system had been running for five minutes. This avoided variations in performance due to transients experienced during the initial startup. The steady state performance maps allowed for the energy savings when rejecting heat to the pool to be determined relative to the system rejecting heat to ambient air.

Site 1

Data collected at Site 1 provided a significant amount of run-time in each mode of operation. Figure 17 shows three distinct performance trends which describe the performance at each of the individual modes of operation including Zone 1 (downstairs), Zone 2 (upstairs), and Zones 1&2 (downstairs and upstairs). The highest performance was measured in the Zone 1 mode with a COP ranging from 3.0-4.3 depending on outdoor conditions.

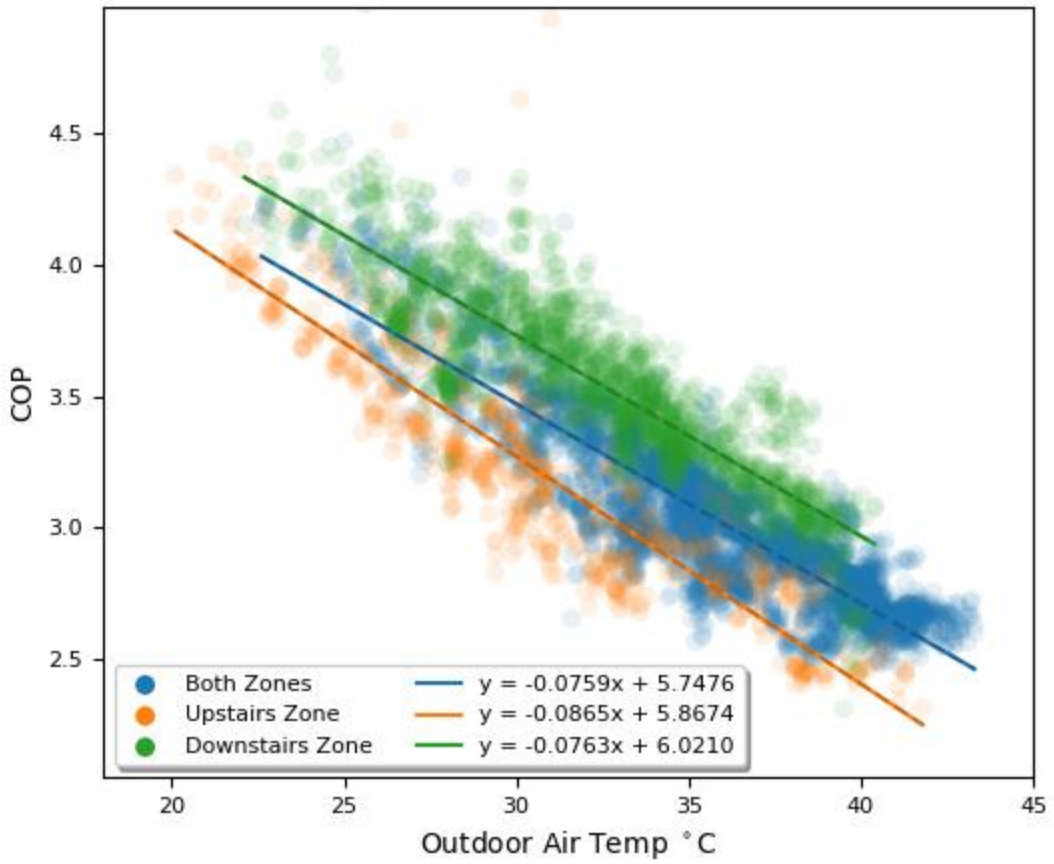

Figure 17: COP vs. ambient air temperature for baseline equipment at Site 1

The COP for Site 1 shows clear performance differences based on the zoning arrangement due to changes in the measured airflow between modes. For each zoning arrangement, there is a clear trend showing efficiency going down as outdoor air temperatures increase. This is consistent with typical air-source air conditioners due to the higher temperature difference between outside air and inside.

Site 2

At Site 2 the observed run-time was much lower than Site 1 with 10-times fewer runtime hours. Figure 18 shows a plot of the COP versus ambient air temperature for each zoning arrangement. Very few observations were made with both zones operating so that mode was not included. The results show that performance trends were much less stable compared to Site 1 as indicated by the lower r-squared values. This was likely due to the reduced run-time hours.

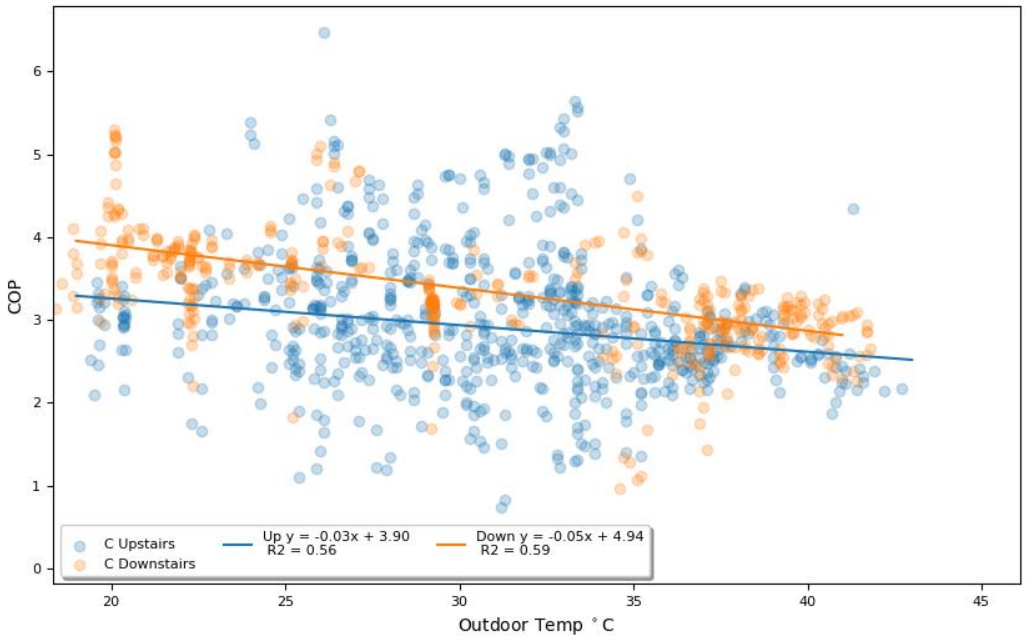

Figure 18: COP vs. ambient air temperature for baseline equipment at Site 2

The baseline performance at Site 2 was generally lower than Site 1. Refrigerant monitoring indicates that the system appears low on refrigerant charge. The performance ranged from a COP of 2.6 during very hot conditions to 4.0 during cooler conditions.

Pool-source performance

After collecting baseline data on the air conditioner performance, the retrofit technology was installed allowing condenser heat to be transferred to the pool. About one month of data was collected with the retrofit technology installed. Minimal operation was observed for Site 2 so the field test analysis focuses on Site 1 performance. Figure 19 shows the air conditioner performance at Site 1 when rejecting waste heat to the swimming pool plotted against outdoor air temperature. While outdoor air temperature does not directly impact the performance when rejecting heat to the pool, it does allow a comparison of performance to be made between air-source (baseline) and pool-source performance. The COP when rejecting heat to the pool had a much narrower range with most of the results for the Downstairs zone ranging between 4.3-4.4 and is also on the higher end of the performance relative to the baseline.

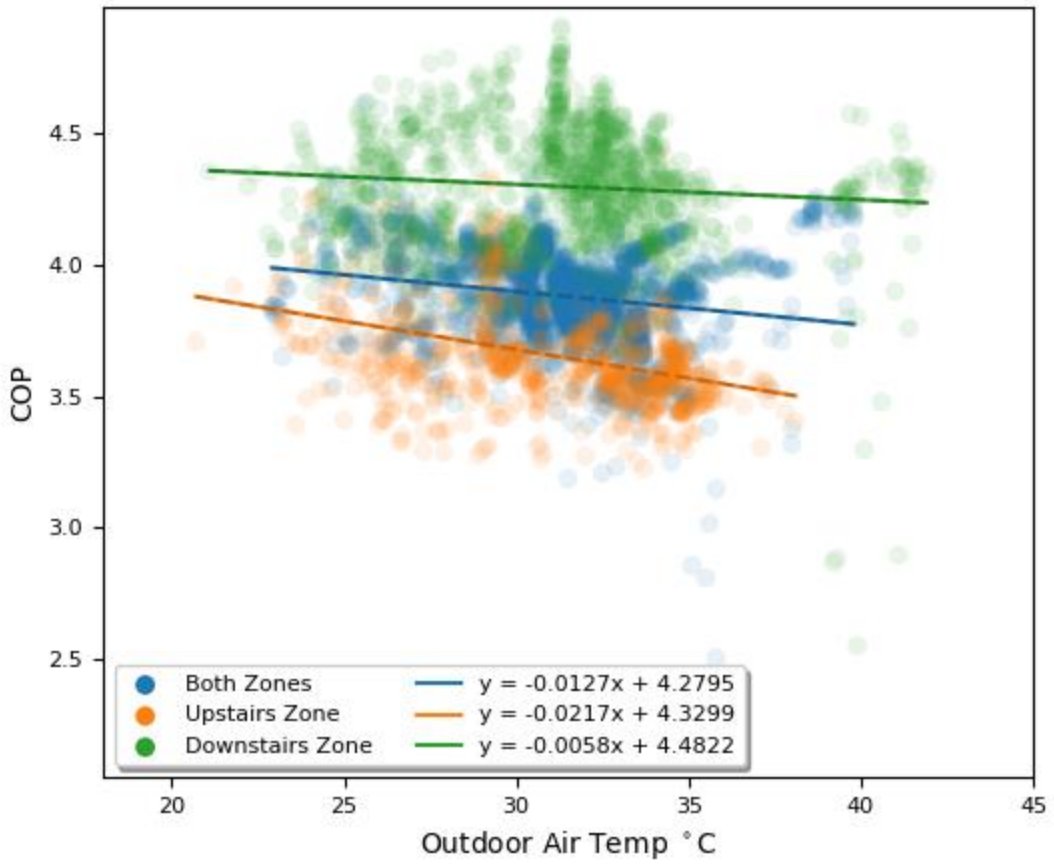

Figure 19. Pool-source COP vs. ambient air temperature for retrofit equipment

The flatter COP profile can be explained by the relatively small changes in pool temperature during the monitoring period compared to outdoor air temperature. The pool temperature only varied between 24°C-30°C (75°F-86°F) compared to the ambient air which varied from 20°C-42°C (68°F-108°F).

Energy Savings

The impact of the retrofit on air conditioning energy use was significant, particularly at higher ambient conditions. Overall, the pool-source condenser operated at 13% higher efficiency than the air-source condenser when not considering the pool pumping power and 6% higher efficiency when contributing all the pool pumping power during air conditioner operation. Pool pumps often run as much as 8-hours per day during the swimming season and it was found that the modest additional resistance associated

with the retrofit had minimal impact on pool pumping energy. Ideally, all pool pumping related to air conditioning would also count toward pool cleaning, but the authors are not aware of a pool controller that includes such a feature.

Rejecting heat to the pool was 31% more efficient than rejecting heat to ambient air when outdoor temperatures were 32.2°C (90°F) and above. Both the cooling capacity was higher, and power draw was lower during hotter outdoor air conditions. The data suggests that the pool-source and air-source systems performed comparably when ambient temperatures dropped to about 25°C (77°F). These results depend on the temperature conditions of the pool which for this case averaged 26.2°C (79.2°F) when used as a heat sink during air conditioning events.

Figure 20 and Figure 21 show the air conditioner power and cooling capacity for the air-source and pool-source modes plotted against outdoor air temperature. The results illustrate the lower variation in these performance metrics when rejecting heat to the pool. Both power and capacity are consistent when rejecting to the pool at levels similar to the air source system operating at an outdoor air temperature of 25°C (77°F). The overall energy savings measured was 57.5 kWh (13%) over the course of the nine-week monitoring period. If you contribute all the pumping power during air conditioning operation, this savings drops to 30.8 kWh (7%).

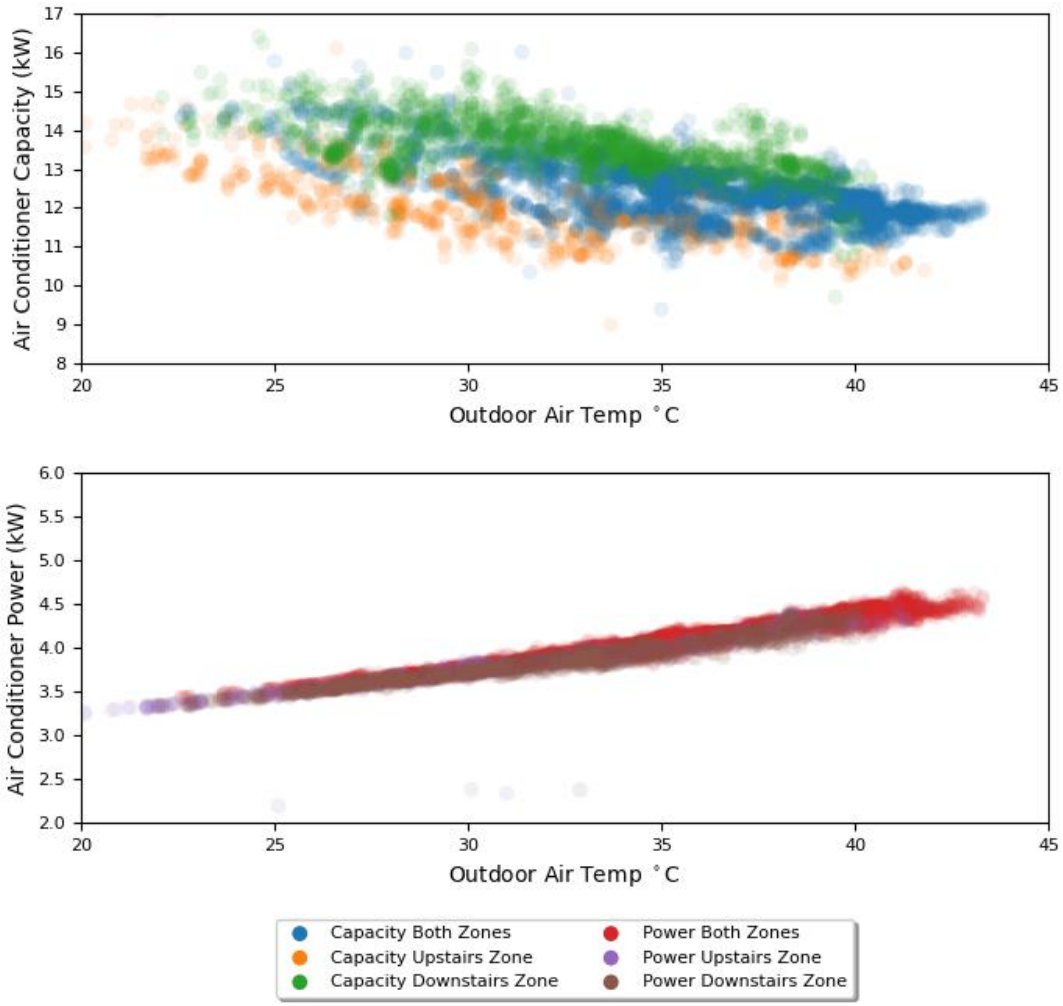

Figure 20. Air conditioner capacity and power for air-source (baseline)

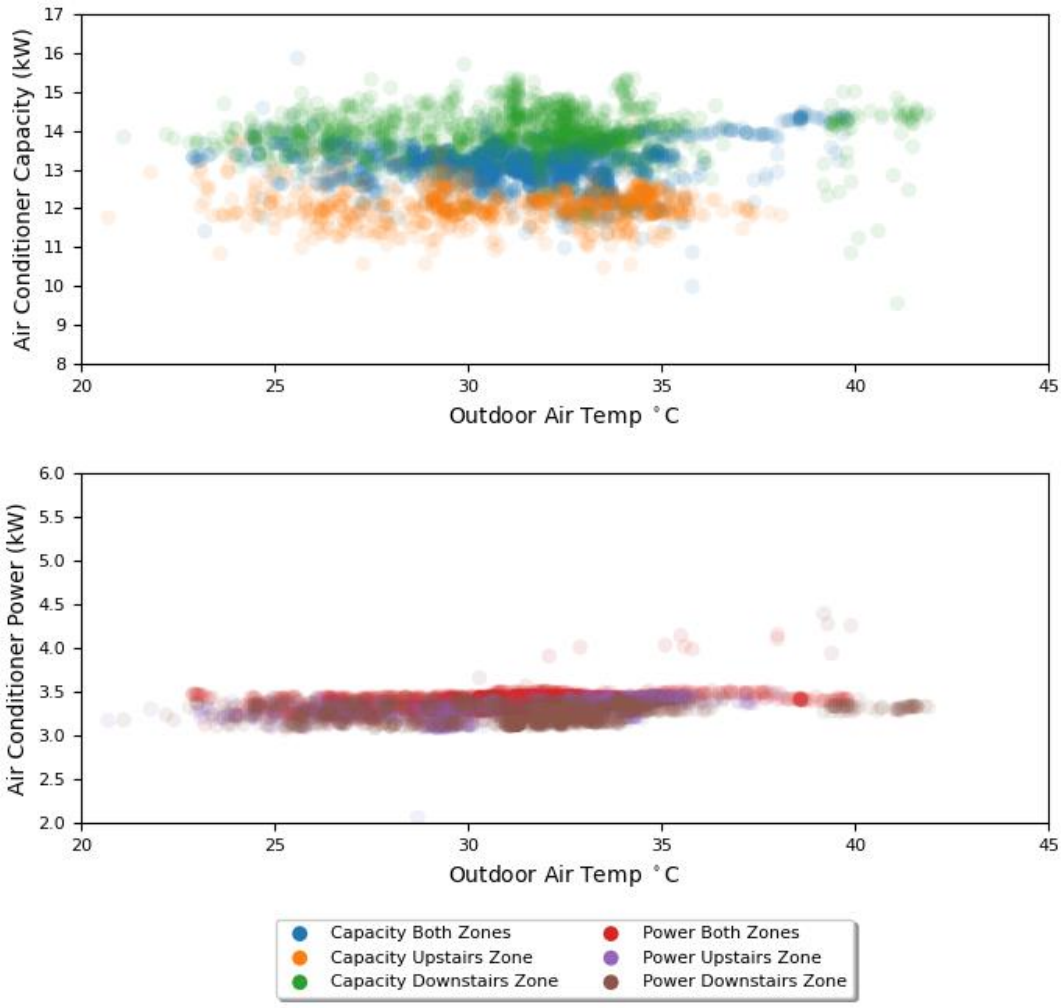

Figure 21. Air conditioner capacity and power for pool-source (retrofit)

Discussion

The retrofit system also provides "free" pool heating by sending heat to the pool that would otherwise be lost to the environment. Using the validated pool thermal model, the additional heat from the air conditioner increased the average pool temperature by 1.4°C in the month immediately following the installation. Figure 22 shows a histogram representing the number of hours the pool temperature fell within each one-degree temperature bin. It shows the pool with heat from the air conditioner has

significantly more hours of warmer pool temperatures. Over the nine-week monitoring period, there were 289 more hours above 27°C (80.6°F) compared to the pool without added heat from the air conditioner. This technology can therefore improve the efficiency of air conditioning while also offsetting fuel used for heating a pool.

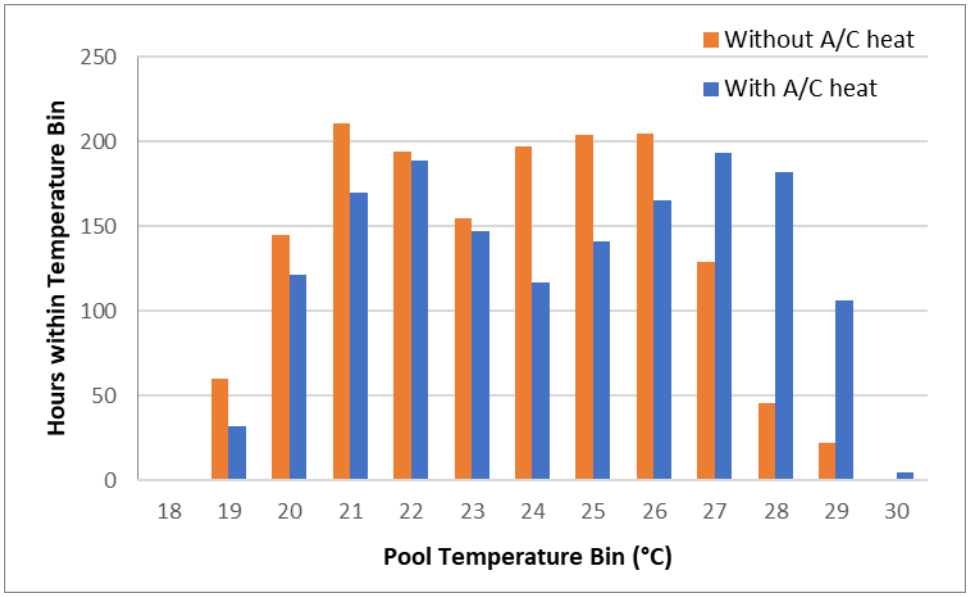

Figure 22. Modeled pool temperature conditions during nine-week monitoring period

Lastly, the energy savings from this approach is highly dependent on the relative size of the pool and air conditioning load. A smaller pool would result in lower energy savings and warmer pool temperatures. To predict potential energy savings in different applications, a pool thermal model would be needed to simulate pool temperature conditions as a function of pool characteristics, climate, and air conditioning loads.

Pool Model Validation

The focus of the validation effort was to assess the accuracy of model predictions of pool temperature given appropriate input data. An accurate pool thermal model is necessary for estimating energy savings of the pool-coupled heat pump system as it is the key variable for estimating heat pump COP and the capacity for the pool to absorb additional heating or cooling loads. The system model was validated

using the field data collected on the two pools in the study. Figure 23 shows the hourly pool temperature predicted by the model compared to the measured pool temperature for Site 1. During this test there was 7,360 MJ of heat rejected to the pool by the air conditioning system from August 16th-October 20th. Some gaps appear in the measured data where data loss occurred.

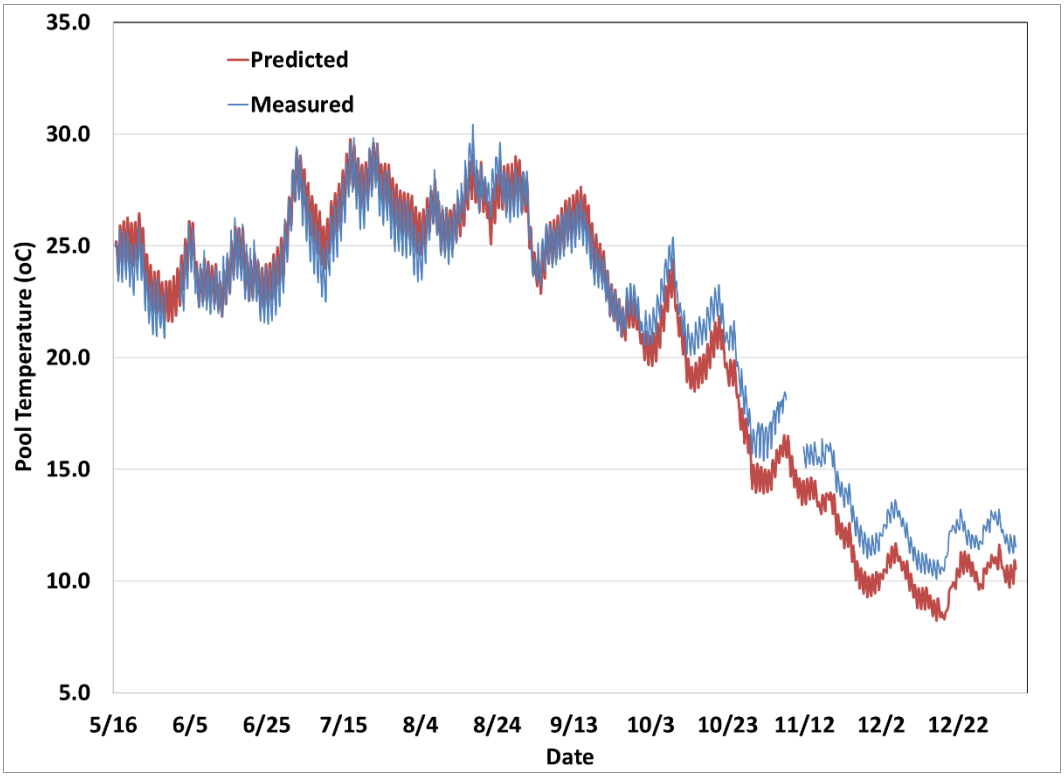

Figure 23. Predicted pool temperature versus measured pool temperature for Site 1

Figure 23 shows good agreement between the predicted and measured pool temperatures. The predictions in the warmer months were generally closer to the measured value than predictions in the cooler months. The average root mean squared (RMS) error in the warmer months was 0.7°C whereas the average RMS error in the cooler months was 1.8°C. The average RMS error of the model predictions for all hours was 1.2°C. Figure 24 shows the parity plot of predicted temperature plotted against the measured temperature. A perfect model would result in a one-to-one relationship which is illustrated by the red line in the plot. This plot illustrates the tendency of the model to predict lower water temperatures when pool conditions are colder. It is unclear what is causing the underprediction by the

model during colder conditions. The sensitivity of shading conditions was evaluated showing that eliminating all pool shading would only marginally improve model predictions suggesting that a change in shading due to solar position was not the cause for the bias.

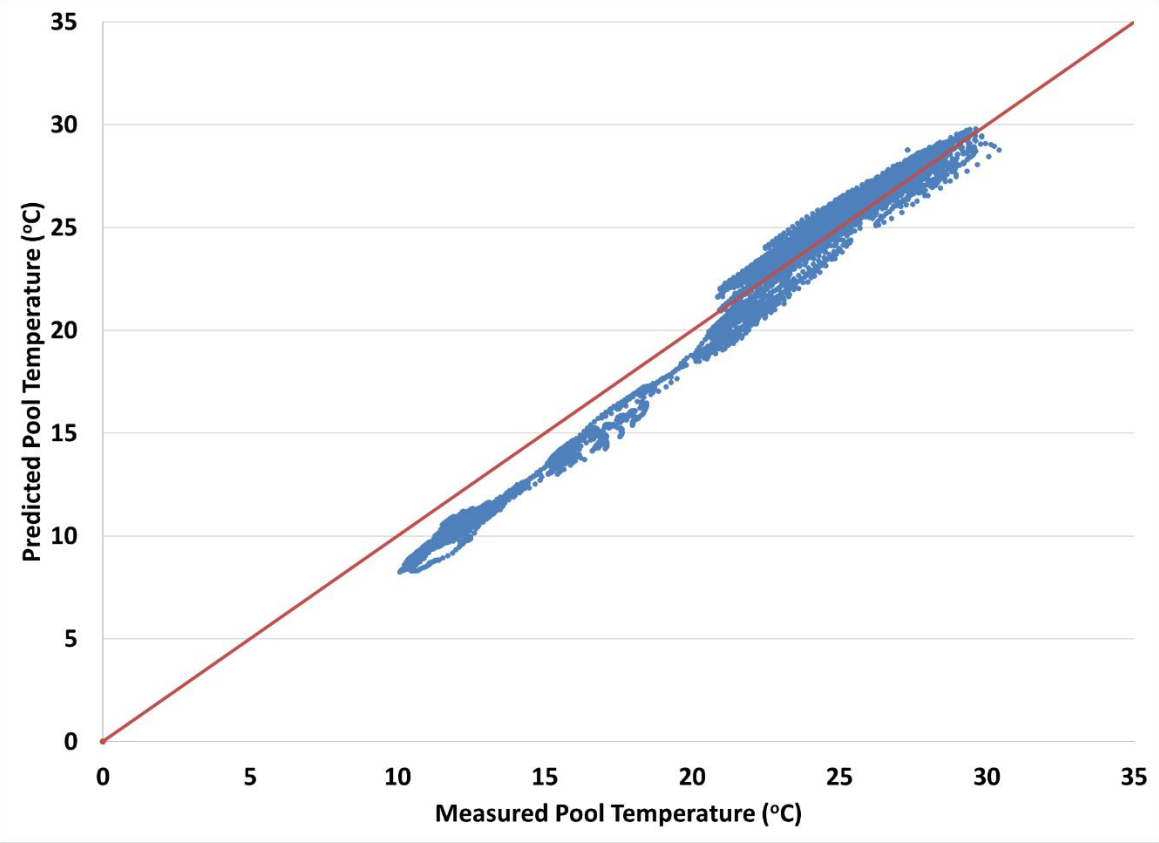

Figure 24. Predicted pool temperature plotted against measured pool temperature with line representing a one-to-one relationship for Site 1

Figure 25 shows the hourly pool temperature predicted by the model compared to the measured pool temperature for Site 2. During this test there was 3,873 MJ of heat rejected to the pool by the air conditioning system from August 16th-October 11th. Some gaps appear in the measured data where data loss occurred.

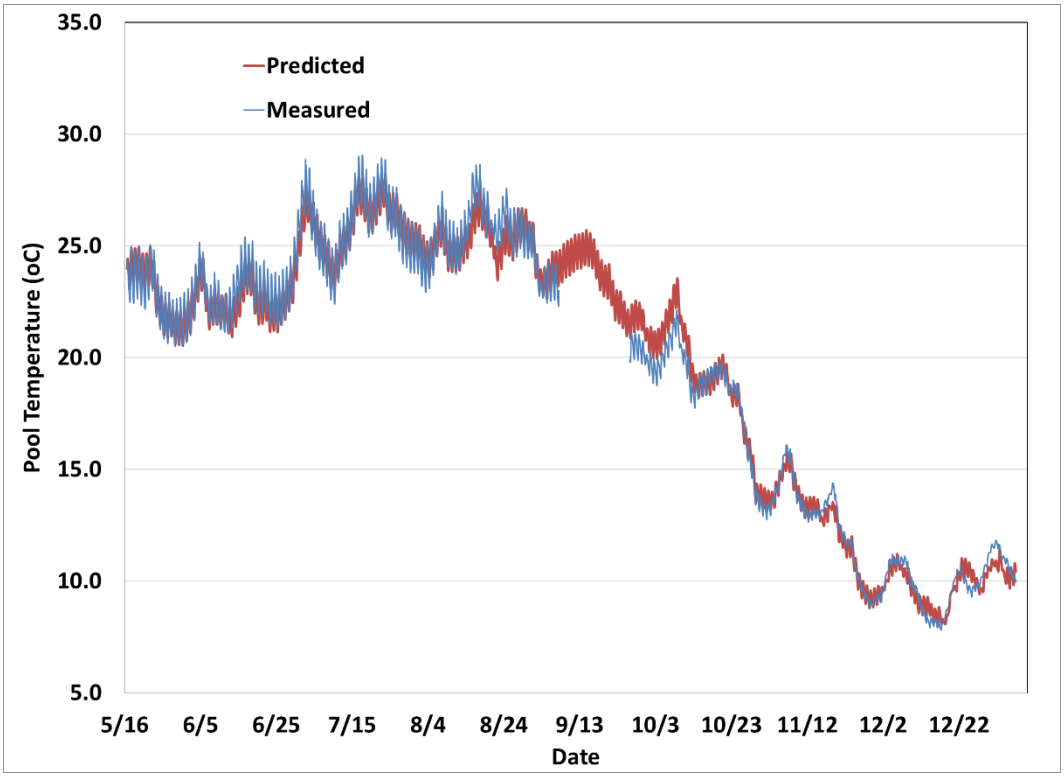

Figure 25. Predicted and measured pool temperatures versus time of year for Site 2

The temperature predictions for Site 2 in Figure 25 show better tracking of actual pool temperatures during colder conditions. The average RMS error in the hotter months was 0.6°C while the average RMS error in the cooler months was 0.4°C. The average RMS error of the model predictions for all hours was 0.6°C. Figure 26 shows the predicted pool temperatures plotted against the measured pool temperature illustrating good temperature predictions across all observed hours.

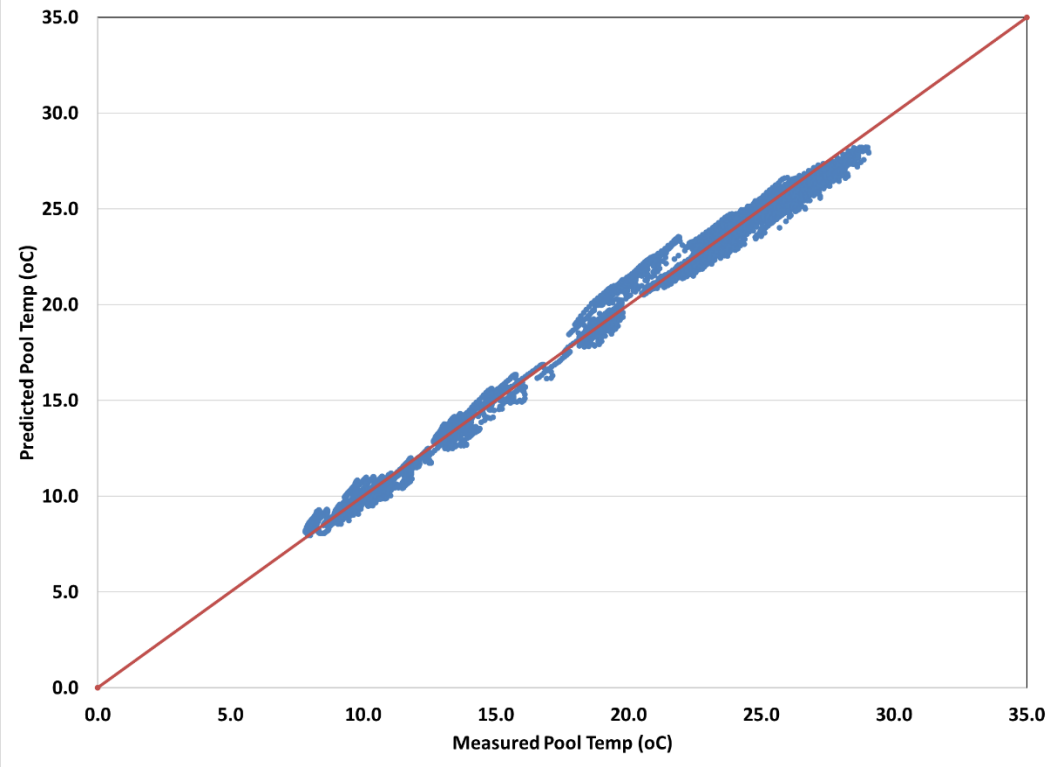

Figure 26. Predicted pool temperature plotted against measured pool temperature with line representing a one-to-one relationship for Site 2

The model predicted pool temperatures showed good agreement with measured values suggesting the pool model can be used to create reasonably accurate energy use estimates for the pool-coupled heat pump system. For Site 1, the pool temperature predictions in the summer were generally better than those in the winter. The model tended to predict lower pool temperature conditions for Site 1 in the winter which would result in lower estimates for heating efficiency for the heat pump system absorbing heat from the pool. For Site 2, the model predicted pool temperatures in the winter fit the measured data better with an average RMS error that was 1/3 of the model error for Site 1. Site 2 also showed similar RMS error for the colder months as the hotter months.

Simulation Results

Simulations were conducted using the validated pool thermal model along with loads from building energy simulations to estimate the energy savings potential of the pool-coupled heat pump technology, as well as the impact on pool temperature conditions. The technology tested is currently only supported

commercially for air conditioning operations of the heat pump, but this study also explored the potential to use the pool as a heat source in the winter.

Energy savings of the technology were evaluated for a wide range of scenarios to describe the broad potential of the technology to reduce HVAC energy use in California. The key parameters that were considered in the analysis were pool volume, surface area, shading level, heat pump efficiency, house type, pool temperature setpoint, and climate zone. Table 9 shows the various parameters that were considered for evaluating the technology performance in California.

Table 9. Simulation parameters considered for parametric analysis of pool-coupled heat pump

Pool Volume	Pool Surface Area	Shading Level*	HVAC Efficiency**	House Type	Pool setpoint	Climate Zone
37.85 m^3 (10,000 gal.)	24.8 m^2 (267 ft^2)	Low Shading	High Efficiency	One-Story Model	32.2°C (90°F)	California climate zones 1-16
56.78 m^3 (15,000 gal.)	37.3 m^2 (401 ft^2)	Some Shading	Medium Efficiency	Two-Story Model	30.0°C (86°F)	
75.71 m^3 (20,000 gal.)	49.7 m^2 (535 ft^2)	High Shading	Low Efficiency			
94.64 m^3 (25,000 gal.)	62.1 m^2 (668 ft^2)					

* Specific shading factors considered are outlined in Table 5
** Specific efficiency ratings outlined in Table 8

Pool surface area is a sensitive parameter since the majority of heat transfer between the pool and its surroundings occurs at the surface. For the simulations, the pool surface area was assumed to be rectangular with an aspect ratio of 2:1, and the depth was assumed to be 1.524 meters (5 ft.). This allowed the relavent parameters to be calculated based on the input volume.

The simulation parameters investigated were meant to cover a range of potential installations. Overall, there were 2,304 different model runs to evaluate all combinations of parameters shown in Table 9. For a particular installation, the model inputs can be refined to reflect more specific project details resulting in a more accurate estimate of energy savings and pool temperature impacts.

Cooling Performance

The cooling performance was evaluated for each of the simulations to determine the impact of the retrofit technology on cooling energy use, including during peak times defined as between 4pm and 9pm, and pool temperature.

Energy Savings

The energy savings are presented in a series of boxplots below. Each boxplot represents a group of simulations that includes all shading parameters and pool sizes considered. Results are generated for different equipment efficiencies, house model type, and pool setpoint temperature. Figure 27 through Figure 29 show the cooling energy savings in each climate zone for the two-story model with a 32.2°C (90°F) pool temperature setpoint.

In general, the pool with larger thermal mass and lower sun exposure resulted in higher energy savings. Larger pools can absorb more heat with smaller changes in temperature compared to smaller pools. This results in lower pool temperatures and better performance when used as a heat sink. Similarly, pools with higher amounts of shading have lower solar gains which allow pool temperatures to remain lower than pools with more sun exposure. Some climate zones were shown to achieve very little or even negative cooling energy savings depending on the specific simulation. Climate zones with very low cooling loads, such as CZ01, would not be a good candidate for this technology due to the limited savings potential.

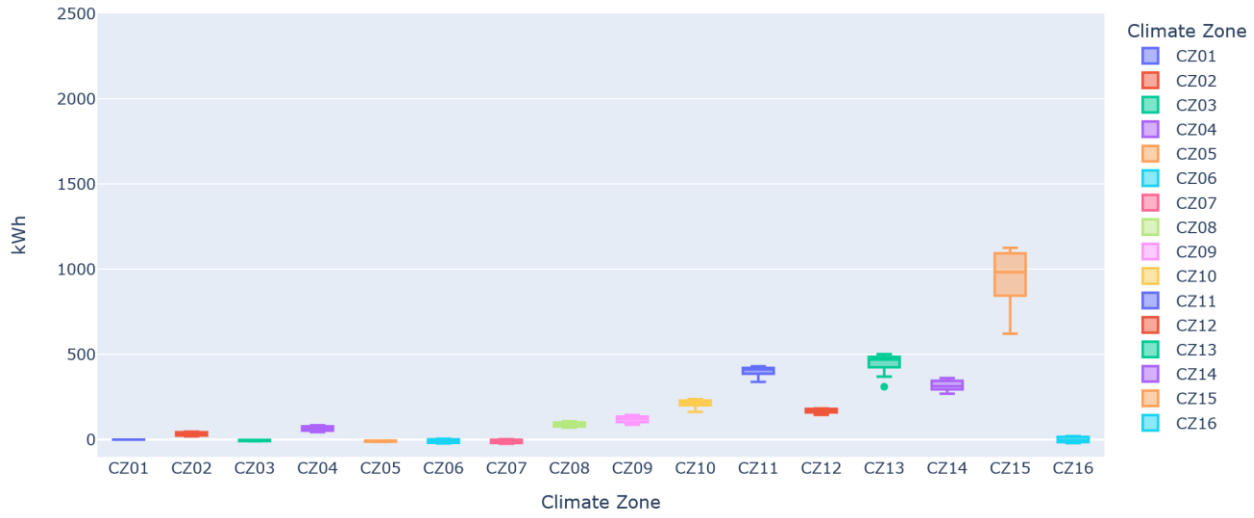

Figure 27. Cooling energy savings (Two-story model, High-COP, 32.2°C setpoint)

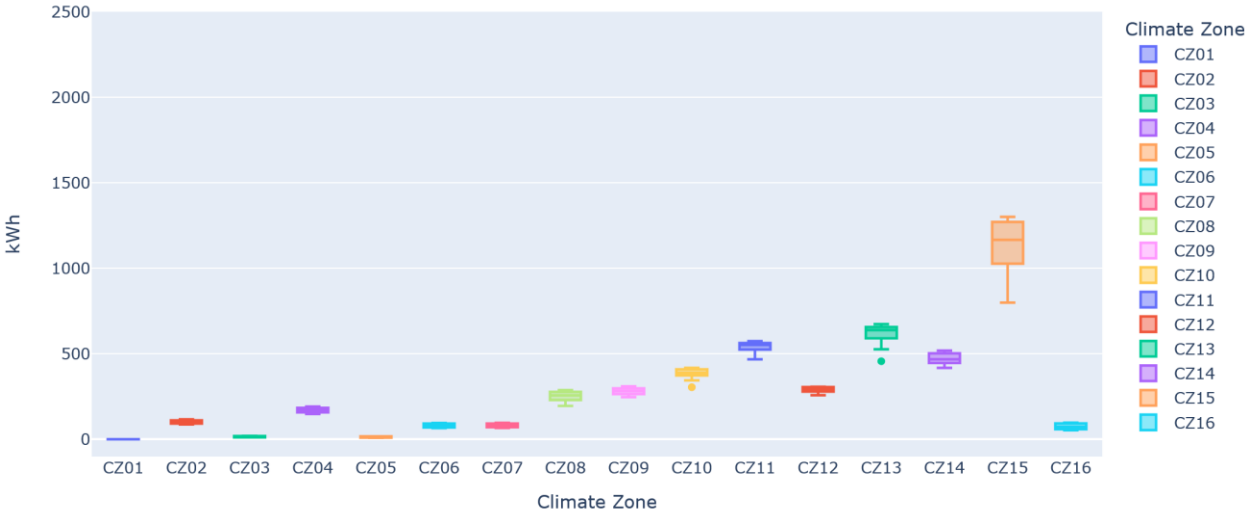

Figure 28. Cooling energy savings (Two-story model, Mid-COP, 32.2°C setpoint)

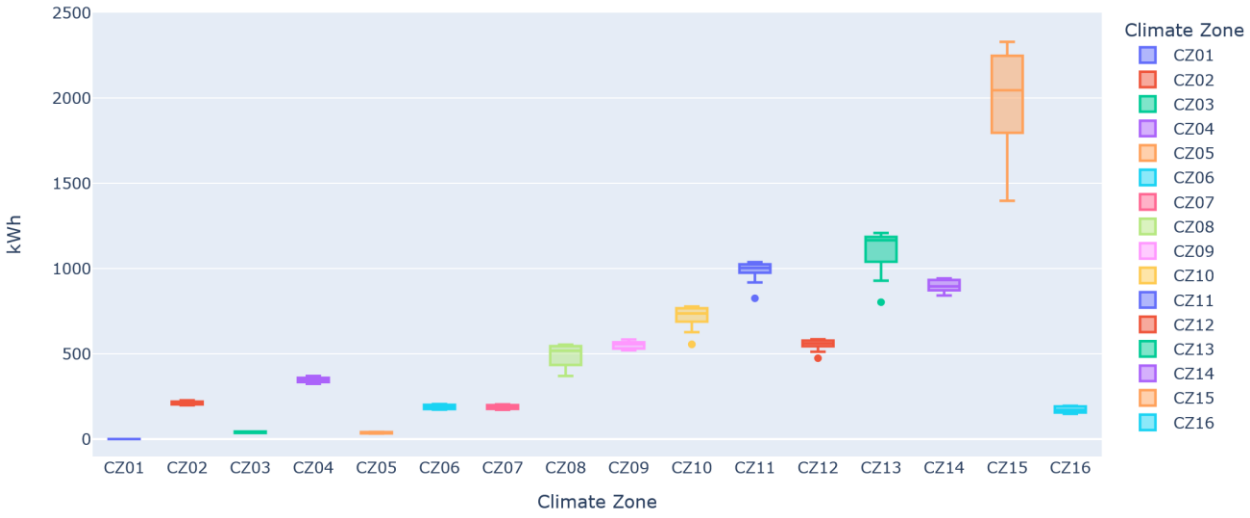

Figure 29. Cooling energy savings (Two-story model, Low-COP, 32.2°C setpoint)

The results show that installing the retrofit technology on an existing air conditioner that has a lower efficiency rating results in higher energy savings. The low-COP air conditioner showed about two-times as much energy savings as the high-COP air conditioner. Climate zone also had a big influence on the potential for energy savings. Some climate zones show low energy savings (heating dominated climates) and even negative savings in some circumstances, while others showed relatively high savings. Climate zone 15 showed the highest savings with the potential to reduce air conditioning energy use by 2,000 kWh annually.

It can also be useful to review the percentage reduction in air conditioning energy use to understand the relative impact of the retrofit. Figure 30 shows the percent air conditioning savings for the two-story model with different air conditioning efficiencies showing a range from -12%-37%. The climate zones that achieved the highest percentage savings were warmer climates that have higher cooling energy use and should be the target for this technology. The colder climate zones showed cases of negative cooling energy savings, but the overall cooling energy use was low for those climates leading to relatively small increases in energy consumption as seen in Figure 27 through Figure 29. Figure 30 also illustrates the impact the baseline air conditioner efficiency has on the result. Lower efficiency air conditioners benefit

more from the retrofit technology with savings of 15-30%.

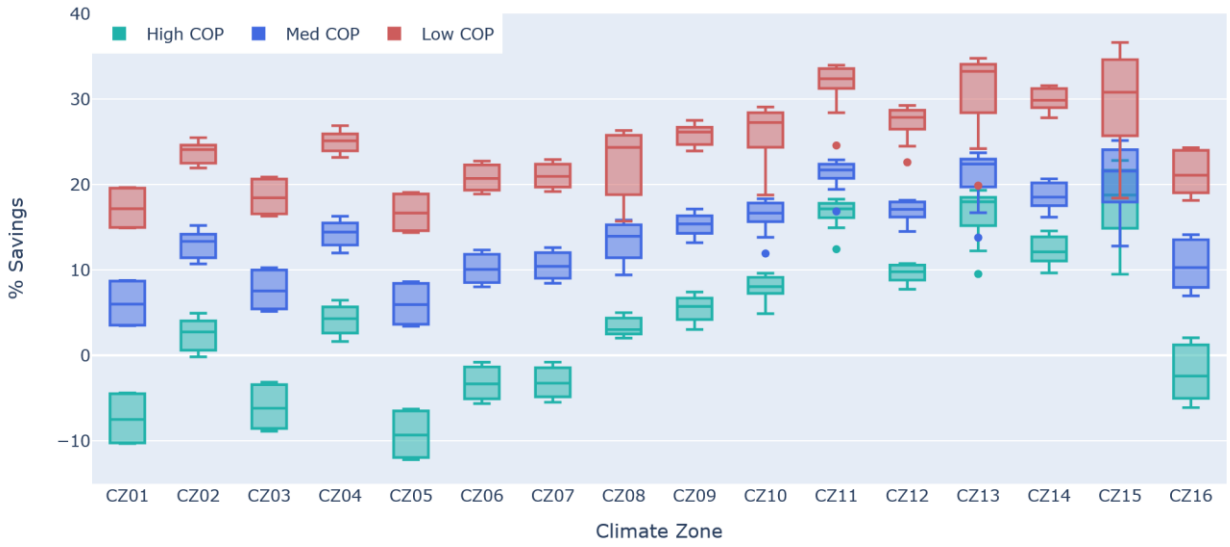

Figure 30. Percentage cooling energy savings with different air conditioner efficiencies (Two-story model, 32.2°C setpoint)

Simulation results evaluating the other parameters are provided in Appendix A. These include results for the two-story prototype model with a lower pool temperature setpoint of 30.0°C (86°F), and results for the one-story model. Reducing the pool setpoint temperature resulted in lower energy savings. When operating with a lower setpoint, there is less thermal capacity in the pool to absorb air conditioner waste heat. The lower setpoint resulted in more air-source operation and lower energy savings potential. It is observed that the boxplots become larger in the scenarios with a lower pool setpoint temperature, especially in the climate zones with more cooling energy use. This is a result of the system switching to air-source mode when the pool surpasses its setpoint reducing energy savings. This is most apparent in climate zone 15, which has the largest cooling requirements of the California climate zones, since sun exposure and pool size conditions cause some of the simulations to reach the setpoint more often than others. For example, the highest savings for climate zone 15 was for the largest pool with the highest shading which switched to air-source cooling (surpassed the setpoint) 32% of all cooling hours. By contrast, the simulation showing the lowest savings in climate zone 15 was for the smallest pool with the most sun exposure that relied on air-source cooling 45% of all cooling hours due to overheating.

The percentage energy savings for the two-story model with a 30.0°C (86°F) setpoint showed a much wider range of results depending on shading condition and pool volume for the hotter climate zones (CZ8-CZ13) compared to the results for the higher setpoint. This suggests some of the pools were experiencing overheating relative to the setpoint causing the system to revert to the air-source condenser.

The results for the single-story prototype model showed similar trends to the two-story model; however, given the lower cooling requirements for the home, the energy savings from the pool-source technology is lower for the one-story model. While the one-story model resulted in lower energy savings compared to the two-story model, the percentage reduction in air conditioner energy use was similar.

Peak Energy Savings

Many utilities in California have time-of-use rate schedules that result in higher electricity pricing when the electric grid is experiencing stress from high loads. The is considered a "peak" period and often occurs between the hours of 4-9pm in California. An analysis was conducted evaluating the results during this peak period to show the impact of the technology during the most challenging demand on California's electric grid. Figure 36 shows the result for the case of the two-story model with the mid-COP air conditioner and 32.2°C setpoint. Simulation results for the other simulations are provided in Appendix A.

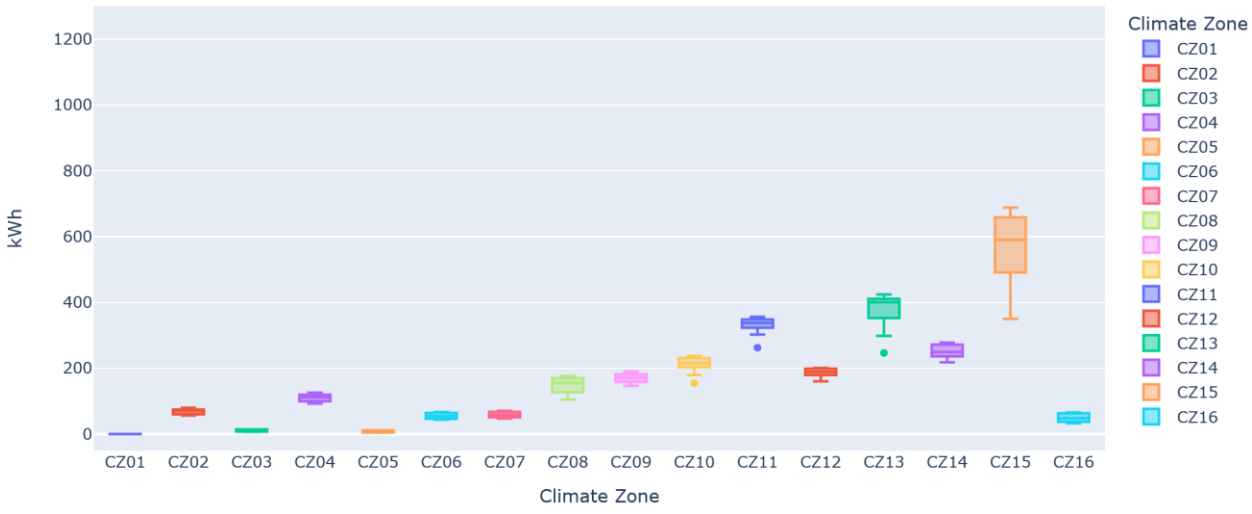

Figure 31. Peak cooling energy savings (two-story model, mid-COP, 32.2°C setpoint)

The energy savings results during peak show that a substantial fraction of the overall energy savings occurs during the peak hours from 4-9pm. For climate zones with more than 100 kWh of cooling energy savings, the simulations showed 30-60% of the energy savings occurred during the peak. A higher percentage of peak savings was observed for simulations with the more efficient air conditioner than with the less efficient air conditioner. However, like the results for total cooling energy savings, more peak energy savings were found when retrofitting the technology with a lower efficiency air conditioner.

Pool Temperature Impacts

The impact of the technology on pool temperatures was also evaluated in the simulations. The heating provided by the air conditioning heat rejection is dependent on the cooling load in the house, pool size, and weather conditions. A small pool absorbing heat from a house with high cooling loads will experience more pool heating than a large pool absorbing heat from a house with lower cooling loads. The former scenario will lead to warmer pool temperatures and reduced energy saving potential. Figure 32 shows the impact on pool temperatures for the simulations showing the average temperature difference between the natural pool temperature and the pool temperature with air conditioner heat rejection from May 1 to September 30. The results are broken out by pool size and climate zones with each bar representing the average impact for all shading conditions and air conditioner efficiency.

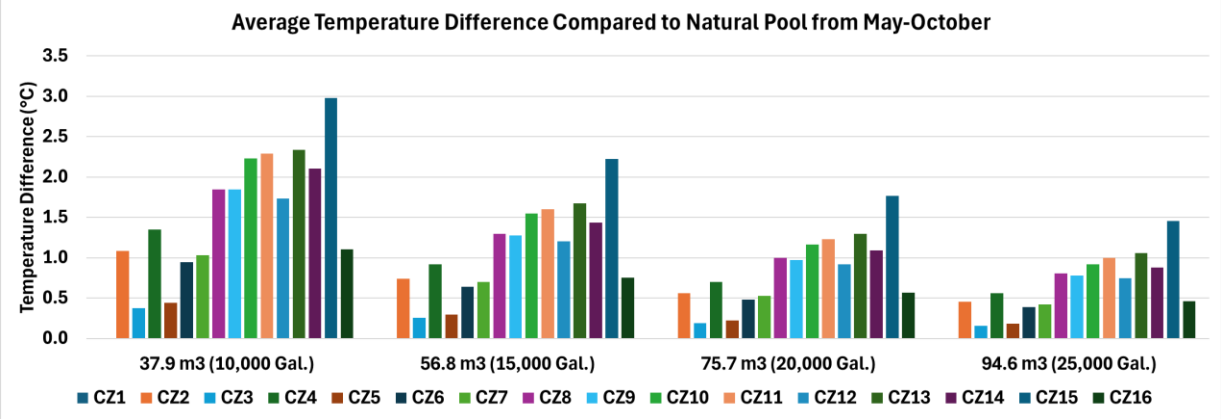

Figure 32. Average pool temperature difference from May 1 to September 30 between natural pool and pool with A/C heat rejection for all simulations

The results in Figure 32 show that the technology increases the average pool temperature during the cooling season by several degrees in many climate zones. The smaller pool sizes and hotter climate zones resulted in more pool heating.

Site 1 House Comparison

To evaluate the simulation tool further, the energy savings results using the simplified inputs were compared to the Site 1 data collected in the field. Table 10 shows the simulation parameters used to test the model against the field test results measured for Site 1.

Table 10. Simulation parameters used to evaluate model accuracy compared to field test results for Site 1

Pool Volume	Pool Surface Area	Shading Level	HVAC Efficiency	House Type	Pool setpoint	Climate Zone
94.64 m^3 (25,000 gal.)	62.1 m^2 (668 ft^2)	Low Shading	Medium Efficiency	Two-Story Model	32.2°C (90°F)	California climate zone 12

The simplified inputs differed from the actual conditions used to validate the pool thermal model in the earlier section. The pool volume was consistent with the actual test but the surface area for the simulation was based on simplified assumptions about average pool depth rather than the measured surface area. The shading conditions also differed slightly from the shading observed at Site 1. The air conditioner performance was based on the Goodman GSX series 13 SEER (Medium Efficiency) unit rather than the performance map created for the unit measured at Site 1. The house for Site 1 was a two story with about 20% more conditioned floor area than the model for generating loads for the simulation. The pool setpoint was accurate to the conditions at Site 1 in that the pool-coupled heat pump never shut off on high temperature and was never observed to go over 90°F during the retrofit monitoring period. Lastly, the weather data for the simulation was based on TMY weather data for climate zone 12 rather than the actual weather observed during the retrofit period.

To evaluate the accuracy of the model to predict the actual amount of energy saved relative to the field

test, the hourly model predictions during the specific nine-week retrofit period were compared to the field test results. This process found that the model underpredicted the actual energy savings observed in the field estimating only 31.1 kWh of energy savings compared to the measured 57.5 kWh. This discrepancy can be explained by several factors. The field test house was larger and used a different thermostat setpoint schedule relative to the model that led to 36% higher cooling loads over the period evaluated. Another source of error comes from the fact that the environmental conditions differed between the model and field test. The average outdoor air temperature during cooling hours was 86°F for the field test versus 79°F for the model. This leads to differences in air-source system performance resulting in lower energy savings estimates for the model. Furthermore, the pool temperature conditions in the model during cooling hours were lower than the field test, but only differed by 0.9°C (1.6°F).

While the absolute energy savings predicted by the simplified model differed from the measured results, the fractional cooling energy savings showed good agreement. The model predicted 11% cooling energy savings for the scenario that most closely matched the field test versus 13% cooling energy savings measured during the nine-week monitoring period. This demonstrates the ability of the model to accurately predict fractional savings without detailed input parameters.

These results suggest that the accuracy of the pool-coupled air conditioner model, like other building energy modeling software, is sensitive to differences in the assumed versus actual meteorological conditions. Furthermore, having more specific input assumptions that represent the conditions of the field test will result in better predictions. In the test case evaluated here, the actual building cooling loads were significantly higher than the prototype building which resulted in lower energy savings estimates.

Heating Performance

The manufacturer of the technology demonstrated in the field test does not support use of the pool as a

heat source for a heat pump heating operation. However, simulations were conducted to evaluate the potential impact if the technology was used in this manner. The simulation parameters were the same with the exception of the pool temperature setpoint which was set at 4.4°C (40°F) for all simulations to avoid freezing temperature conditions in the pool.

Energy Savings

The heating energy savings are presented in a series of boxplots. Each boxplot represents a group of simulations that includes all shading parameters and pool sizes considered. Results are generated for different equipment efficiencies, and for each house model type. Figure *33* shows the heating energy savings in each climate zone for the two-story model with the mid-COP heat pump. The results for other simulation parameters are presented in Appendix A.

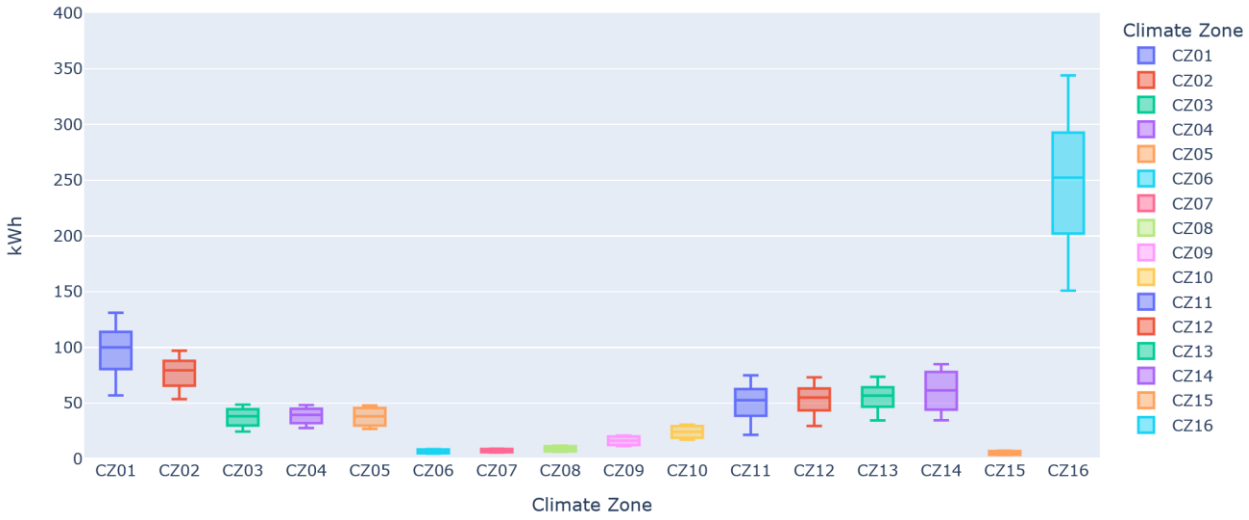

Figure 33*. Heating energy savings (two-story model, mid-COP)*

The heating energy savings results showed lower savings potential for the pool as a heat source during the winter in California than as a heat sink during the summer. As expected, a similar pattern emerged showing climate zones with minimal heating loads (coastal climates in southern, CA) showed little savings potential. Some of the colder climate zones showed higher heating energy savings than cooling energy savings including climate zones 1 and 16, but the savings in these zones ranging from 30-350 kWh is still much lower than the cooling energy savings potential in other parts of California.

Figure *34* show the percentage heating energy savings for the pool-source system relative to the air-source for the two-story model. Similar results for the one-story model are presented in Appendix A. The results show that the opportunity for savings in the winter with the pool-source system is much lower than it is for cooling. However, none of the simulations showed negative savings showing some value in all climate zones. Both house models showed similar results with savings between 2-16%.

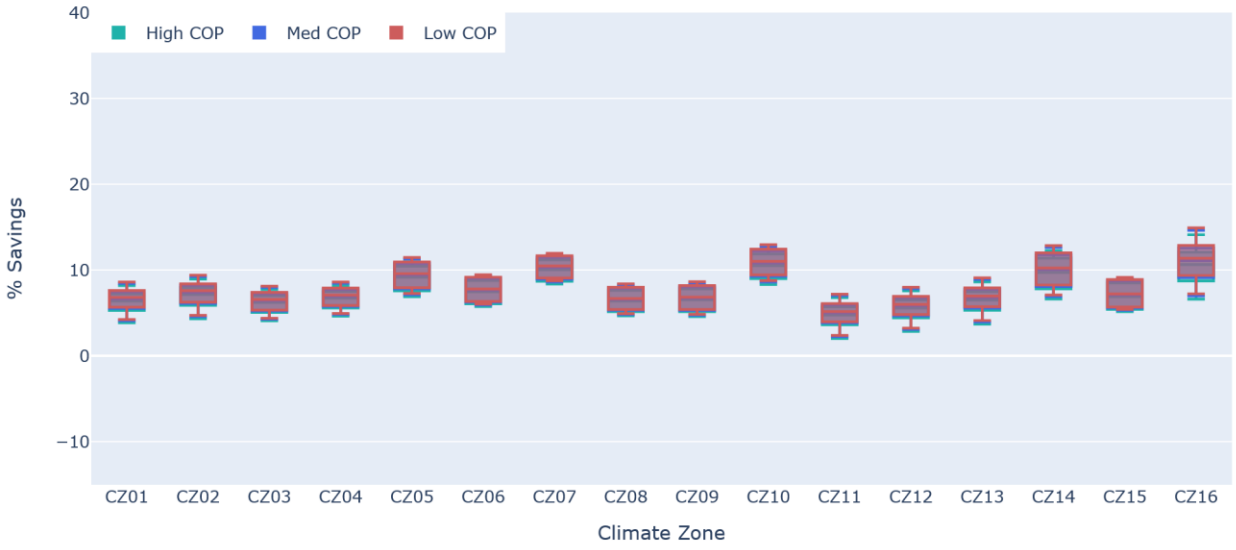

Figure 34*. Percentage heating energy savings with different air conditioner efficiencies (Two-story model)*

Unlike the cooling energy impacts, using the pool as a heat source for heating did not result in any negative savings values suggesting there is no downside to using the technology for heating applications. There were also far fewer instances of the pool exceeding the low temperature setpoint of 40°F. Overcooling only occurred in climate zone 16 where ambient temperatures often drop below freezing. It should be noted that the model was not rigorously validated under these very cold conditions, and pool equipment may need to be winterized in some of these climates preventing their use for this application. The results could improve with the use of existing solar thermal pool heaters or solar blankets to reduce heat rejection at the surface of the pool. These strategies could be explored further in future work.

Stakeholder Feedback

The stakeholders in this project evaluation included the manufacturer and HVAC installers. The following is a summary of feedback received from each of these stakeholders throughout the project.

Manufacturers

Discussions with the manufacturer of the technology provided insight on their view of the primary market for the technology. This product is marketed as a pool heating system which is reflected in the recommendations that the manufacturer provides for specific applications. As part of the recommendation, they provide guidance to prospective customers on the number of hours of runtime the air conditioner would need to maintain the pool at around 27-30°C temperatures. They used a combination of air conditioner capacity and pool surface area to make this determination, and for the sites in this study they recommended the air conditioner run for 7.9 hours per day for Site 1 and 4.1 hours per day for Site 2. They note that adding a pool cover would reduce the required hours for adequate pool heating. Clearly meeting the estimated air conditioning runtime would depend on the cooling load rather than the pool heating needs and is likely to be met on hotter days than cooler ones. The other topics discussed with the manufacturer were what types of air conditioning equipment works with the technology. They recommend against using this technology on variable capacity equipment due to the presence of additional sensors that may cause a fault when the technology interrupts the refrigerant flow or condenser fan operation. The technology does work with heat pump units, but only in the cooling mode. The manufacturer does not currently support using the pool as a heat source for a heat pump in heating mode due to the expectation that the pool does not have enough thermal capacity to avoid overcooling. Simulation using the pool thermal model in this project show that this approach could be beneficial in some climate zones and should be a topic for further research.

HVAC Installers

The installer of the technology was contacted to discuss the complexity of the installation and overall potential from their point of view. The installation process required the same skillset as many other

HVAC installations, but the fact that the technology was new to the installer meant that the installation team had to take more time to review installation guidelines and steps. The first installation took about twice as long as the second due to this lack of familiarity. With a familiar installation crew, the process would be similar to other HVAC installations. There is also a need to install plumbing on the pool equipment that HVAC installers may or may not be comfortable with. This project worked with a separate pool contractor for the pool equipment installation which is similar to the process for a solar thermal or mechanical pool heating system.

Chapter 4. Conclusions

This thesis evaluated the potential to use swimming pools as heat sinks and sources for heat pumps. A field test was conducted to evaluate the impact on performance for an air conditioner that rejects heat to a swimming pool and used to validate a pool thermal model used to simulate the system in different California climate zones. The field demonstrations and model simulations show that the technology evaluated can reduce cooling energy use of existing air conditioners while also providing pool heating. The simulations performed based on loads from two single-family prototypes show air conditioning energy savings over 500 kWh per year in multiple climate zones with a significant fraction of the cooling energy savings coming during peak times (4pm-9pm). Using the pool as a heat source during the winter showed a benefit as well but the savings were lower with most climate zones showing less than 100 kWh of savings. The systems that achieved the highest savings were the inland climate zones 11-15. These climate zones have relatively high heating and cooling loads resulting in more energy savings. In addition, retrofitting the technology on existing systems with lower efficiency tends to increase the energy savings potential. The installation complexity and cost could impact adoption rates, but it is expected that costs would come down as contractors became familiar with the installation process. Unfortunately, these costs could prevent the system from being cost-effective based strictly on the energy savings alone, but if installed in place of a traditional pool heater that may be a better pathway toward achieving cost effectiveness.

It should be noted that the pool thermal model has not been rigorously validated at very cold temperatures or with a full winter of heat loads extracted from the pool. Furthermore, the technology manufacturer does not currently support the use of the system as a heat source in the winter. Future work should explore this functionality of the system further to validate the findings presented here. Below are some observations from the field studies that could help with maximizing energy savings and guide measure development:

- The pool modeling tool developed for this thesis should be used to estimate the energy savings from a particular installation. The more information provided to the model the better the prediction for energy savings will be. It is expected that the percentage cooling energy savings will likely be the best predictor of actual performance since the total energy savings is based on loads from an EnergyPlus prototype. If the utility can estimate cooling energy use for a home, then combining that estimate with the percentage savings result will likely provide a better estimate for total energy savings.
- The pool temperature setpoint should be set as high as possible to maximize pool-source heat rejection and energy savings. This setpoint temperature will not necessarily be maintained by the system but instead be considered the maximum allowable pool temperature for the homeowner.
- The technology does not have a sophisticated way to interact with the existing pool pump controls. It is the manufacturer's recommendation to always send water to the pool-refrigerant heat exchanger to avoid issues related to controls, but they do have a control strategy that allows the system to simulate a solar thermal pool heating system. For systems with long plumbing runs to the heat exchanger, a three-way valve can be used along with the built-in solar thermal controls for the pool pump to avoid additional pumping power when the air conditioner is not running.
- The system is not designed to turn the pool pump on and off so the pool pump must be running to reject heat to the pool. For the demonstrations, the pool pumps were scheduled to perform filtering operations during the afternoon to coincide with air conditioning energy use. A variable speed pool pump allows for optimal control since the pump can be set at low speeds over longer periods of time for filtering allowing the system to be available for air conditioning heat rejection over more hours of the day.

References

AHRI (Air-Conditioning, Heating, and Refrigeration Institute), (2023). AHRI Standard 210/240. *Performance Rating of Unitiary Air-conditioning & Air-source Heat Pump Equipment.*

Aydin, M.S., A. Gultekin, A., B. Dehgan (2015). *An Experimental Performance Comparison between Different Shallow Ground Heat Exchangers.* 2015. Proceedings World Geothermal Congress, 2015.

Bowen, I.S. (1926). *The Ratio of Heat Losses by Conduction and by Evaporation from any Water Surface.* Physical Review V27: p. 779-787.

CPUC (California Public Utilities Commission) (2011). *CA Energy Efficiency Strategic Plan*. January 2011 Update.

CIMIS, California Irrigation Management Information System. Hourly Report for Davis, CA, (2024) Department of Water Resources, https://cimis.water.ca.gov/.

DOE (Department of Energy) (2024). *EnergyPlus.* V23.2. https://energyplus.net/

EIA (Energy Information Agency) (2019). *Efficiency requirements for residential central AC and heat pumps to rise in 2023*. https://www.eia.gov/todayinenergy/detail.php?id=40232#

EIE (Energy Information Agency) (2023). *Internation Energy Outlook 2023.* https://www.eia.gov/outlooks/ieo/

Figliola, R.S., D.E. Beasley (2006). *Theory and Design for Mechanical Measurements.* 4th ed. ISBN-13: 978-0-471-44593-7

Hahne, E., R. Kubler (1994). Monitoring and Simulation of the Thermal Performance of Solar Heated Outdoor Swimming Pools. Solar Energy. Vol. 53 pp. 9-19.

Harrington, C., M. Modera (2013). *Swimming pools as heat sinks for air conditioners: California feasibility analysis.* Energy and Buildings 59 pp.252-264.

Harrington, C., J. Garcia, T. Pistochini (2018). *Waste-heat recovery from an air conditioner for swimming pool heating*. San Diego Gas and Electric Emerging Technologies Program. ET16SDG1011.

IEA (International Energy Agency) (2023). *Energy Efficiency - The Decade for Action.* IEA 8th Annual Global Conference on Energy Efficiency.

ICC (International Code Council) (2006). *2006 International Energy Conservation Code.*

Incropera F.P., D.P. DeWitt (2007). *Introduction to Heat Transfer*. 5 ed.: Wiley

Maxwell, E. (1987). *A Quasi-Physical Model for Converting Hourly Global Insolation to Direct Normal Insolation.* NREL TR/215-3087. Solar Energy Research Institute (National Renewable Energy Laboratory)

Miller, P., K. Griffin (1986). *How Insulated Are California's Homes? Field Inspection and Survey Data on Residential Insulation.* California Energy Commission Report.

Najib A., A. Zarrella, V. Narayanan, R. Bourne, C. Harrington (2020). *Techno-economic parametric analysis of large diameter shallow ground heat exchanger in California climates*. Energy and Buildings 228

NREL. (2024). *Geothermal Heat Pump Basics.* https://www.nrel.gov/research/re-geo-heat-pumps.html#:~:text=Although%20climate%20changes%20seasonally%2C%20a,10%2D16%C2%B0C accessed August 2024

Proctor Engineering, *Central Valley Research Homes.* (2013). https://www.proctoreng.com/dnld/CVRHProjectWholeHouseConcept.pdf. [Accessed Jan 2021].

Rawlings, R., J. Sykulski (1999). *Ground source heat pumps: a technology review*. Building Services Engineering Research and Technology. 20(3): p. 119-129.

Singh, S., R.V. Sharma (2017). *Numerical analysis for ground temperature variation*. Geothermal Energy 5:22 DOI 10.1186/s40517-017-0082-z

Smith, C.B., K.E. Parmenter (2016). *Energy Management Principles (Second Edition).* (2016). Elsevier ISBN 9780128025062. https://doi.org/10.1016/B978-0-12-802506-2.00008-2.

Spitler, J.D., M.S. Mitchell (2016). *Advances in Ground-Source Heat Pump Systems: 8 – Surface water heat pump systems.* Pages 225-246. https://doi.org/10.1016/B978-0-08-100311-4.00008-X

Vignola, F., A. McMahan, C. Grover (2013). *Solar Energy Forecasting and Resource Assessment*. Ch. 5.3. ISBN: 9780123971777.

Woolley, J., C. Harrington, M. Modera (2011). *Swimming pools as heat sinks for air conditioners: model design and experimental validation for natural thermal behavior of the pool*. Building and Environment 46, 187–195.

Appendix A. Simulation Model Results

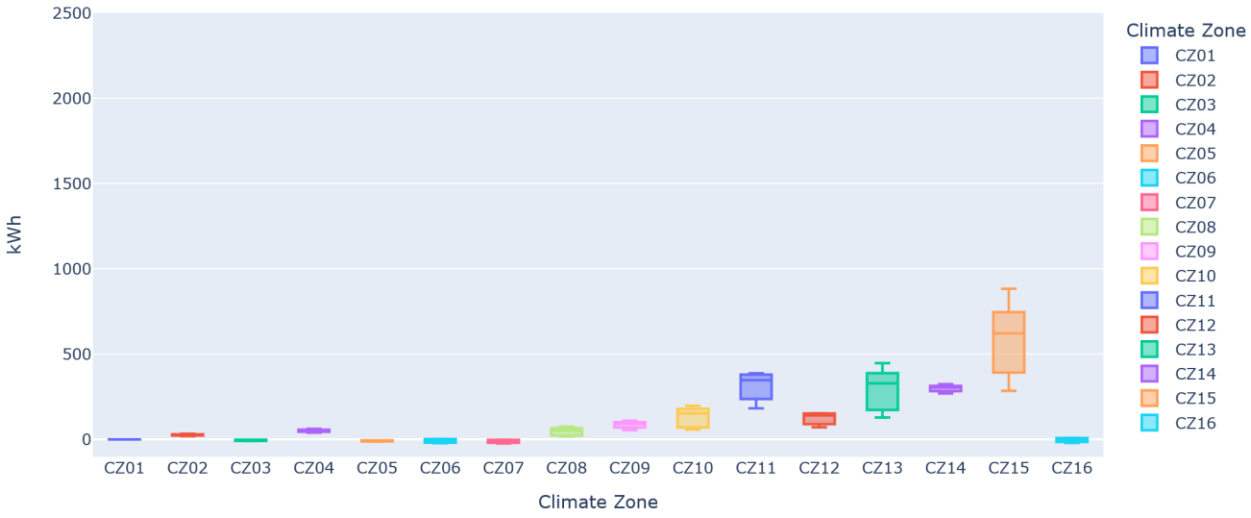

Figure 35. Cooling energy savings (Two-story model, High-COP, 30.0°C setpoint)

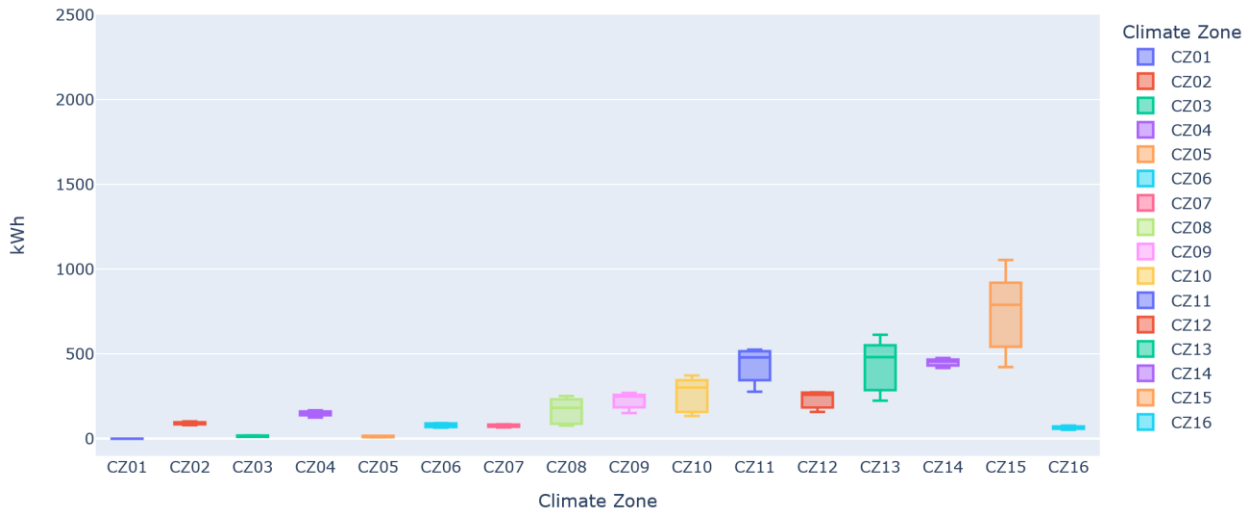

Figure 36. Cooling energy savings (Two-story model, Mid-COP, 30.0°C setpoint)

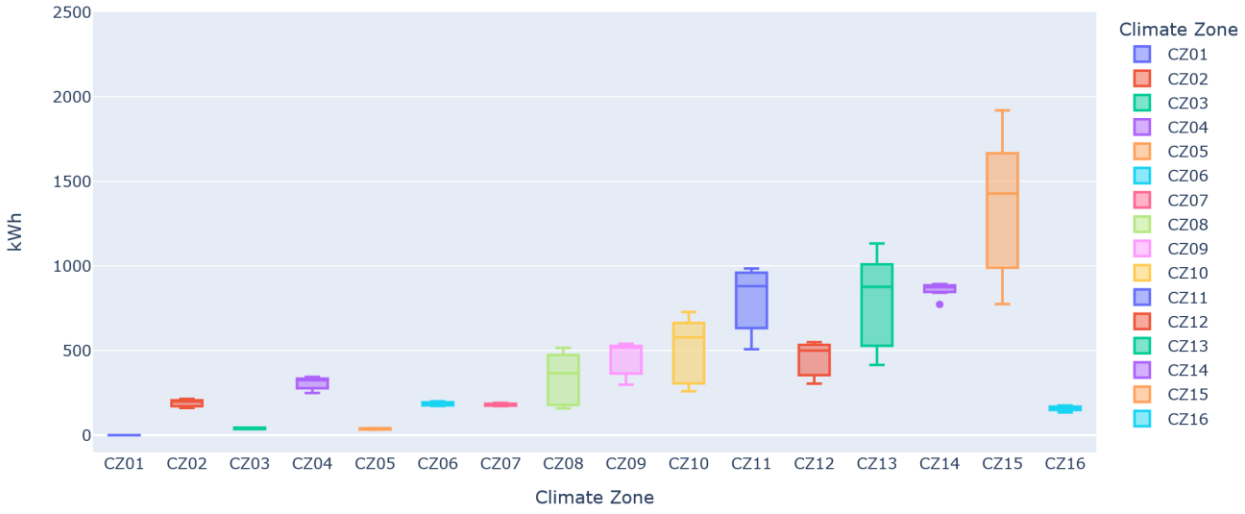

Figure 37. Cooling energy savings (Two-story model, Low-COP, 30.0°C setpoint)

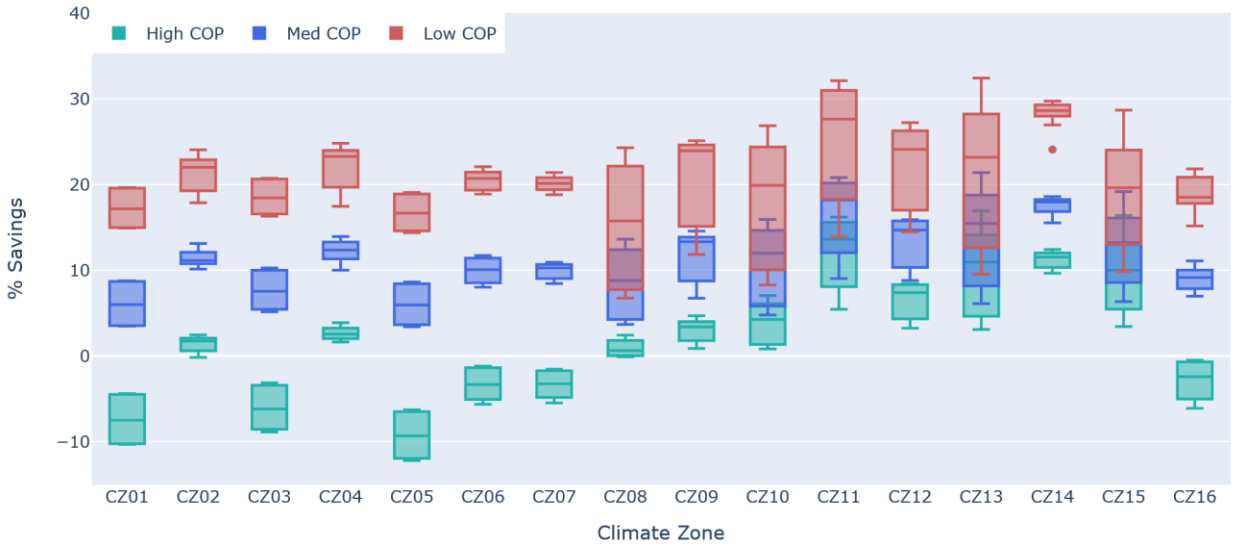

Figure 38. Percentage cooling energy savings with different air conditioner efficiencies (Two-story model, 30.0°C setpoint)

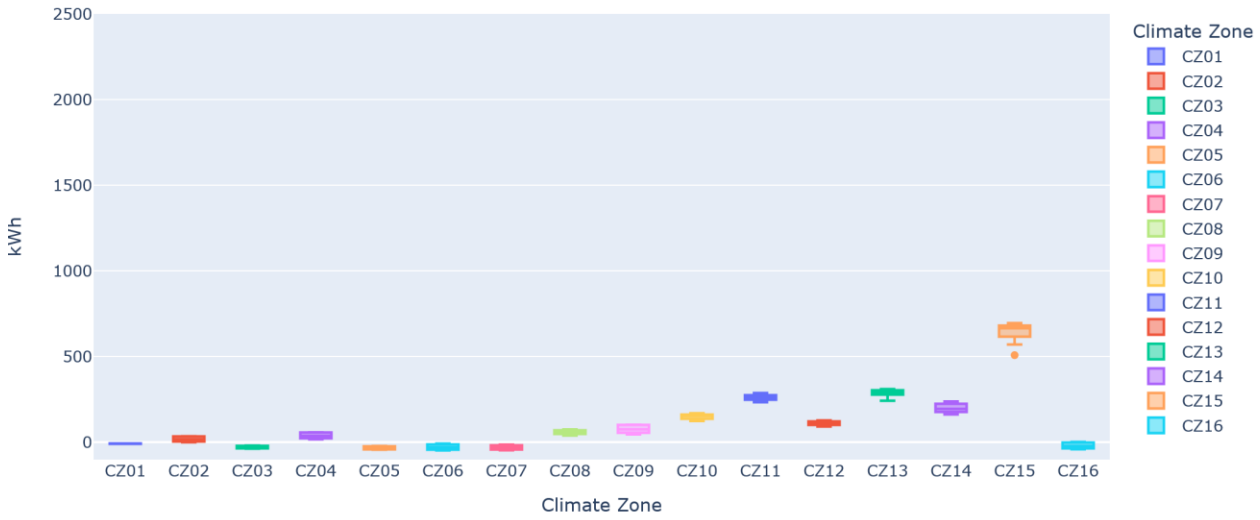

Figure 39. Cooling energy savings (One-story model, High-COP, 32.2°C setpoint)

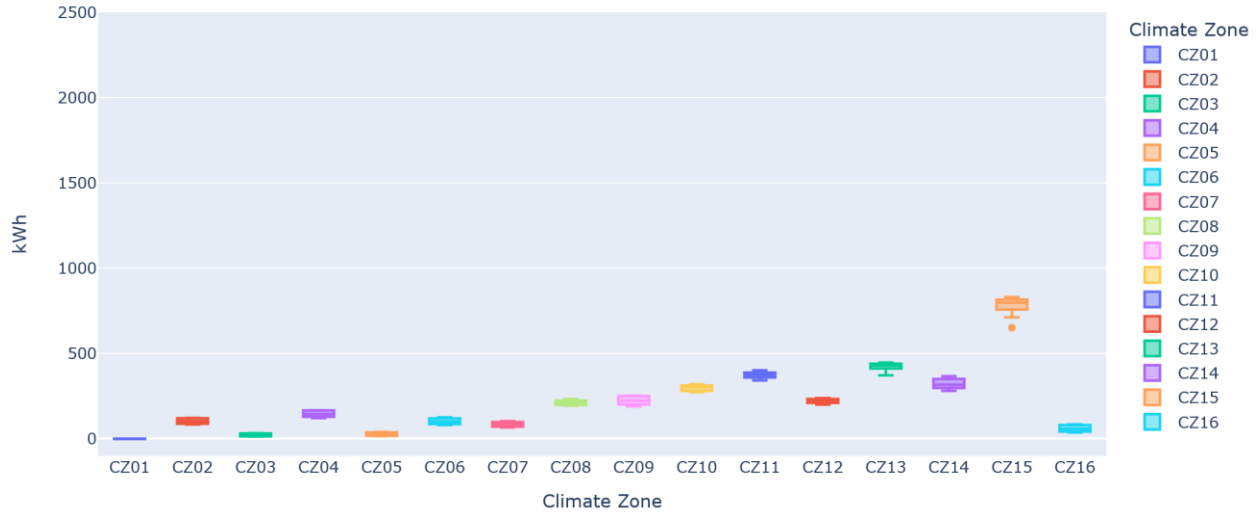

Figure 40. Cooling energy savings (One-story model, Mid-COP, 32.2°C setpoint)

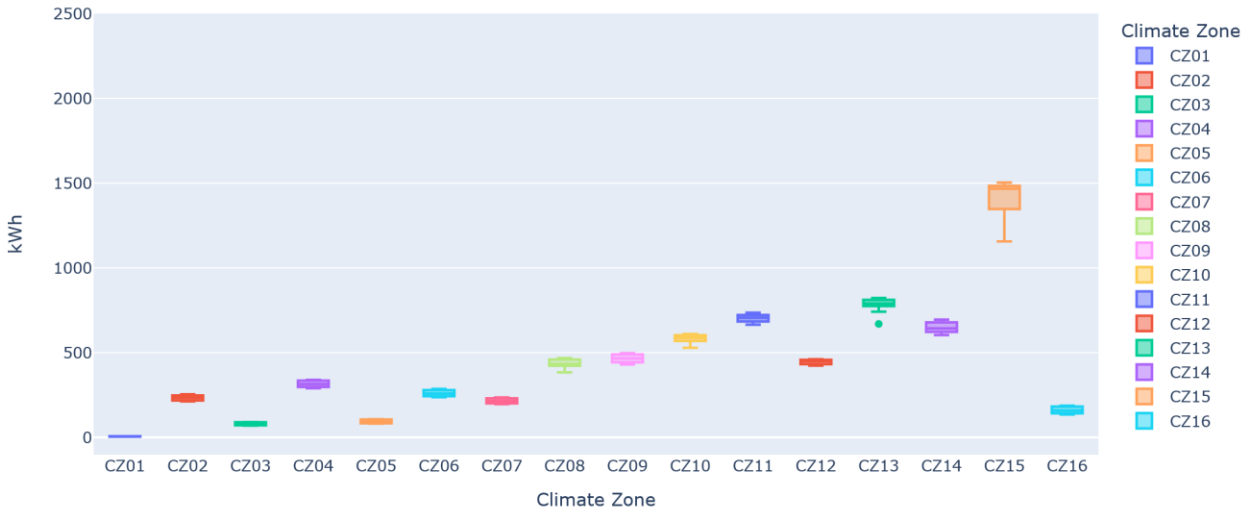

Figure 41. Cooling energy savings (One-story model, Low-COP, 32.2°C setpoint)

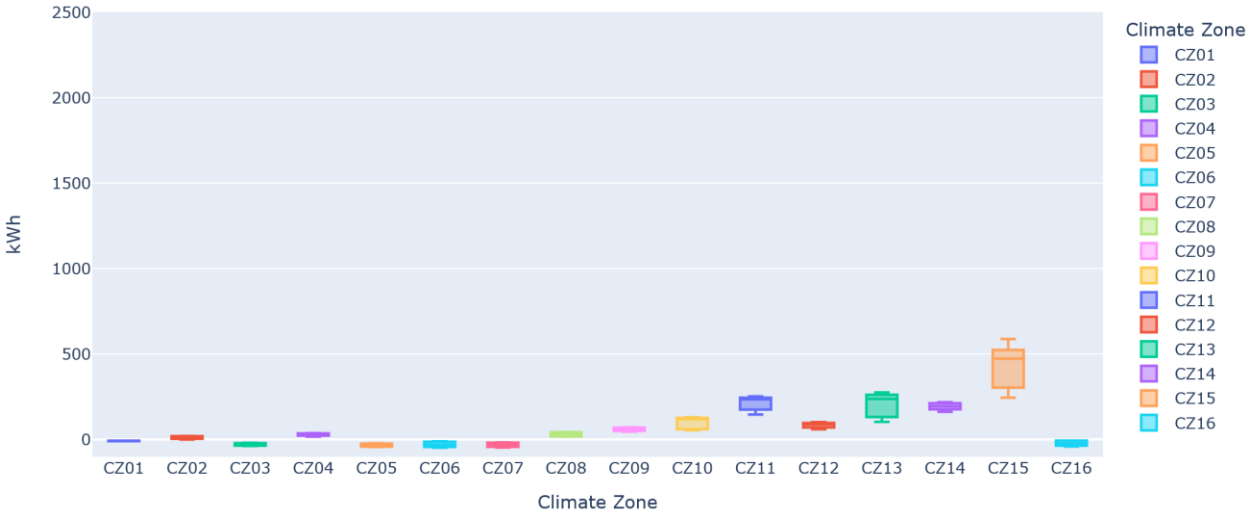

Figure 42. Cooling energy savings (One-story model, High-COP, 30.0°C setpoint)

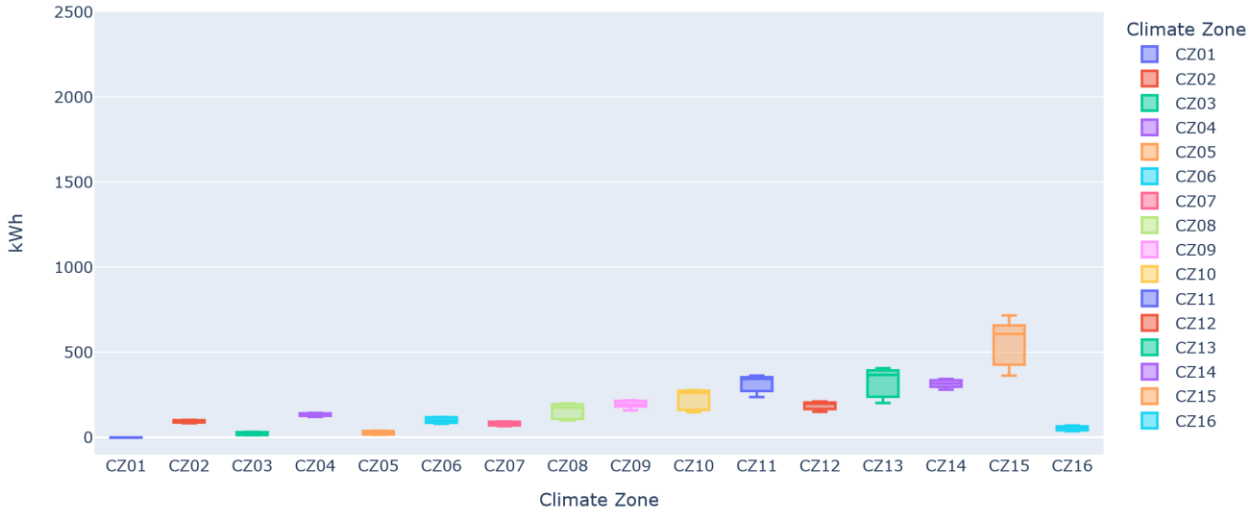

Figure 43. Cooling energy savings (One-story model, Mid-COP, 30.0°C setpoint)

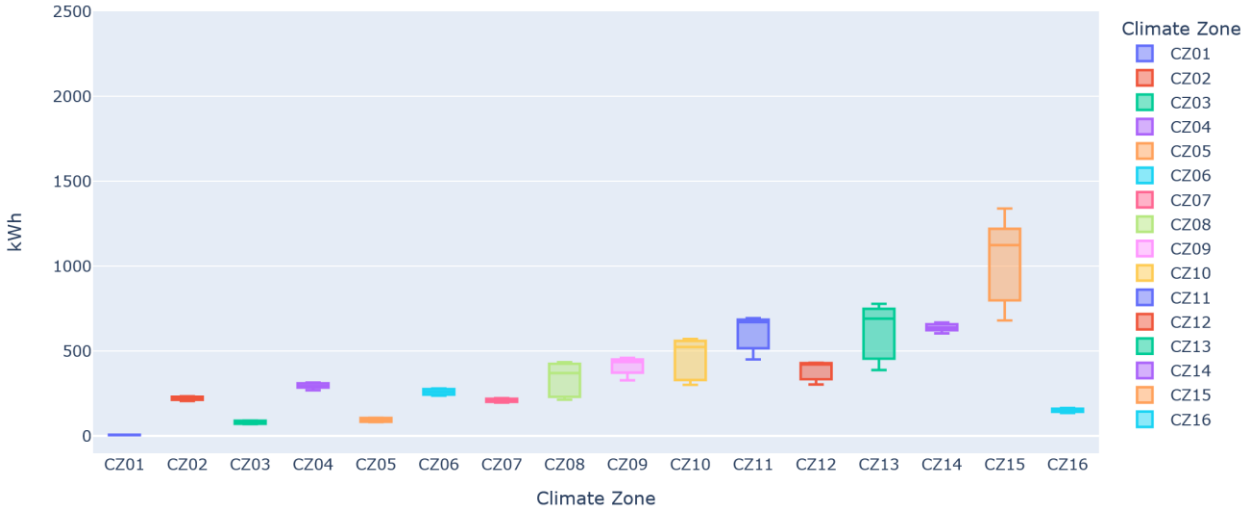

Figure 44. Cooling energy savings (One-story model, Low-COP, 30.0°C setpoint)

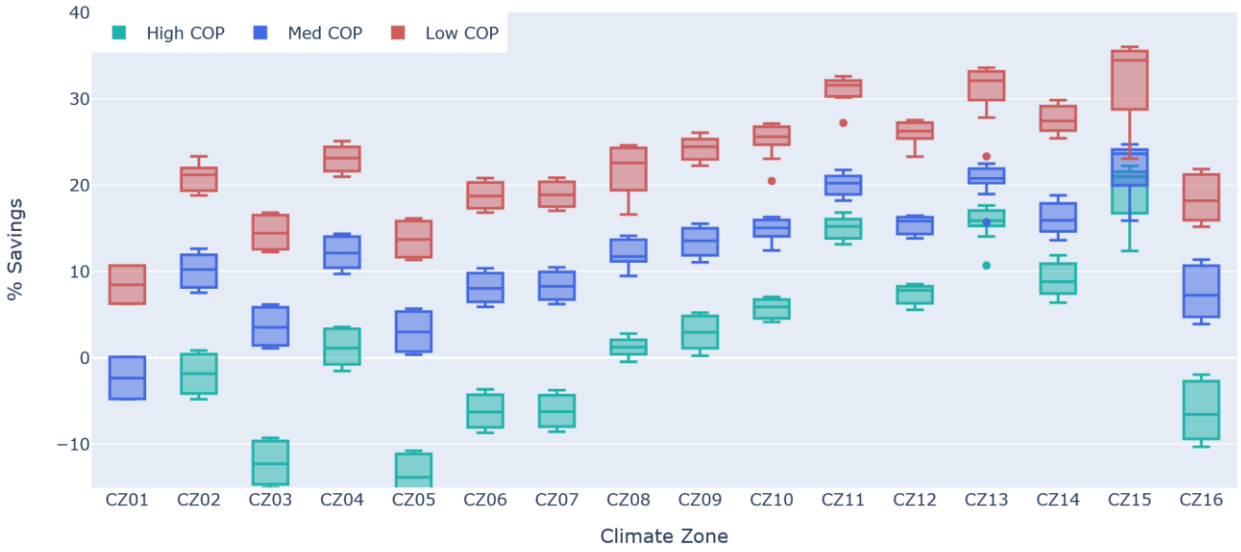

Figure 45. Percentage cooling energy savings with different air conditioner efficiencies (One-story model, 32.2°C setpoint)

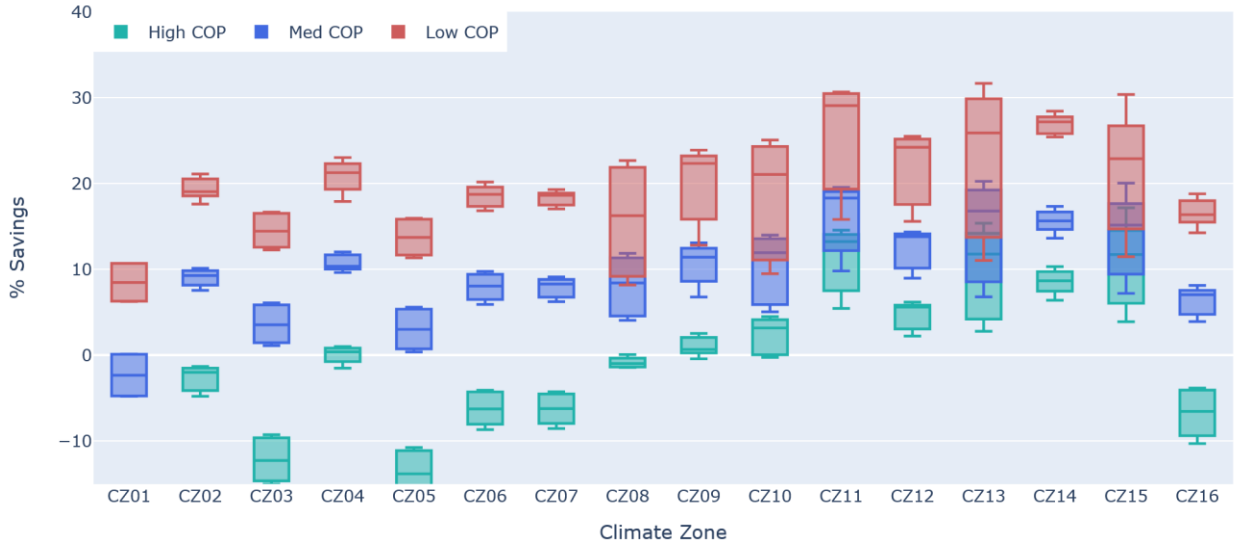

Figure 46. Percentage cooling energy savings with different air conditioner efficiencies (One-story model, 30.0°C setpoint)

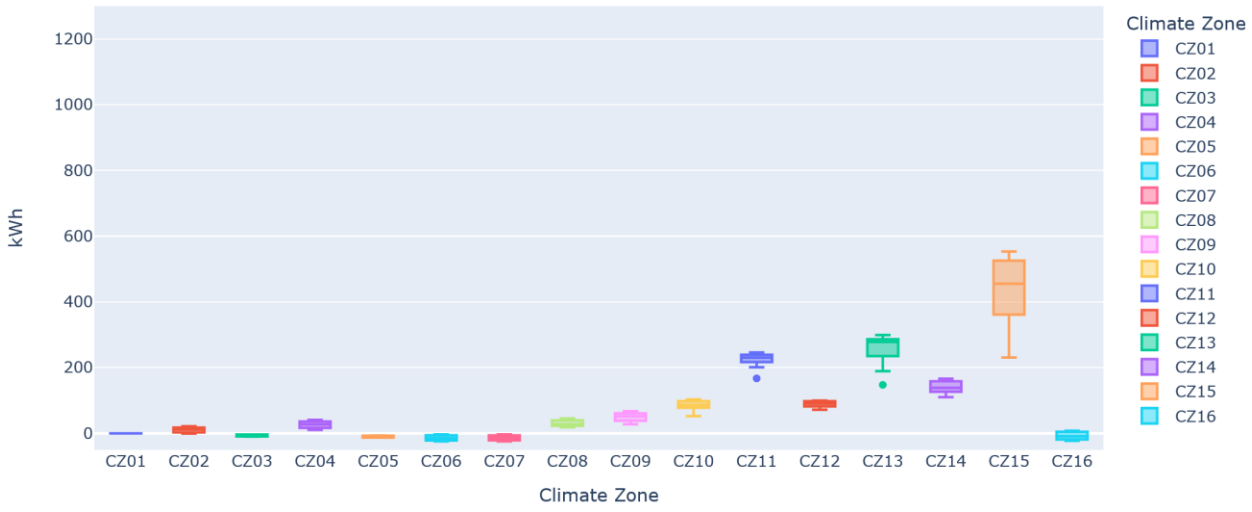

Figure 47. Peak cooling energy savings (two-story model, high-COP, 32.2°C setpoint)

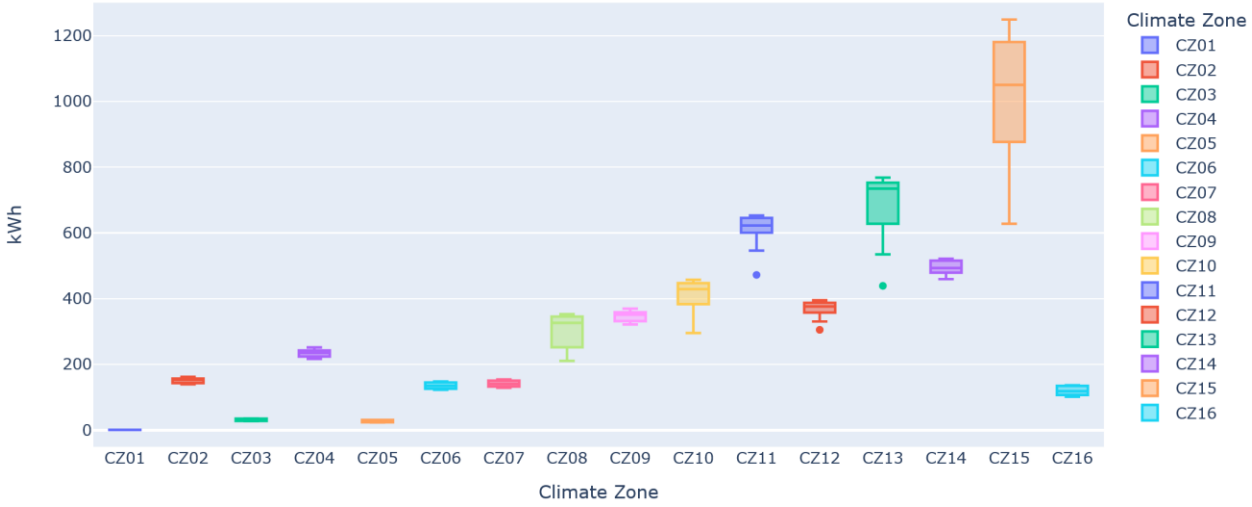

Figure 48. Peak cooling energy savings (two-story model, low-COP, 32.2°C setpoint)

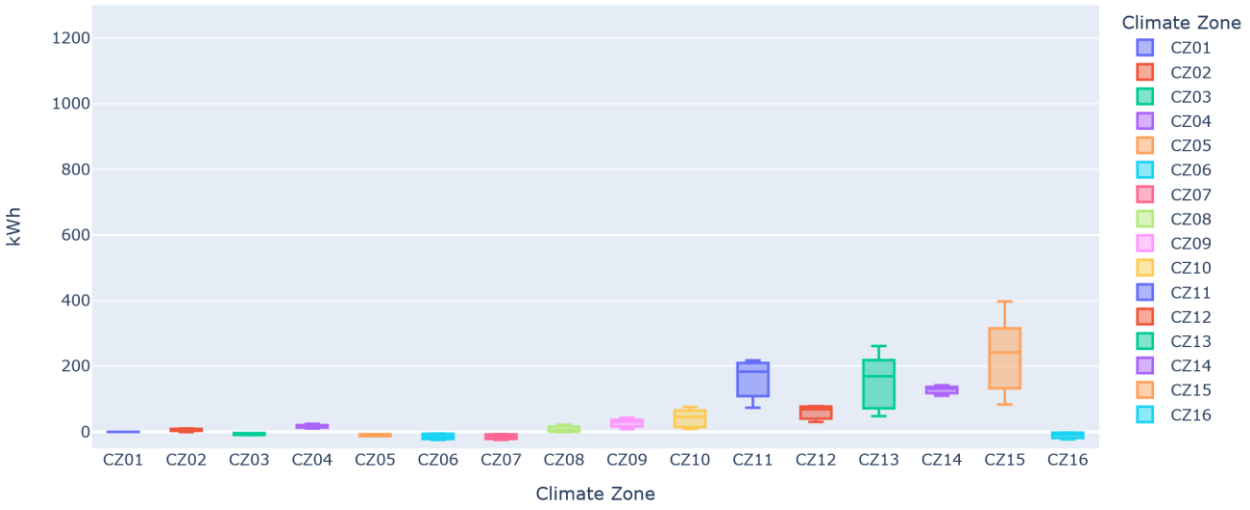

Figure 49. Peak cooling energy savings (two-story model, high-COP, 30.0°C setpoint)

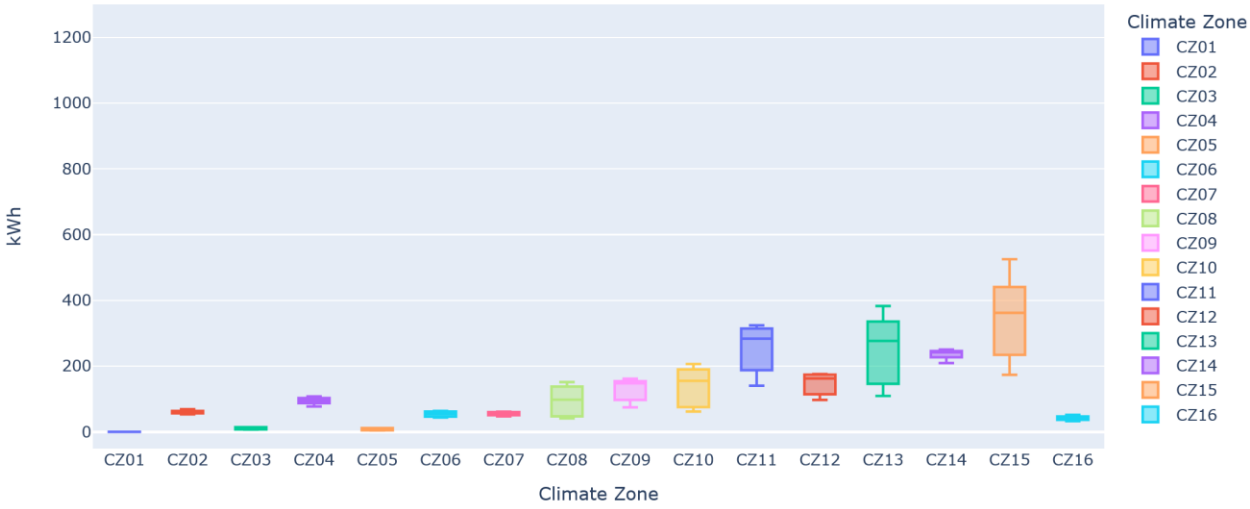

Figure 50. Peak cooling energy savings (two-story model, mid-COP, 30.0°C setpoint)

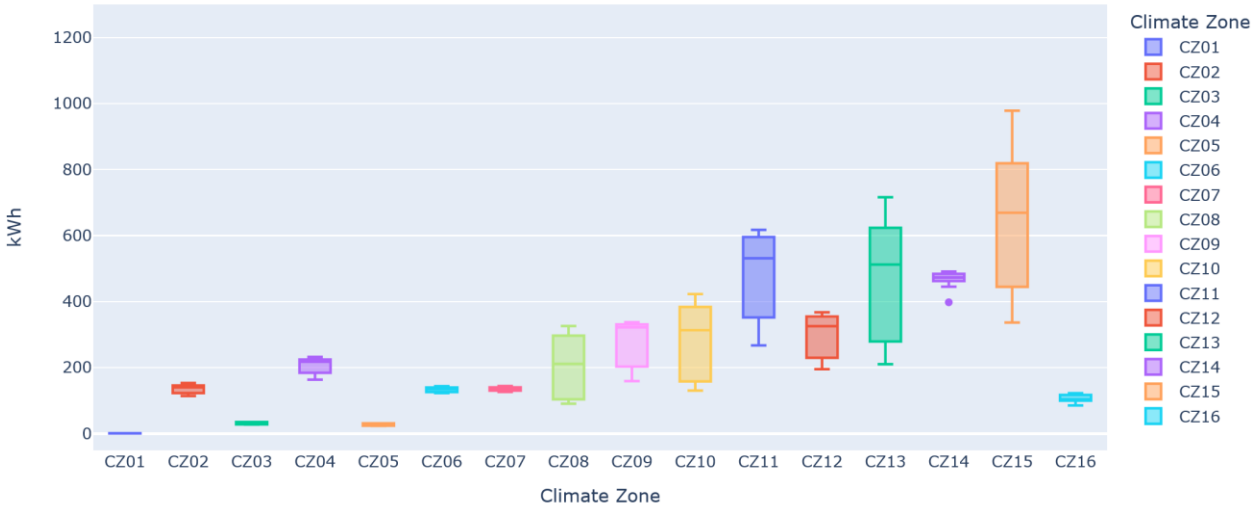

Figure 51. Peak cooling energy savings (two-story model, low-COP, 30.0°C setpoint)

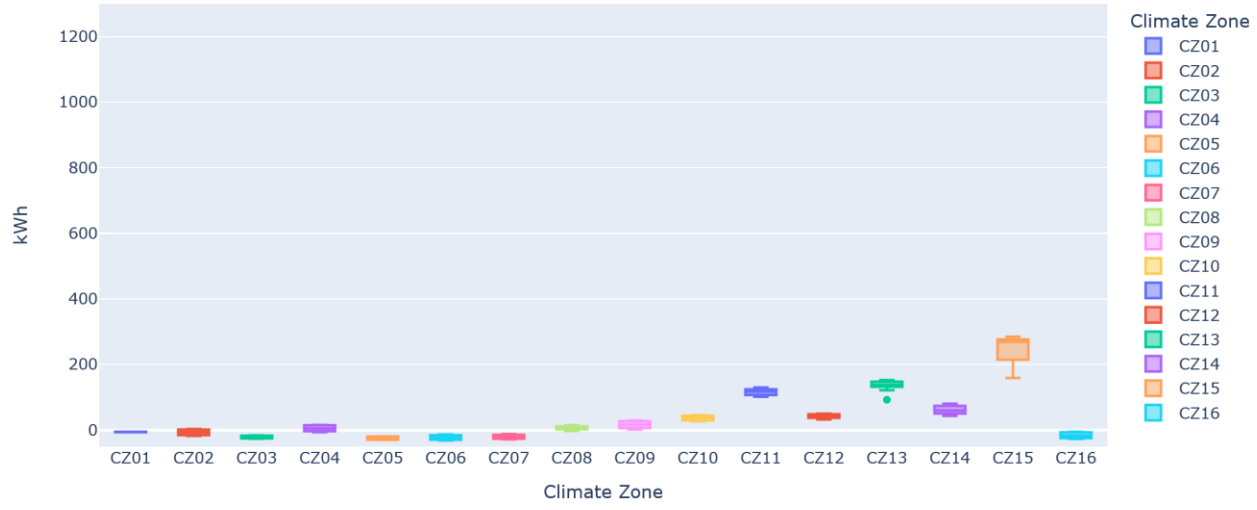

Figure 52. Peak cooling energy savings (One-story model, high-COP, 32.2°C setpoint)

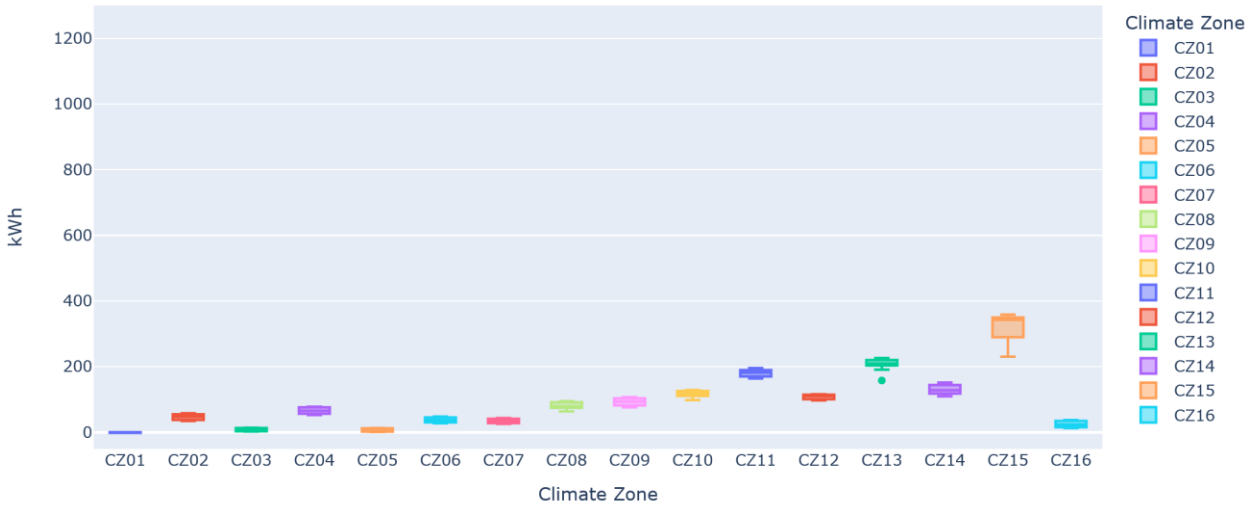

Figure 53. Peak cooling energy savings (One-story model, mid-COP, 32.2°C setpoint)

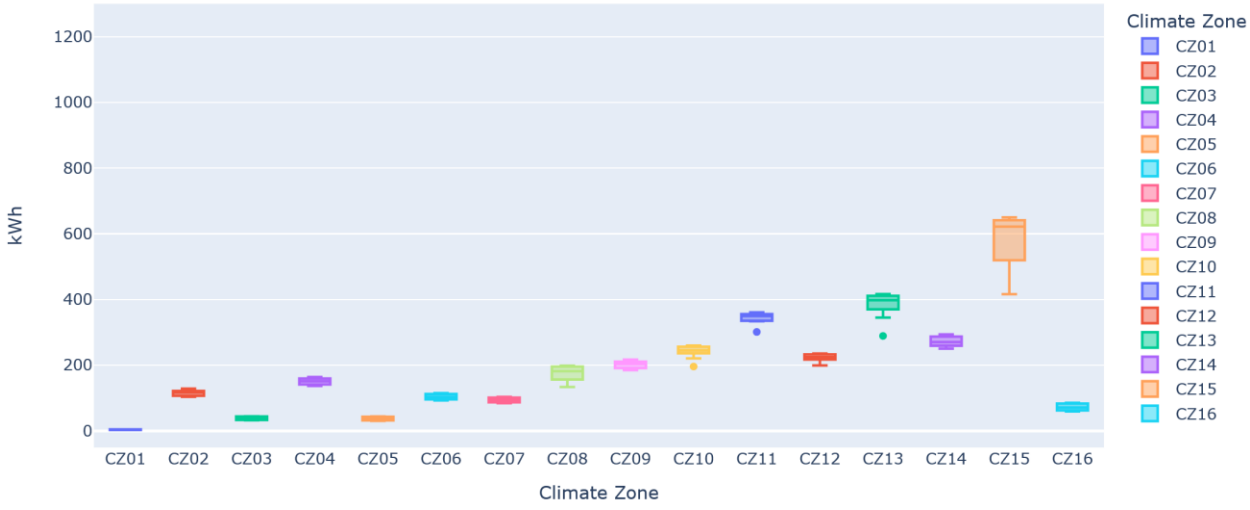

Figure 54. Peak cooling energy savings (One-story model, low-COP, 32.2°C setpoint)

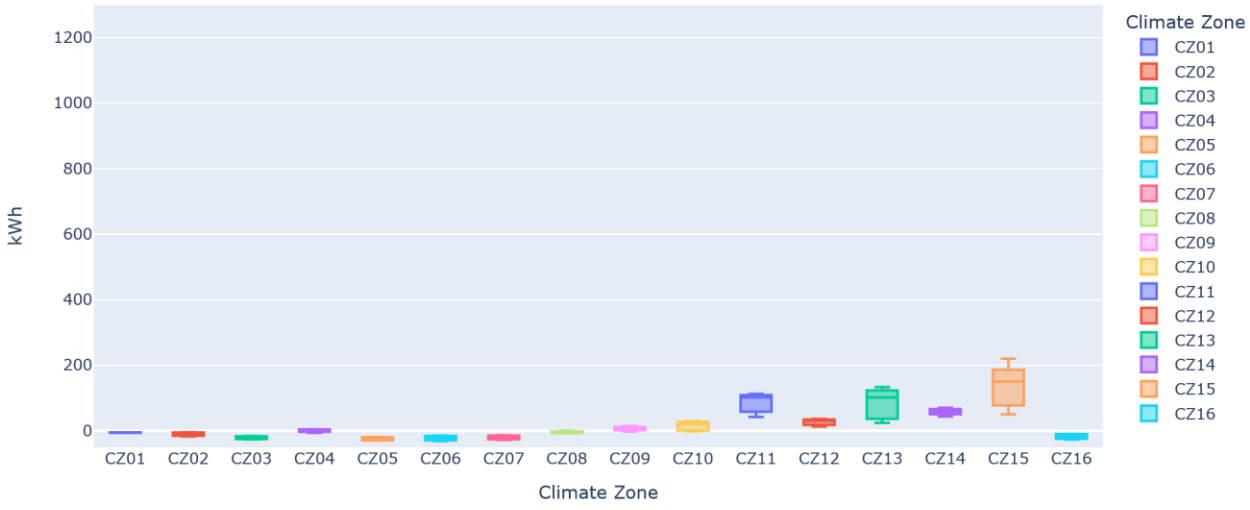

Figure 55. Peak cooling energy savings (One-story model, high-COP, 30.0°C setpoint)

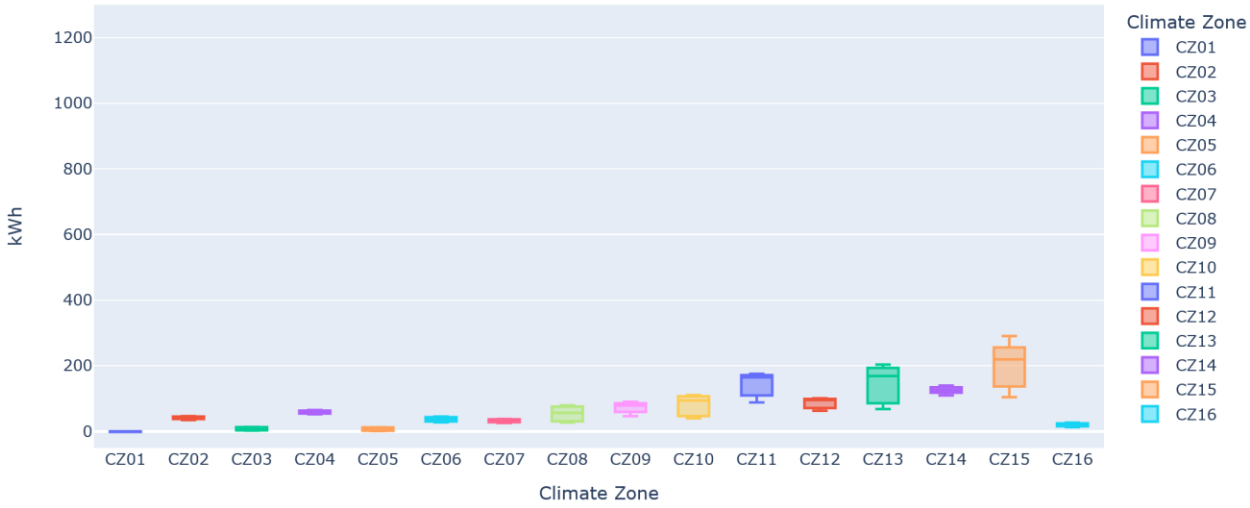

Figure 56. Peak cooling energy savings (One-story model, mid-COP, 30.0°C setpoint)

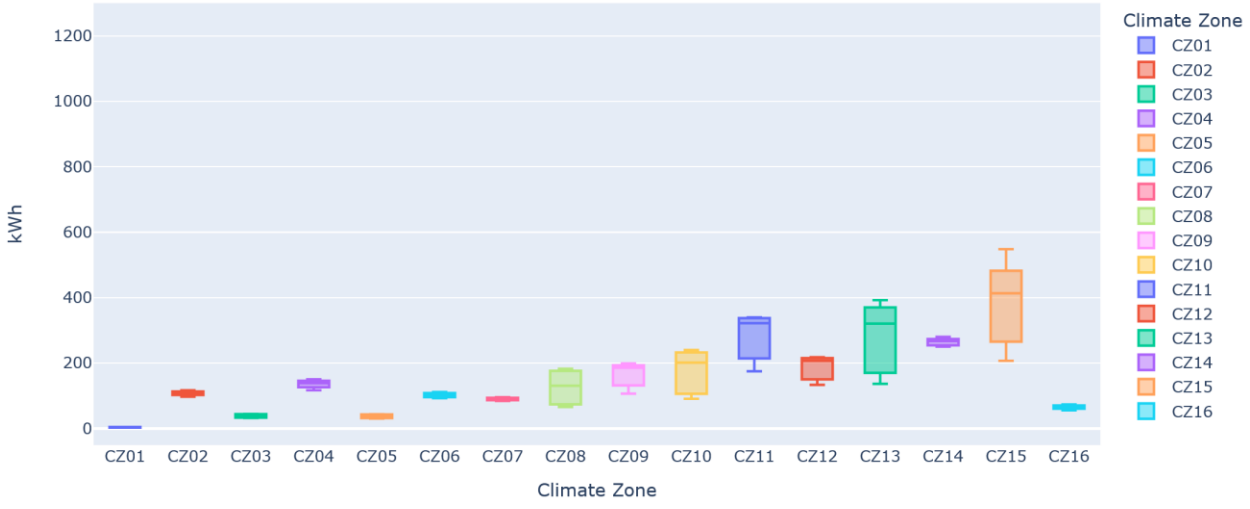

Figure 57. Peak cooling energy savings (One-story model, low-COP, 30.0°C setpoint)

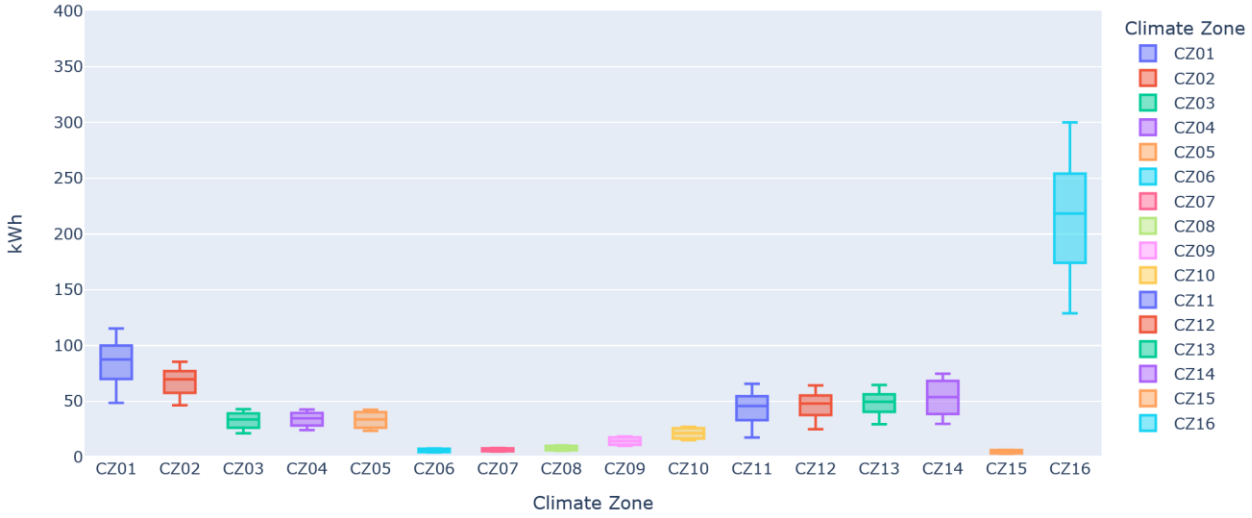

Figure 58. Heating energy savings (two-story model, high-COP)

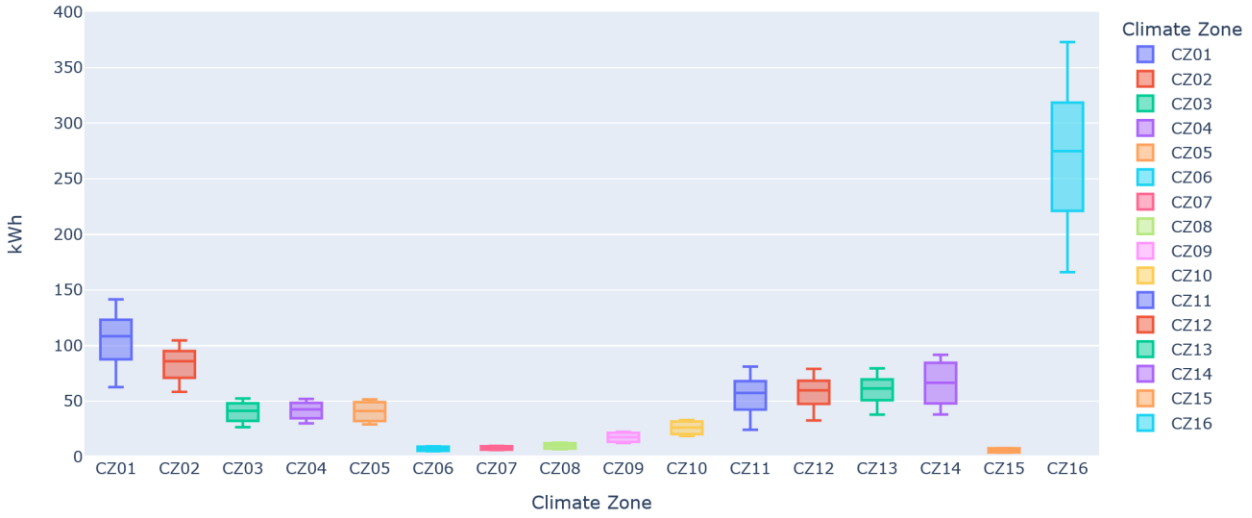

Figure 59. Heating energy savings (two-story model, low-COP)

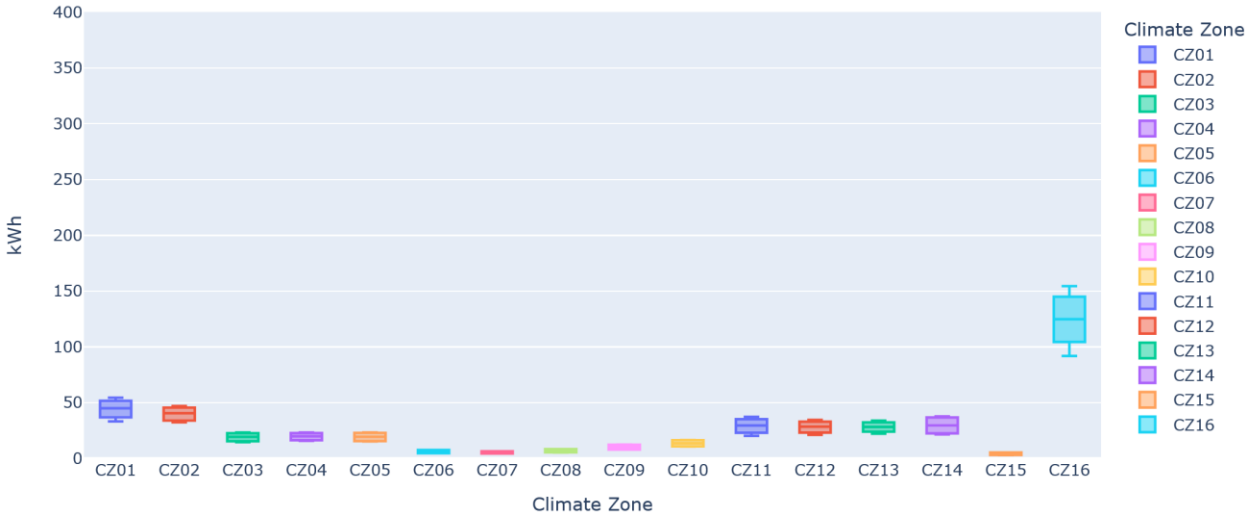

Figure 60. Heating energy savings (One-story model, high-COP)

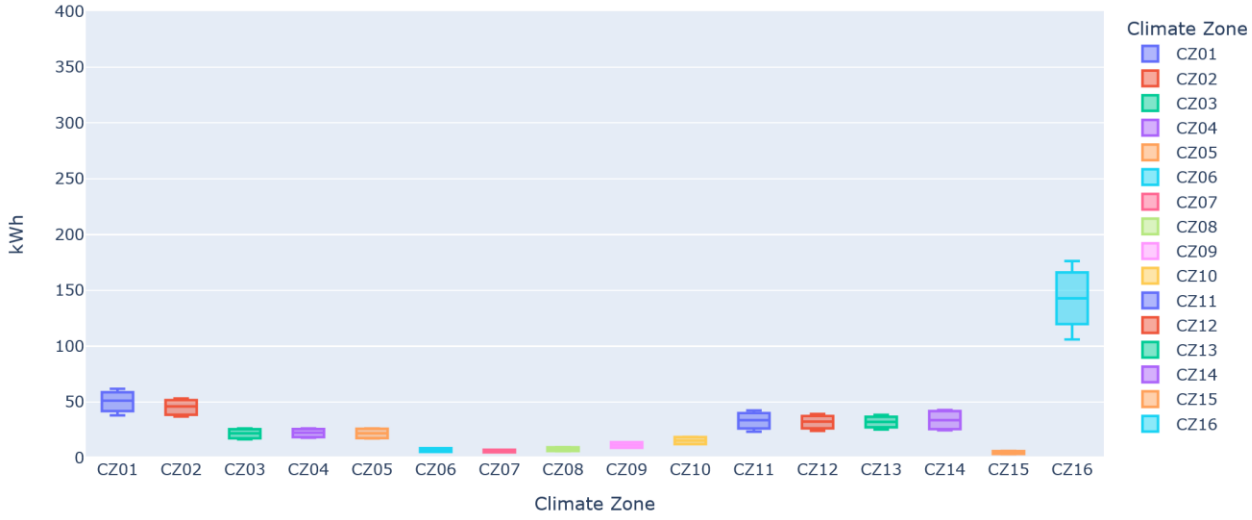

Figure 61. Heating energy savings (One-story model, mid-COP)

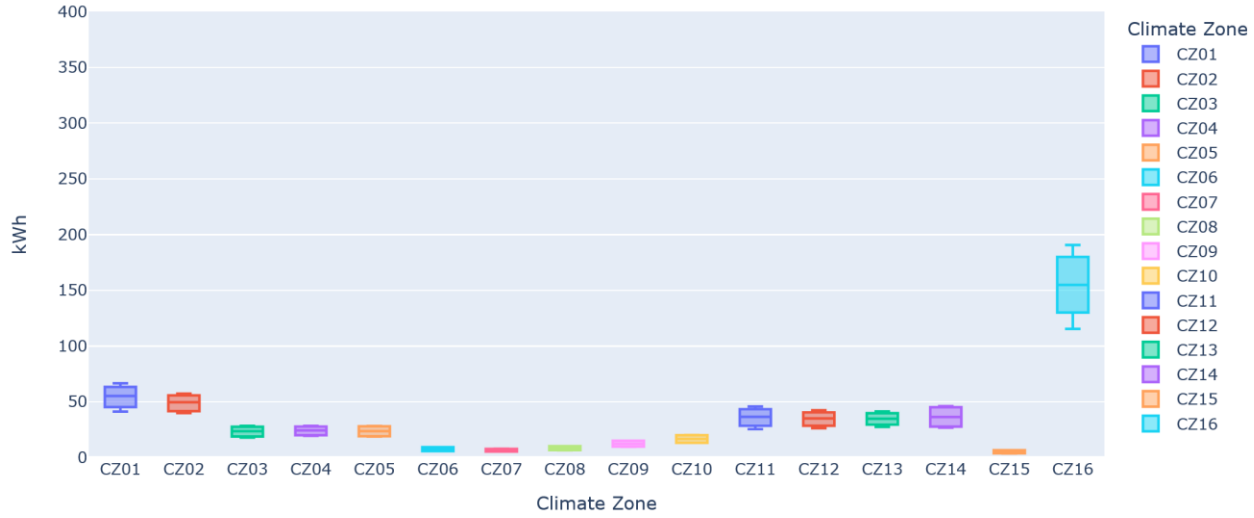

Figure 62. Heating energy savings (One-story model, low-COP)

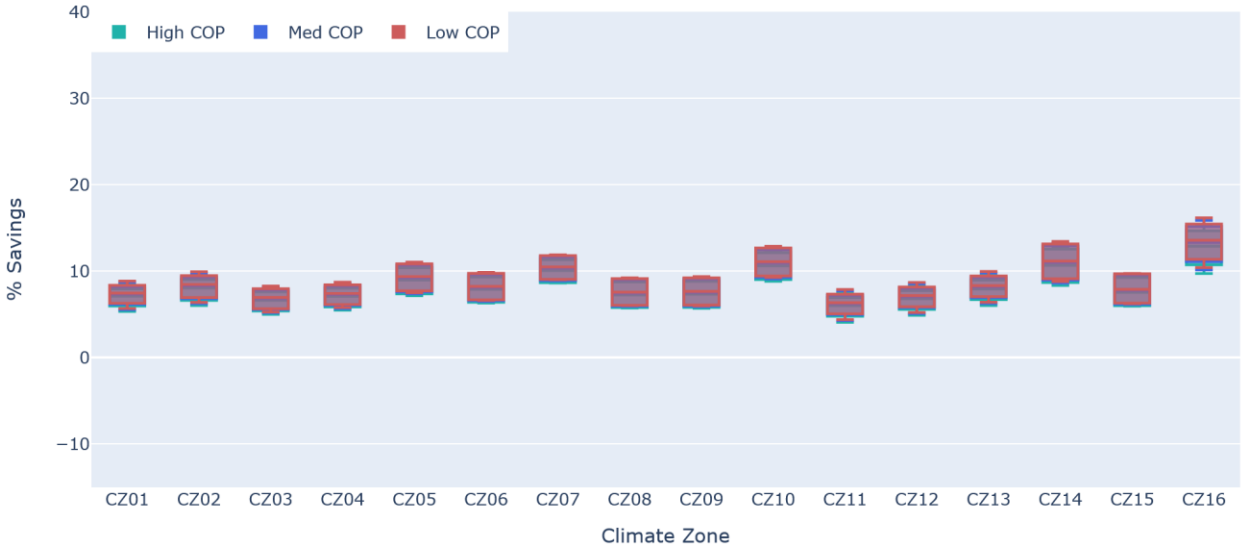

Figure 63. Percentage heating energy savings with different air conditioner efficiencies (One-story model)